Application of Physiographic Science to the Northland Region: Preliminary Hydrological and Redox Process-Attribute Layers

Clint Rissmann, Lisa Pearson, Jessie Lindsay, Matt Couldrey
and Abigail Lovett

Land and Water Science Report 2018/11
June 2018

Application of Physiographic Science to the Northland Region: Preliminary Hydrological and Redox Process-Attribute Layers

Prepared by
Rissmann, C., Pearson, L., Lindsay, J., Couldrey, M., and Lovett, A.

Land and Water Science Ltd.
www.landwaterscience.co.nz
61c Leet Street
Invercargill, 9810
New Zealand

Corresponding Author
Clint Rissmann
Contact number: 03 214 3003
Email: clint@landwatersci.net

Document Information
Land and Water Science Report No: 2018/11
Report Date: 29.06.2018
Project Number: 18001-NRC

Reviewed By: Susie Osbaldiston
Organisation: Northland Regional Council
Position: Groundwater Management Scientist
Review Date: 12.06.2018

Document Status: Final

Citation Advice
Rissmann, C., Pearson, L., Lindsay, J., Couldrey, M., and Lovett, A. (2018). Application of Physiographic Science to the Northland Region: Preliminary Hydrological and Redox Process-Attribute Layers. Land and Water Science Report 2018/11. p88.

Disclaimer: This report has been prepared by Land and Water Science Ltd. (Land and Water Science) exclusively for, and under contract to Northland Regional Council. Land and Water Science accepts no responsibility for any use of, or reliance on any contents of this report by any person or organisation other than Northland Regional Council, on any ground, for any loss, damage, or expense arising from such use or reliance. Information presented in this report is available to Northland Regional Council for use from 1 June 2018.

Table of Contents

List of Figures

Section 2

Section 4

Section 5

Section 6

Section 7

List of Tables

Section 4

Section 5

Section 6

Section 7

Abstract

Water quality outcomes can vary spatially across the landscape, even when there are similar land use pressures. These differences are often the result of natural spatial variation in the landscape, which alters the composition of the water through coupled physical, chemical and biological processes. The physiographic approach is an integrated or 'systems view,' predicated upon the spatial coupling between landscape attributes and the key processes (e.g. hydrological and redox) governing water quality outcomes in surface water and shallow groundwater. In this application of physiographic science to the Northland Region, existing geospatial data, multidisciplinary knowledge, and water quality and hydrochemical data have been used to produce a preliminary classification of the hydrological (H-PAL) and redox (R-PAL) process-attribute layers. Although preliminary, both the H-PAL and R-PAL are considered a current best estimate of the likely key hydrological and redox gradients, that in addition to land use, are thought to govern spatial variation in water quality outcomes across the Northland region.

The preliminary hydrological process-attribute layer includes mapping:

- Hydrological domain for water source
- Overland flow
- Lateral flow
- Artificial drainage
- Deep drainage

The preliminary redox process-attribute layer includes mapping:

- Soil reduction potential
- Geological reduction potential
- Combined soil and geological reduction potential

Knowledge of how and why water quality outcomes vary in space, and ultimately in time, is a powerful basis for more effective and targeted management of natural resource use including the identification of what mitigations are likely to be best suited to a particular setting to improve water quality. Future work looks to further refine and subsequently test the validity of the mapping produced here in terms of its ability to estimate spatial variation in surface water and shallow groundwater quality across the Northland Region. Accompanying this report is a GIS map package.

1 Introduction

Water quality can vary spatially across the landscape, even when there is similar land uses or pressures in a catchment. These differences occur because of natural spatial variation in landscape attributes, which alters the composition of the water through coupled physical, chemical and biological processes. Previous research has noted that spatial variation in landscape attributes can account for more than twice the variability in water quality than land use alone (Johnson et al., 1997; Hale et al., 2004; King et al., 2005; Dow et al., 2006; Shiels, 2010; Becker et al., 2014). The role of landscape variability over water quality outcomes is especially true for countries such as New Zealand, which is often recognised as one of the most complex geological regions in the world (Johnson et al., 1997). In addition to providing critical context to better understand and model land use losses, such as nutrients and sediment, the physiographic method provides a greater opportunity to target and implement mitigations that are both environmentally and cost-effective.

In New Zealand, the physiographic method is being developed and applied nationally by Land and Water Science via several projects at local, catchment, regional and national scales. The Our Land and Water National Science Challenge, Physiographic Environments of New Zealand (PENZ) programme has been developed to apply the physiographic method at the national scale. The PENZ programme requires alignment of project funding and an in-kind contribution from Regional Councils who chose to participate. Council project funding is required to support the development of hydrological and redox process-attribute layers, which will be complemented by additional field sampling of surface water and groundwater, undertaken by regional councils. The number of additional sites and samples identified for sampling is directly related to coverage and completeness of existing datasets and the spatial scale at which the physiographic method is to be applied. The primary outcome of the application of physiographic science at the regional scale is that regional councils' will have a tool/model to make more informed resource management decisions to achieve requirements under the National Policy Statement for Freshwater Management (NPSFM; Ministry for the Environment, 2014).

This project is a collaboration between Land Water Science and Northland Regional Council and is aligned with the PENZ programme. The primary aim of this project was to develop an understanding of the physiographic background to inform the application of the physiographic approach. To achieve this, a hydrological process attribute layer and a redox process-attribute layer were developed for the Northland region. A summary of datasets required, methods used, and results are provided in this report. In addition, a discussion of the results in the context of the application of the physiographic approach to the Northland Region is provided, followed by a summary of recommendations and next steps.

2 Background to Physiographic Science

It is widely recognised in hydrochemical and geochemical literature that there are four key process families governing the composition of freshwater - atmospheric, hydrological, redox and weathering (Moldan & Černý, 1994; Clark & Fritz, 1997; Güler & Thyne, 2004; Kendall & McDonnell, 2008; Tratnyek et al., 2012). Of these process families, hydrological and redox processes are often considered the most significant in governing variation in water quality outcomes (Moldan & Černý, 1994; Langmuir, 1997; Wieder et al., 2004; Tratnyek et al., 2012; Eriksson, 2012). The fundamental premise of the physiographic approach is that spatial variation in water composition (quality and hydrochemistry) can be understood by identifying and mapping the spatial coupling between *process signals* in water and *landscape attributes*. Land use intensity can also be incorporated into the approach to account for the modification of landscape attributes through human endeavours such as higher nutrient loading rates and modification of soil hydrological properties via artificial drainage (see Rissmann et al., 2018).

Until recently a systematic approach to mapping the integrated landscape controls over surface and shallow groundwater quality has been lacking. In this section, a conceptual overview of the physiographic method for identifying and mapping the critical attributes of the landscape that control spatial variation in water quality outcomes is presented (Figure 2.1).

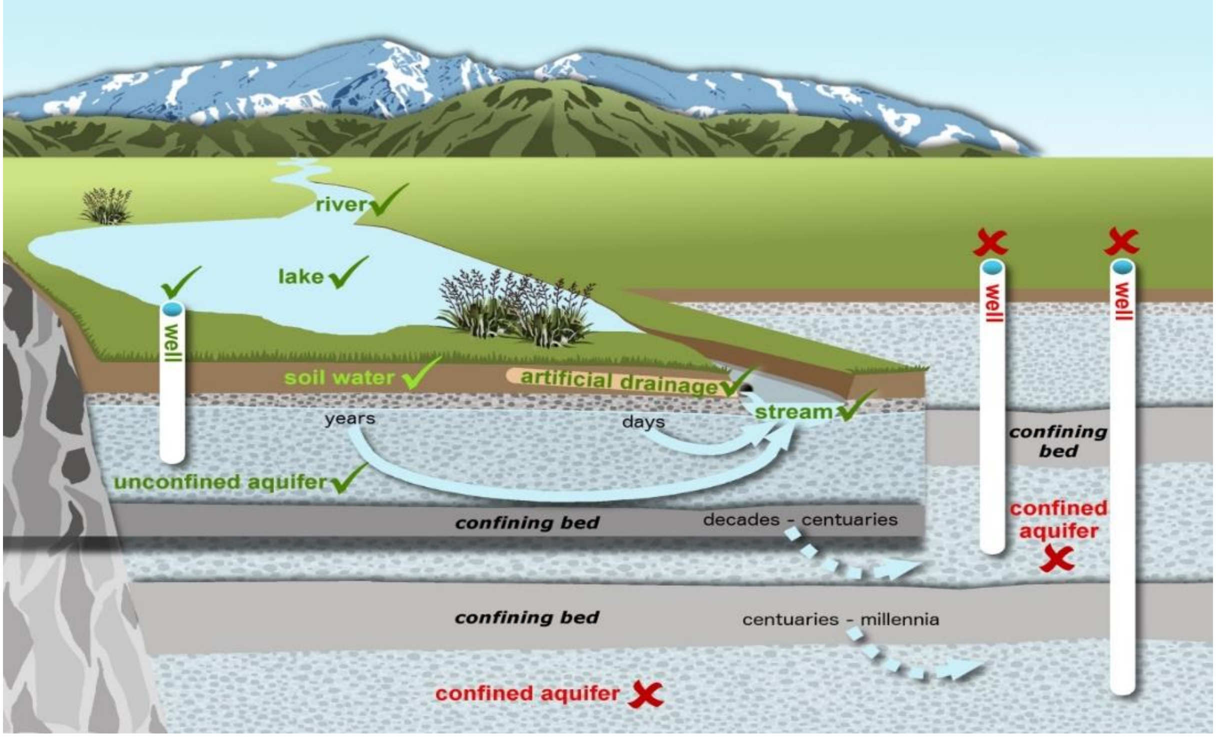

Figure 2. 1: Illustration of the connectivity of near-surface water resources, including soil water, surface and shallow groundwater (Hughes et al., 2016). Green tick marks show the hydrologically connected settings included in the physiographic approach, whereas red crosses identify settings that are excluded.

For example, spatial variation in the concentration of sodium (Na), chloride (Cl), and the stable isotopes of water ($\delta^{18}O/\delta^{2}H-H_2O$, V-SMOW) in precipitation (*atmospheric process signals*) are known to be governed by altitude and distance from the coast (*landscape attributes*) (Clark & Fritz, 1997; Langmuir, 1997; Wieder et al., 2004; Kendall & McDonnell, 2008); spatial variation in the Na, Cl and $\delta D/\delta^{18}O$ in surface and shallow groundwater (*hydrological process signals*) are known to vary according to water source and connectivity between recharge domains (*landscape attribute*) (Clark & Fritz, 1997; Kendall & McDonnell, 2008; Inamdar, 2011); spatial variation in groundwater pH and hence alkalinity (*weathering process signals*) are governed by the acid neutralising capacity (ANC) (*landscape attribute*) of soil and rock, as well as its degree of weathering (Wright, 1988; Moldan & Černý, 1994; Giller & Malmqvist, 2004; Lydersen et al., 2004), and; aquifer reduction potential (*redox process signals*) varies according to the permeability (residence time) and abundance of electron donors within an aquifer (*attribute*) (Krantz and Powars, 2002; McMahon and Chapelle, 2008; Rissmann, 2011; Beyer et al., 2016; Wilson et al., 2018).

The signals in water are used to verify the effective properties of the landscape. This process is important for (i) linking landscape compartments (i.e., land surface, soil, aquifer, surface waters); (ii) understanding the relative significance of each compartment over water composition, and; (iii) refining pre-existing maps of landscape attributes that may not have been mapped with water in mind, or do not contain the key attributes governing water quality outcomes.

With this integrated perspective in mind, the ultimate aim of the physiographic method is to produce a number of classed process-attribute GIS layers that depict the spatial coupling between process signals in water and landscape attribute gradients. The steps for physiographic mapping of the landscape are summarised in Figure 2.

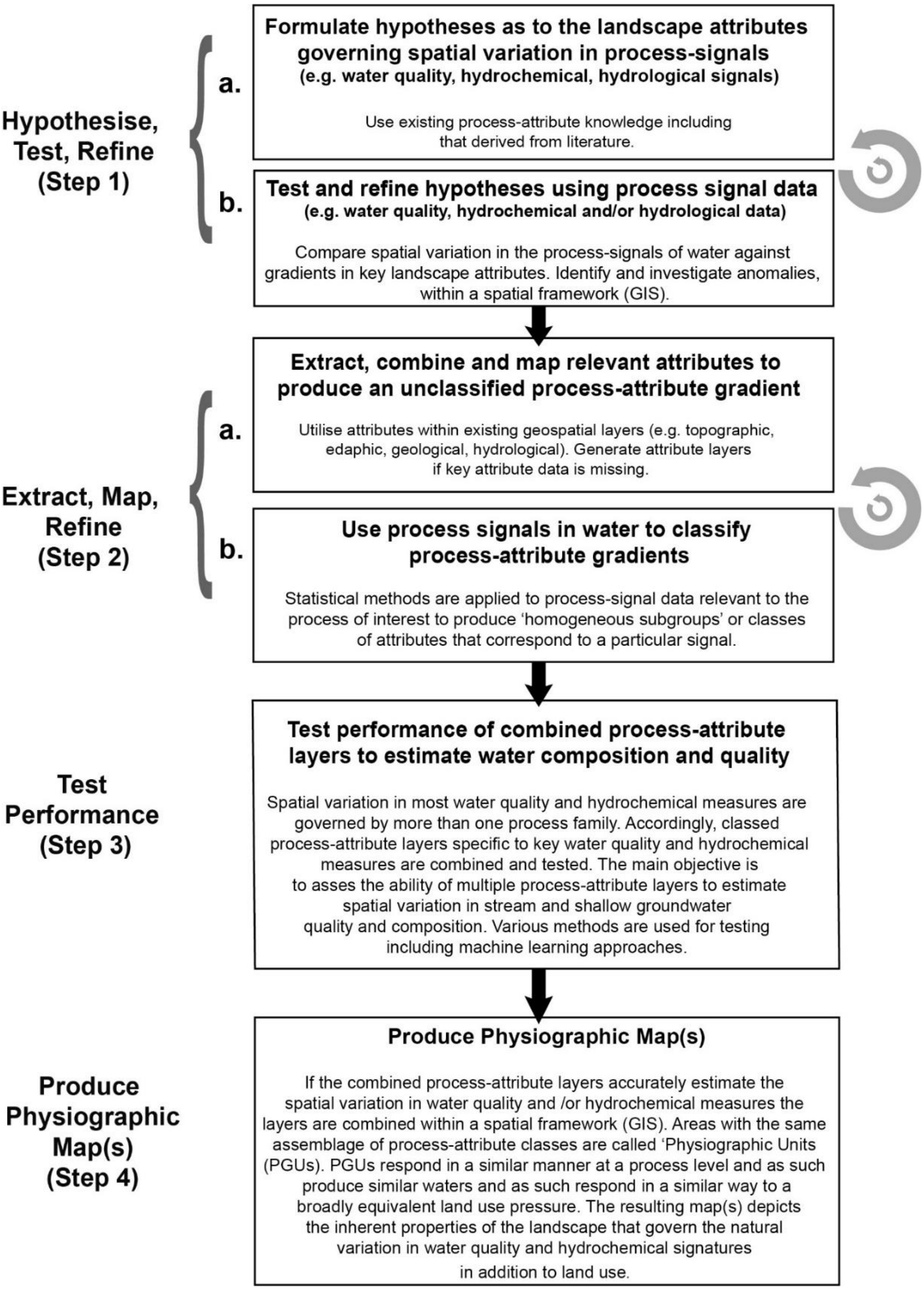

Hypothesise, Test, Refine (Step 1)

a. Formulate hypotheses as to the landscape attributes governing spatial variation in process-signals (e.g. water quality, hydrochemical, hydrological signals)

Use existing process-attribute knowledge including that derived from literature.

b. Test and refine hypotheses using process signal data (e.g. water quality, hydrochemical and/or hydrological data)

Compare spatial variation in the process-signals of water against gradients in key landscape attributes. Identify and investigate anomalies, within a spatial framework (GIS).

Extract, Map, Refine (Step 2)

a. Extract, combine and map relevant attributes to produce an unclassified process-attribute gradient

Utilise attributes within existing geospatial layers (e.g. topographic, edaphic, geological, hydrological). Generate attribute layers if key attribute data is missing.

b. Use process signals in water to classify process-attribute gradients

Statistical methods are applied to process-signal data relevant to the process of interest to produce 'homogeneous subgroups' or classes of attributes that correspond to a particular signal.

Test Performance (Step 3)

Test performance of combined process-attribute layers to estimate water composition and quality

Spatial variation in most water quality and hydrochemical measures are governed by more than one process family. Accordingly, classed process-attribute layers specific to key water quality and hydrochemical measures are combined and tested. The main objective is to asses the ability of multiple process-attribute layers to estimate spatial variation in stream and shallow groundwater quality and composition. Various methods are used for testing including machine learning approaches.

Produce Physiographic Map(s) (Step 4)

Produce Physiographic Map(s)

If the combined process-attribute layers accurately estimate the spatial variation in water quality and /or hydrochemical measures the layers are combined within a spatial framework (GIS). Areas with the same assemblage of process-attribute classes are called 'Physiographic Units (PGUs). PGUs respond in a similar manner at a process level and as such produce similar waters and as such respond in a similar way to a broadly equivalent land use pressure. The resulting map(s) depicts the inherent properties of the landscape that govern the natural variation in water quality and hydrochemical signatures in addition to land use.

Figure 2. 2: Summary of steps to develop the physiographic mapping method (Rissmann et al. 2018a).

Step 1: Hypothesise and Test

Firstly, hypotheses as to the likely landscape attributes governing spatial variation in a particular process signal are formulated (Step 1a). Hypotheses may be informed by international peer review literature, prior technical reporting and/or a working knowledge of a catchment, or regional scale landscape controls over variation in water composition. For example, in addition to land use intensity the dissolved oxygen (DO) and nitrate (NO_3^-) concentration in surface waters are expected to vary according to the landscape attributes soil drainage class and the abundance of electron donors (mainly organic carbon) in soil and shallow aquifers (Rissmann, 2011; Beyer et al., 2016; Beyer and Rissmann, 2016).

Using the above example, the hypothesis is then tested by interrogating the relationship between field measures of DO and NO_3^- and soil drainage class, soil carbon content and the likely electron donor abundance of the shallow aquifer associated with a given surface and/or groundwater monitoring site and associated capture zone (Step 1b). The key question is whether in-stream or shallow groundwater process signals vary in the hypothesised manner within and between capture zones. Various hydrochemical, graphical and multivariate methods are used during this phase (Rissmann et al., 2016; 2018). Pre-existing geospatial layers (e.g. Digital Elevation Model (DEM), soil, geological) are used as the source of landscape attribute data.

During the hypothesis testing stage, a spatial disconnect between process signals and a key landscape attribute suggests decoupling of the hypothesised process-attribute relationship. For example, across a significant area of Southland a disconnect was observed between soils mapped as poorly drained (reducing) and the occurrence of elevated nitrate (>8.0 mg/L NO_3^-N) in shallow groundwaters beneath these soils (see Central Plains Physiographic Zone after Hughes et al., 2016). Elsewhere, aquifers underlying poorly drained soils showed little sign of anomalous NO_3^-, indicating considerable removal within the soil zone by reduction (Beyer et al., 2016). Further investigation into the nature of this anomaly indicated that these soils crack in response to soil moisture deficit, with autumn recharge of high NO_3^- waters bypassing the reducing soil zone and rapidly recharging the underlying strongly oxidising aquifer (Rissmann et al., 2016; Hughes et al., 2016). Accordingly, where the correlation between a given process signal and geospatial representations of landscape attributes are anomalous, further investigation as to the character of the attributes within an area may be necessary.

Step 2: Extract Landscape Attributes, Map and Classify

Once the hypotheses have been tested and subsequently refined to incorporate any anomalous signals, an unclassed process-attribute layer is produced by extracting the key landscape attributes that govern process signatures from pre-existing geospatial layers (Step 2a). For example, attribute data on soil chroma, redox segregations, organic carbon content and texture were extracted from pre-existing geospatial layers (e.g., NZLRI, regional soil layers, S-Map) and combined to produce an unclassified process-attribute layer that defines a soil zone reduction potential gradient for Southland (Killick et al., 2015; Beyer et al., 2016; Rissmann et al. in prep.). Similarly, data on the abundance of electron donors (i.e., organic carbon, glauconite and iron sulphides) associated with shallow aquifers were extracted and mapped from pre-existing geological (Q-Map (Turnbull & Allibone, 2003); Rock 2 in NZLRI (Lynn et al., 2009)) and petrochemical (Petlab; Strong et al., 2016)) datasets (Rissmann, 2011). Critically, the method utilises the smallest scale polygons associated with soil series mapping as the basis for delineating process-attribute gradients. At this stage, additional information provided by regional or catchment scale surveys of attribute properties are incorporated (e.g. finer scale soil mapping, LiDAR, radiometric imagery (see Rissmann et al., 2017)).

Following the mapping of each process-attribute gradient, water signals are used to classify the attribute gradient into key classes that are associated with relatively homogenous process signals in water (Step 2b; Rissmann et al., 2016). The number of classes is finite and often correlated with the number of distinctly different attributes that make up an attribute gradient. For example, pH and alkalinity in Southland shallow groundwater were observed to vary strongly between six key rock/sediment classes, decreasing across the carbonate > ultra-mafic > mafic > intermediate > felsic > and carbonaceous continuum (Rissmann et al., 2018). Shallow aquifers associated with each of these rock/sediment categories showed statistically significant differences in pH and alkalinity as well as major ion abundances. The role of different rock, sediment and soil attributes over pH and alkalinity is well established in the international peer-reviewed literature and has been used by many authors to spatially map the likely impact of acid rain over the pH and alkalinity of aquatic ecosystems across North America and Europe (Wright, 1988; Giller & Malmqvist, 2004; Lydersen et al., 2004). In another example, mapping of soil drainage class has historically been informed by soil redox indicators, soil colour (chroma) and the abundance of redox segregations (mottles) (Lynn et al., 2009). It is perhaps not surprising, therefore, that the redox signatures in soil drainage waters are also correlated with soil drainage class (Beyer et al., 2016; Beyer and Rissmann, 2016; Rissmann et al., 2018). Many other such relationships exist and can be used to estimate the likely process signals in water and the number of classes within a region.

Therefore, although there is an obvious benefit in having a significant water sampling dataset it is not essential, as much can be inferred from knowledge of how landscape attributes influence different process signals in water. Mapping of 'likely' process-attribute classes can be used for targeted water quality sampling, minimising the number of samples that are required for validation. Further, as the approach is looking at process signals, not trend, historical water quality data is a valuable source of process signal information for the initial evaluation of process-attribute gradients and likely classes (see Rissmann et al., 2016).

Step 3: Test Performance

As the spatial variation of most water quality and hydrochemical measures is controlled by more than one process, the combination of classed process-attribute layers is necessary in order to best estimate spatial variation in water quality and/or hydrochemical measures (Rissmann et al., 2016; Snelder, 2016). For example, the concentration of NO_3^- in a stream may be controlled by both the overall redox setting in a capture zone and the degree of hydrological connection to low NO_3^- waters sourced from reducing parts of a catchment or a hydrologically connected recharge domain with naturally low NO_3^- (i.e. Alpine recharge domain).

Selection of the process-attribute layers to be combined will depend on the objectives of the study and the processes considered to exert the greatest control over spatial variability. For example, if understanding and estimating the spatial variation in nitrogen (N) and phosphorous (P) is the key objective, then the hydrological and redox process-attribute gradients should be combined. If the objective is to better understand and estimate spatial variation in the process level controls over water source and recharge mechanism, then the atmospheric and hydrological attribute-process layers should be combined. If the purpose is to better understand and estimate spatial variation in the process level controls over the major ion concentration, pH and alkalinity of water, then the atmospheric, hydrological, and weathering process-attribute layers should be combined. Finally, if the objective is to better understand and estimate both water quality and hydrochemical variation, then all four process attribute layers should be combined.

For the regional 'Physiographics of Southland' project, all four-classed process-attribute layers representing each key process family were combined, and both a simple hierarchal sorting (Rissmann et al., 2016) and a more sophisticated machine learning approach (Random Forest (RF) (Snelder, 2016) were applied. The two key questions formulated for testing were: (i) can the process-attribute classes within the capture zone of a monitoring point independently estimate spatial variation in water quality and hydrochemistry for surface and shallow groundwaters? and; (ii) do water quality and hydrochemical measures change in a manner consistent with the process level understanding used to develop the layers?

In the RF models of Snelder (2016), the classed process-attribute layers representing each key process family were used as predictor variables and the water quality and hydrochemistry as response variables. Snelder (2016) found the mapping accurately estimated spatial variation in surface water quality and hydrochemistry for most key measures. Further, the response characteristics evident in partial response plots derived from the RF modelling were consistent with the underlying process level understanding used to develop each layer. The performance of the physiographic approach to estimate groundwater signatures from bores across the region was less accurate (Snelder, 2016). However, mapping still readily identified and constrained all previously recognised groundwater NO_3^- and P hotspots, and correctly estimated water source and aquifer redox status (Rissmann et al., 2012; Rissmann, 2012; Rissmann et al., 2016). Furthermore, the strong performance for surface water suggested the approach could be used to accurately estimate the shallow groundwater contribution most relevant to the surface water network. This interpretation is consistent with the established knowledge that the zone of water table fluctuation is often the key driver of the young groundwater exported to streams (Molenat et al., 2008; Inamdar, 2011). This issue occurs as groundwater wells are drilled for the security of supply, not for targeting the shallow aquifer component most critical to stream. Accordingly, regional groundwater datasets may vary as to their representativeness, with well depth and the degree of confinement critical considerations.

For the ‘Physiographics of Southland’ project, estimation of the spatial variability in surface water sediment and *E. coli* was not as well constrained, although variation in these measures between monitoring sites with significantly different assemblages of process-attribute classes were statistically significant and as hypothesised (Hughes et al., 2016). In the Waituna case study provided here, additional effort was made to improve the spatial mapping of the landscape controls governing variation in steady-state sediment and *E. coli* measures, with some significant improvements (Rissmann et al., 2018). This was accomplished by mapping landscape gradients in percentage excess rainfall occurring as overland flow and artificial drainage density (Pearson, 2015a and b). These attributes were not initially included in the science component of the regional scale project. At regional scales, greater variability in the landscape attributes governing sediment loss to streams necessitates that additional attributes be considered (e.g. rock strength) (Rissmann et al., 2017).

The strong performance of the physiographic method to estimate spatial variation in water composition suggests the scale of geospatial layers used are appropriate. However, it is noted that most surface water monitoring networks are biased towards larger order streams and that some geospatial layers have limited resolution for drainage basins <8 km^2 (Rissmann et al., 2017). At this level of resolution, additional fine-scale geospatial data may be required to improve mapping of process-attribute gradients, such as radiometric imagery (Rissmann et al., 2017).

Finally, if the process-attribute mapping can be used to accurately estimate water quality and/or hydrochemical composition across monitoring sites, then it is assumed that it can be used for areas without monitoring data given similar land use intensities. This assumption is based upon the recognition that process-attribute gradients are just as relevant for areas without water quality data (as noted in Step 2).

Step 4: Produce Physiographic Map(s)

Following testing, process-attribute layers are combined to produce a “Physiographic Map”. Areas with the same assemblage of attribute-process classes are identified as Physiographic Units (PGUs). Combining classed process-attribute layers to produce PGUs, essentially self-classifies at the process level, the landscape attributes that govern variation in shallow ground and surface water quality and/or hydrochemistry. Relevant here is that PGUs respond in a similar manner at the process level and as such also respond in a similar manner to a broadly equivalent land use pressure.

As with Step 3 above, the Physiographic Map that is produced will depend on the objectives of the study. If traditional water quality contaminants are the key focus, then the process-attribute layers representing the hydrological and redox process layers are combined and areas that share the same characteristics are identified. A more complex Physiographic Map is produced when all four process-attribute layers are combined. For the Southland region, *c.* 30 PGUs were identified based on the combination of regional hydrological and redox process-attribute layers. Several hundred (*c.* 300) PGUs were produced when all four process-attribute layers were combined. Ultimately, the number of PGUs is finite and dependent upon the inherent complexity of the landscape within a given catchment or region.

An example of an important PGU, within the intensively farmed lowland area of Southland, is that characterised by well-drained soils overlying oxidised aquifers that are recharged exclusively by local precipitation - with no flushing by alpine or hill country derived waters. This PGU is commonly associated with elevated groundwater NO_3^- concentrations and contributes NO_3^- rich waters to local streams as baseflow (Hughes et al., 2016). Another PGU that is also recharged exclusively by local precipitation is characterised by well-drained soils that overly reducing aquifers. Nitrate leaching from these soils is rapidly removed in the underlying aquifer with little deleterious impact on hydrologically connected groundwater or surface water bodies (Hughes et al., 2016). Another important PGU is associated with well-drained gravel soils overlying strongly oxidising aquifers that are recharged by Alpine derived waters (Hughes et al., 2016). In this PGU, high NO_3^- concentrations in soil drainage water that reach the underlying aquifer are diluted to low levels by large volumes of low NO_3^- waters. More examples of Southland PGUs are presented in Hughes et al., 2016 and Rissmann et al., 2018.

In addition to accurately estimating spatial variation in water quality, the physiographic method has the advantage of being able to explain, at the process level, ‘how’ and ‘why’ water quality and composition vary despite similar levels of land use intensity (Hughes et al., 2016; Rissmann et al., 2016; Snelder et al., 2016). As such, the method adds value by providing the underlying context to questions of state and trend and when communicating with stakeholders the likely reason for the variation in water quality outcomes between different catchments or farms (Hughes et al., 2016; Rissmann et al., 2018). For example, the question of *Why is* NO_3^- *increasing in this stream or aquifer but not in others?* For the same reasons, the physiographic mapping can be used to provide context to other useful tools and numerical models commonly used to estimate land use losses and catchment loads (i.e. OVERSEER Nutrient Budgets, CLUES, LUCI, SPASMO etc.).

In the following report, Steps 1 to 2a in the Physiographic Method are applied to the Northland Region for the development of a hydrological process attribute layer (H-PAL) and a redox process attribute layer (R-PAL).

3 Northland Environmental Setting

A qualitative assessment of the relationships between nationally available soil, geological, elevation, and hydrological geospatial layers with radiometric survey imagery collected in the Northland region was provided by Rissmann et al., (2017). To avoid repetition, this report includes a summary of key environmental setting information only, and the reader is referred to Rissmann et al. (2017) and other resources referred to in the following text for more detailed information.

3.1 Climate and Hydrology

Rainfall is abundant throughout the Northland region and ranges from a mean annual average of 1,000 mm in coastal areas to 2,000 mm at higher elevations (Chappell, 2013). High-intensity rainfall events (e.g., 47 mm/hr) associated with the passage of tropical or subtropical storms can lead to flooding (Chappell, 2013). An extensive network of rivers and streams exists across the 13,000 km^2 region, with over 1,400 individual source-to-sea catchments. Due to the narrow landmass, most rivers in the region are short (<30 km) and have small catchments. Major rivers flow into harbours or estuarine environments, rather than directly to the open ocean (Northland Regional Council, 2011; Ballinger et al., 2014). The largest river in Northland is the Northern Wairoa (near Dargaville), with a catchment area of 3,650 km^2, 7 main tributaries, and is tidally influenced for about 100km.

Sediment is a key pollutant of surface water in the region and is easily mobilised during high-intensity rainfall events which result in rapid overland flow. Overland flow mobilises the highest particulate contaminant load (McKegrow et al., 2007; McDowell, 2008; Monaghan et al., 2010). Almost all monitored rivers in Northland, including those that flow through land with mostly native forest cover, have turbidity and microbial (E. coli) levels worse than the national median (McDowell et al., 2013; Ballinger et al., 2014). Phosphorus, as dissolved reactive phosphorus (DRP) and total phosphorus (TP), are also elevated.

3.2 Geology

Northland is one of New Zealand's oldest geomorphic regions, with no recent (Quaternary) glacial activity, and few regionally significant volcanic ash deposits since the middle of the Miocene (c. 14 Ma ago). The relatively stable nature of the Northland region reflects both the climatic but also the tectonic (faults & uplift) and eruptive (volcanic & intrusive) setting (Isaac, 1996; Edbrooke and Brook, 2009). Specifically, sedimentary succession is characterised by the Permian-aged (299 – 252 Ma ago) Waipapa-Composite and Caples terranes (greywacke-argillite/chert/melange) to Quaternary-aged beach sands, with pulses of local intraplate volcanism that include the regionally extensive basalts of the Tangihua Complex, Waipoua Basalts and Kerikeri Volcanic Group. Rock strength and degree of induration, primary texture and provenance are key controls over sediment yields, soil hydrological properties and biogeochemical properties of both soil and aquifers, respectively. Accordingly, recognition of geological gradients provides critical constraint over the variation in water quality outcomes for surface water, shallow groundwater and near coastal environments.

3.3 Hydrogeology

Groundwater in the Northland Region predominantly occurs in four main aquifer types including Jurassic greywacke, Cretaceous sandstone, Cenozoic basalt, and Quaternary sediment (sand, shell, and/or gravel) (Cameron et al., 2001; NRC, 2018). Jurassic greywacke aquifers are at greatest depth and are generally the least productive aquifer systems, although large areas of mudstone associated with the Northland Allochthon are known to host poorly productive aquifers that are locally important sources of streamflow (pers. comm. S. Osbaldiston, May 2018). Basalt from local volcanic activity has intruded into or overlies the sandstone, and forms aquifer systems which are often semi-confined. There are numerous Quaternary sedimentary aquifers which are generally small, shallow, and located in coastal regions, for which confinement varies with depth. Aquifers are predominantly recharged through rainfall, mainly during winter when lowest evapotranspiration occurs (Cameron et al., 2001). Surface water recharge is known to occur through lake beds in some local areas (e.g., Pakaraka, Aupouri), however, there is little knowledge of river recharge in the region.

The water quality of groundwater is variable throughout Northland due to geological composition of each aquifer system. For example, the Aupouri aquifer has higher sodium and chloride concentrations in comparison to inland basalt aquifers, primarily due to leaching of marine materials and the proximity to the coast. In 2001, nitrate-nitrogen (NO_3-N) concentrations were below the New Zealand Drinking Water guidelines (11.3 mg/L) for all monitored sites. NO_3 concentration in groundwater is elevated (3 - 6 mg/L, NO_3-N) in a few small areas, where well-drained volcanic soils overlay fractured rock. In these areas, land surface recharge (winter rainfall) drives water movement and recharge of underlying aquifers. Elsewhere, due to poorly drained soils and/or reducing aquifers, nitrate concentrations are thought to be low (Cameron et al. 2001). Phosphorus concentrations in groundwater are considered elevated in aquifers and stream baseflow in places, perhaps due to both a combination of anthropogenic and naturally elevated concentrations in aquifer materials (Unpublished data NRC, 2017; see also Rissmann and Lovett, 2016).

3.4 Soils

The soils of Northland are predominantly Ultic according to the New Zealand Soil Classification (NZSC). Ultic soils are strongly weathered and contain well-structured clay-enriched horizons in the subsoil. Other NZSC orders present include Brown soils (typically silt loams) on younger sedimentary land surfaces; Granular soils, a clay soil formed by the strong weathering of volcanic rocks; Podzol soils that are high in organic matter and are strongly acid beneath the topsoil; Gley soils form in response to prolonged periods of soil saturation; Recent and Raw soils are weakly developed to minimally developed. In Northland, Recent and Raw soils are typically associated with recent beach sands and young alluvial floodplains.

Soil Order can be limiting when attempting to understand the relationship between gradients in landscape attributes such as slope, geology and geomorphic setting and attendant gradients in a soil's physical and chemical properties (Rissmann et al., 2016, TC2, TC3 and TC6). A recent project to refine the understanding of the landscape controls over soil properties that are relevant to water quality outcomes was undertaken for the Northland Region (Rissmann et al., 2017).

Soil texture, permeability, depth to slowly permeable layers, carbon content, and drainage class are the critical attributes determining the pathway water takes across the landscape and the strength of soil zone reduction, respectively (Rissmann et al. 2016a and b). Areas characterised by slow permeability (<4 mm/hr) are more prone to overland flow than soils with high permeability. Areas of well-drained soils with moderate to high infiltration rates favour deep drainage. The proportion of slowly permeable soils in Northland is 56%, the majority of which occur in lowland areas. The proportion of well-drained soils is small (18.7 %), with most of the soils classified as poorly drained (35.7 %) or moderately well (45.6 %) drained. Poorly drained soils are often strongly reducing and therefore have higher denitrification rates than well-drained soils, however, poorly drained soils have a greater tendency to leach phosphorus (P) and are also more prone to overland flow (McDowell et al., 2003).

Soil structure, texture and mineral composition are important attributes governing the evolution of macro-pore (bypass) networks, which are critical pathways for water and hence contaminant transport (Rissmann et al., 2016a and b; Beyer et al., 2016). Although there are a range of soil-related features that may facilitate bypass, we consider the largest and most integrated structures (e.g. soil cracks due to the desiccation of clays and/or pedogenic features) the most important in terms of water quality outcomes (Rissmann et al., 2016b). Specifically, those soils with large and well-integrated macropore structures favour the bypass of the soil matrix and in our experience, are associated with poor water quality outcomes for nitrogen (N), microbes (i.e. E. coli, (M)), and at times phosphorus (P) (Rissmann et al., 2016a).

Across Northland, 68 % of soils are characterised as clay-rich (argillic) and may crack during the summer in response to soil moisture deficit. Consultation with local soil experts can be used to identify soils with large macropore structures that may be associated with contaminant bypass.

Typically, soils that exhibit shrink-swell characteristics tend to be clay-rich and/or are characterised by large and highly conductive pedogenic structures (e.g., massive columnar peds in some areas of 'gumland soils') in contrast to the overall soil matrix. These large macropore networks provide a preferred pathway for water and contaminant transport and influence redox gradients by directly coupling shallow soil and groundwater to the atmosphere (Dif and Bluemel, 1991; Day, 1994; Guney et al. 2007; Beyer et al., 2016a).

The microbial load, free and sorbed N and P, organic carbon (C), and associated carbon to nitrogen (C:N) and carbon to phosphorus (C:P) ratios are important indicators of sediment quality. Developed soils have a higher potential microbial (M), N and P load along with organic carbon characterised by smaller C:N and C:P ratios relative to areas of indigenous land cover with undeveloped/natural state soils. The contaminant content associated with 1 kg of agriculturally derived sediment, therefore, can be large relative to 1 kg of sediment derived from a natural state setting (Cooper and Thomsen, 1988). Recognition of this difference in sediment quality is very important in terms of internal eutrophication of rivers, lakes, lagoons and estuaries.

Soil P-retention or anion exchange varies with soil age and parent material. According to the New Zealand Land Resource Inventory (NZLRI), 19% of Northland mapped soils are characterised by high P-retention (mostly associated with younger volcanic landforms) and 48% by low P-retention, with the rest having moderate P-retention. The ability of soils to sorb P has implications for P leaching, the P-content of sediment lost via farm drainage and/or the P content of stream banks that are eroded during peak flow events.

4 Input data

4.1 Geospatial

Geospatial data was sourced from a number of regional and national datasets. The input geospatial data is summarised in Table 4.1.

Capture zones for the surface water monitoring sites were generated in ArcGIS from the River Environment Classification (REC1) using the easting and northing points provided by Northland Regional Council. These surface water capture zones are used to compare the hydrochemistry data with proportionally weighted landscape attributes in the development of the hydrological and redox layers.

Table 4. 1: Geospatial information used for physiographic classification of the Northland Region.

Data	Reference Layer	Resolution	Used for
Elevation	8m Digital Elevation Model (DEM)	8 m (±0.2 m)	Hydrological domain, slope
Land Cover	Land Cover Database (LCDB v4.1)	1:50,000	Identification of potential agricultural areas, a proxy for land use in hydrological flow pathways and redox interpretation
Climate and Hydrology	Temperature and Rainfall (Chappell, 2013)	25 m processed grid	Hydrological domain
	Isoscape (isotope) map (Baisdan et al. 2016)	4 km processed grid	Hydrological domain
	River Environment Classification (REC 1)	Various	Generation of capture zones from monitoring points using an upstream accumulation of the riverline tool
	Northland SOE SW quality sites + capture zones	(LAWA resolution poor – requires generation from 8 m DEM)	Identify proportion of land area contributing to the monitoring point.
Soils and Geology	Fundamental Soil Layer (FSL)	1:50;000 (from 1:63,360)	H-PAL flow pathways, R-PAL soil reduction potential
	NZ Land Resource Inventory (NZLRI) (Landcare Research, DSIR)	1:63,360	H-PAL domain classification
	Q-map (quarter million geological map)	1:250,000	Hydrological Domain, Geological reduction potential
	Radiometric (NZP&M)	50 m^2	Selection of attributes for H-PAL and R-PAL classification. Can be used to refine soil and geological polygon extent
Hydrogeology	New Zealand Aquifer Potential Map Version 1.0, based on Q-map (Tschritter et al., 2017)	1:250,000	H-PAL domain classification

4.2 Surface water data

Northland Regional Council provided all surface water quality and compositional data collected between 2010 – May 2018 period for 78 sites. Following removal of text from censored values the range and potential outliers of individual measures were evaluated using cumulative probability plots. Mean, median, minimum, maximum and coefficient of variation (C.V) were calculated for each site reducing the data set from 5,411 individual measures to a single measure for each site. Counts of repeat measures were also generated to inform the selection of analytes/measures for multivariate analysis. For those sites with the relevant data, redox category and Terminal Electron Accepting Process (TEAP) were assigned using the Redox Assignment Workbook of Jürgen et al.

(2009) (see section 5.1). The sites with water quality and/or physiographic dataset are shown in Figure 4.1, and site name, location, and available water quality data in Table 4.2.

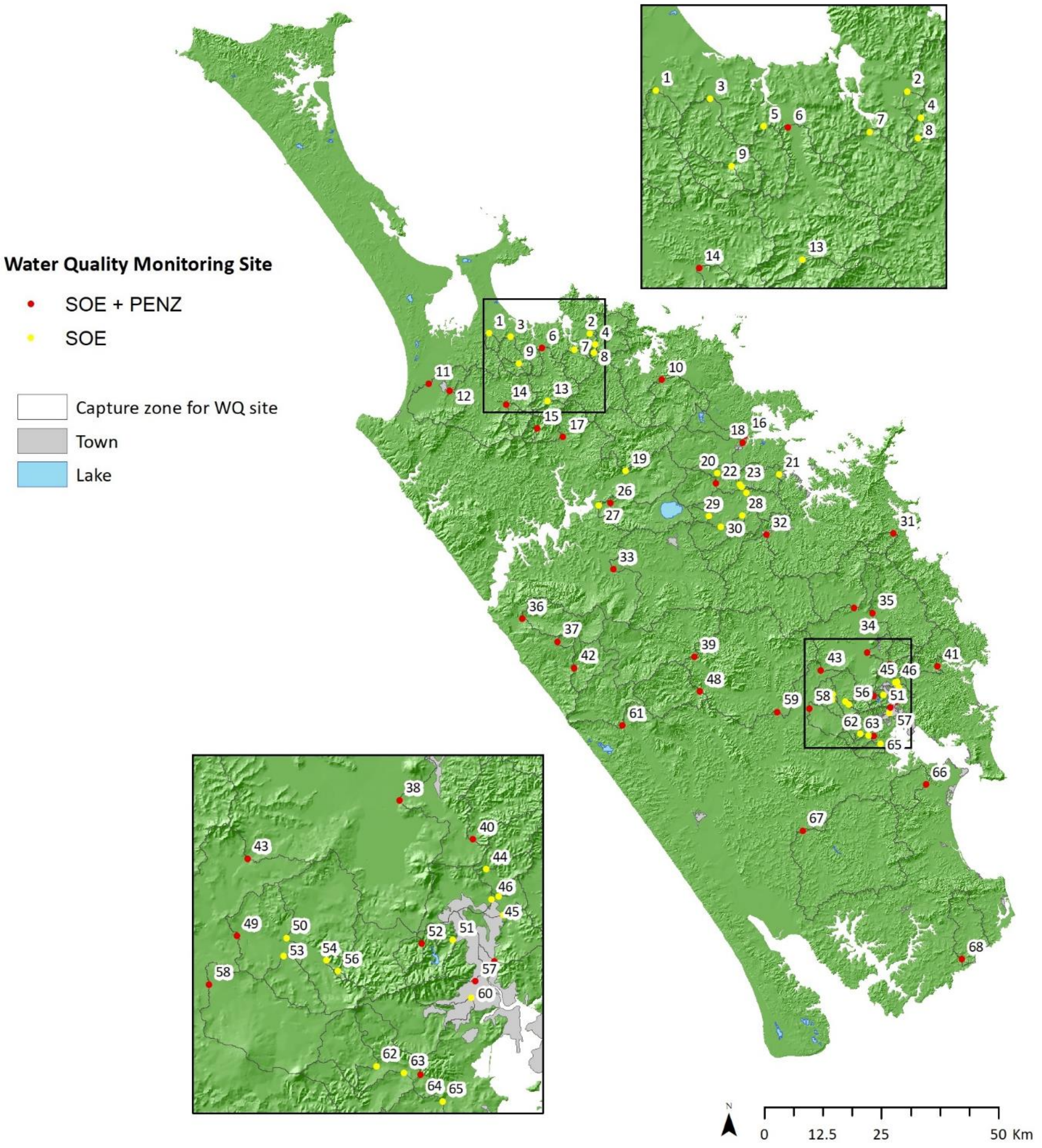

Figure 4. 1: Northland surface water quality monitoring sites and associated capture zones. Sites with State of Environment (SOE) data and PENZ test set are shown in red and sites with SOE data only are shown in yellow (See Table 5.1 for site names).

Table 4. 2: Surface water quality site reference. PENZ indicates where the extended suite of analytes for hydrologically conservative and redox sensitive species were measured, and SOE where standard water quality measures were available.

Site #	Site	Easting	Northing	Hydrochemistry Data
1	Aurere at Pekerau Road	1633459	6125735	SOE
2	Oruaiti at Windust Road	1654906	6125632	SOE
3	Parapara at Taumata Road	1638075	6125035	SOE
4	Stony at Sawyer Road	1656071	6123396	SOE
5	Paranui at Paranui Road	1642652	6122666	SOE
6	Oruru at Oruru Road	1644740	6122563	PENZ & SOE
7	Kenana at Kenana Road	1651704	6122183	SOE
8	Oruaiti at Sawyer Road	1655830	6121640	SOE
9	Parapara at Parapara Toatoa Road	1639905	6119265	SOE
10	Kaeo at Dip Road	1670326	6115833	PENZ & SOE
11	Awanui at Waihue Channel	1620713	6114952	PENZ & SOE
12	Awanui at FNDC take	1625095	6113439	PENZ & SOE
13	Peria at Honeymoon Valley Road	1645966	6111291	SOE
14	Victoria at Victoria Valley Road	1637132	6110554	PENZ & SOE
15	Tapapa at SH1	1643752	6105453	PENZ & SOE
16	Waipapa at Landing	1688150	6103986	PENZ & SOE
17	Mangamuka at Iwitaua Road	1649247	6103622	PENZ & SOE
18	Kerikeri at Stone Store	1687631	6102447	PENZ & SOE
19	Waipapa at Forest Ranger	1662582	6096421	SOE
20	Waipapa at Waimate North Road	1682092	6095939	SOE
21	Waitangi at Wakelins	1695269	6095708	SOE
22	Waitangi at Waimate North Road	1681894	6093741	PENZ & SOE
23	Waitangi at SH10	1686946	6093563	SOE
24	Waiaruhe at Puketona	1687317	6093001	SOE
25	Mania at SH10	1688381	6091736	SOE
26	Utakura at Okaka Road	1659391	6089567	PENZ & SOE
27	Utakura at Horeke Road	1656910	6089081	SOE
28	Watercress at SH1	1687416	6086899	SOE
29	Pekepeka at Ohaeawai	1680346	6086802	SOE
30	Waiaruhe D/S Mangamutu Confluence	1682873	6084561	SOE
31	Punaruku at Russell Road	1719724	6083074	PENZ & SOE
32	Waiharakeke at Stringers Road	1692604	6082806	PENZ & SOE
33	Punakitere at Taheke	1660001	6075453	PENZ & SOE
34	Waiotu at SH1	1711381	6067240	PENZ & SOE
35	Whakapara at Cableway	1715259	6066116	PENZ & SOE
36	Waimamaku at SH12	1640666	6064914	PENZ & SOE
37	Wairau at SH12	1648152	6060041	PENZ & SOE
38	Mangahahuru at Apotu Road Bridge	1714117	6057720	PENZ & SOE
39	Mangakahia at Twin Bridges	1677333	6056762	PENZ & SOE
40	Mangahahuru at Main Road	1718886	6055192	PENZ & SOE
41	Ngunguru at Coalhill Lane	1729072	6054775	PENZ & SOE
42	Waipoua at SH12	1651633	6054443	PENZ & SOE
43	Wairua at Purua	1704273	6053948	PENZ & SOE
44	Mangakino at Mangakino Lane	1719727	6053270	SOE

45	Mangakino U/S Waitaua Confluence	1720522	6051489	SOE
46	Waitaua at Vinegar Hill Road	1720066	6051317	SOE
47	Hatea at Whangarei Falls	1720857	6050300	SOE
48	Opouteke at Suspension Bridge	1678503	6049460	PENZ & SOE
49	Mangere at Knight Road	1703586	6048948	PENZ & SOE
50	Mangere at Kokopu Road	1706785	6048813	SOE
51	Waiarohia at Whau Valley	1717568	6048671	SOE
52	Pukenui at Kanehiana Drive	1715558	6048441	PENZ & SOE
53	Mangapiu at Kokopu Road	1706588	6047656	SOE
54	Mangere at Kara Road	1709388	6047363	SOE
55	Hatea at Mair Park	1720284	6047290	PENZ & SOE
56	Mangere at Wood Road	1710121	6046658	SOE
57	Waiarohia at Second Avenue	1719047	6046013	PENZ & SOE
58	Waipao at Draffin Road	1701772	6045796	PENZ & SOE
59	Mangakahia at Titoki	1694999	6045028	PENZ & SOE
60	Raumanga at Bernard Street	1718760	6044937	SOE
61	Kaihu at Gorge	1661946	6042161	PENZ & SOE
62	Otaika at Cemetery Road	1712613	6040509	SOE
63	Otakaranga at Otaika Valley Road	1714396	6040056	SOE
64	Otaika at Otaika Valley Raod	1715476	6039940	PENZ & SOE
65	Puwera at SH1	1716892	6038226	SOE
66	Ruakaka at Flyger Road	1726626	6029623	PENZ & SOE
67	Manganui at Mitaitai Road	1700359	6019751	PENZ & SOE
68	Hakaru at Topuni	1734330	5992416	PENZ & SOE

4.3 Groundwater data

Northland Regional Council provided all groundwater quality and compositional data collected between 2010 – May 2018 period for 50 groundwater monitoring sites across the region (Figure 4.2, Table 4.3). In addition to groundwater chemical data, NRC provided all attendant data on aquifer on bore depth, screen interval, static water level, aquifer confinement status and aquifer lithology. Following removal of text from censored values the range and potential outliers of individual measures were evaluated using cumulative probability plots. Mean, median, minimum, maximum and coefficient of variation (C.V) were calculated for each site reducing the data set from 2,179 individual measures to a single measure for each site. Counts of repeat measures for each analyte/metric were also generated to inform the selection of variables for multivariate analysis. For those sites with the relevant data redox category and Terminal Electron Accepting Process (TEAP) were assigned using the Redox Assignment Workbook of Jürgen et al. (2009) (see section 5.1).

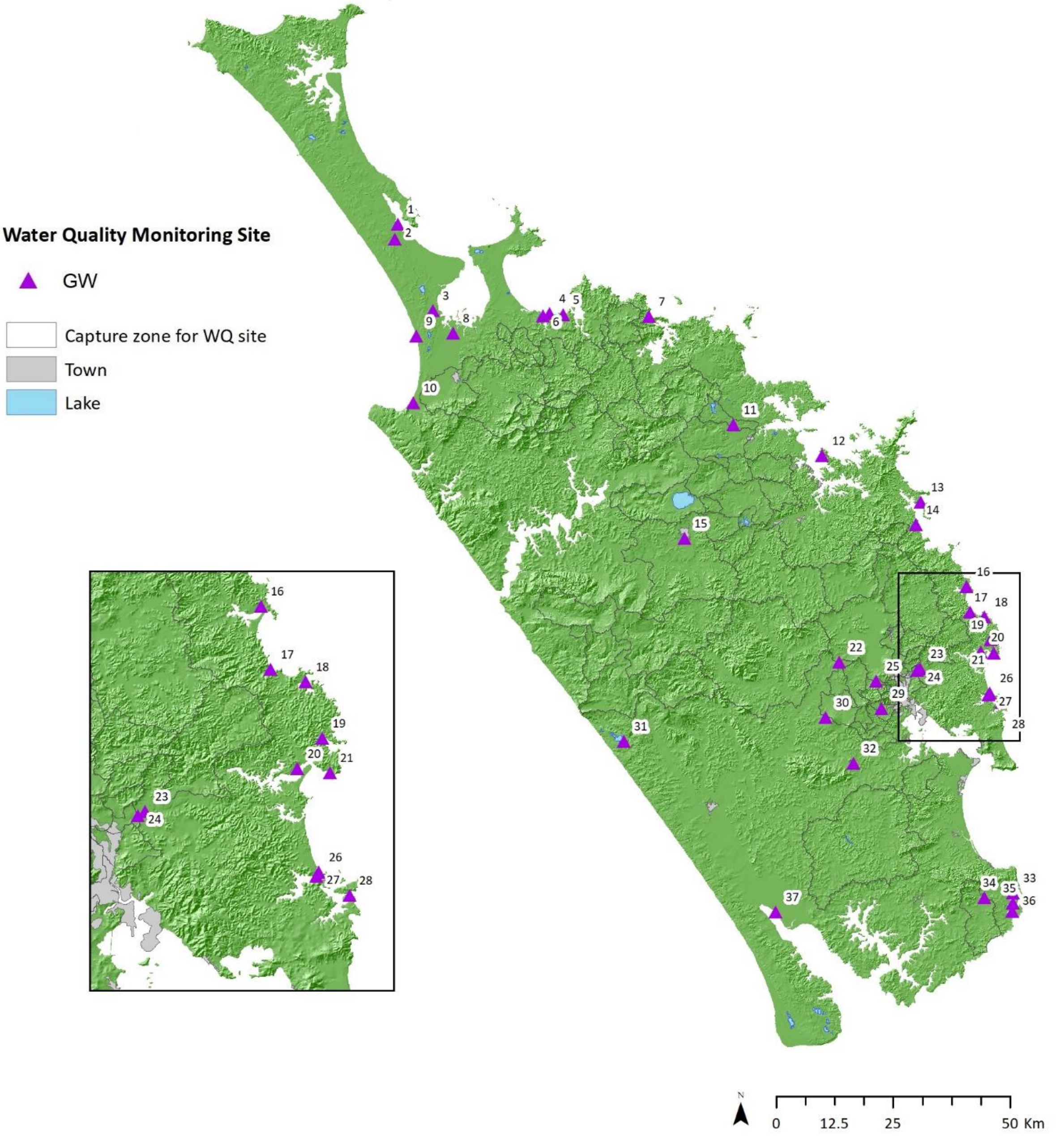

Figure 4. 2: Northland groundwater quality monitoring sites (purple) in relation to surface water capture zones (See Table 5.2 for site names).

Table 4. 3: Groundwater quality site reference.

Site #	Site Name	Easting	Northing
1	Aupouri Groundwater at Houhora BG Fish Club	1611411	6146928
2	Houhora GW at Hukatere Rd (Colville NGMP site)	1610823	6143757
3	Aupouri Groundwater at Far North Farms, Houhora (NGMP site)	1618858	6128533
4	Cable Bay Groundwater at Croquet Club by Stream	1643721	6127891
5	Coopers Beach Ground Water at Youth Camp	1646705	6127658
6	Taipa GW at Taipa High School	1642410	6127448
7	Taupo Bay GW at John Turner	1664972	6127237
8	Awanui GW at Vinac Farms	1623217	6123720
9	Waipapakauri GW at Waipapakauri landing	1615323	6123076
10	Aupouri Groundwater at Long Bore, Ahipara (NGMP site)	1614711	6108940
11	Waipapa GW at 10 Pungaere Rd (D Hop owner)	1682997	6104174
12	Russell GW at 47 The Strand (Dr Jack Phillips)	1701965	6097521
13	GW Bland Bay at M/C Ngatiwai t/Board Camp new bore	1722997	6087720
14	Oakura GW at 3 Te Kapua Street (Patricia Wallis)	1722052	6082846
15	Kaikohe GW a 75 Thorpe Road (Strawbridge, NGMP site)	1672538	6079886
16	Whananaki North GW at WDC Toilets	1732755	6069588
17	Sandy Bay GW at WDC Toilets	1733607	6064226
18	Matapouri Groundwater at Smith P/S Beside Road	1736585	6063147
19	Tutukaka Groundwater at Cnr Matapouri Rd (NGMP site)	1738030	6058312
20	Ngunguru Groundwater at Thompson P/S	1735867	6055687
21	WDC toilet at Whangaumu Bay	1738679	6055379
22	Matarau GW at Osbaldiston Bore	1705599	6053505
23	Glenbervie GW at Barron's Property, Ngunguru Road	1722873	6052070
24	Glenbervie GW at Green's Bore (NGMP site)	1722245	6051689
25	Three Mile Bush GW at Wise Bore	1713490	6049494
26	Pataua North GW at WDC Toilets	1737702	6046865
27	Pataua South GW at Pataua public toilets	1737504	6046493
28	Taiharuru GW at WDC Toilets	1740332	6044876
29	Whangarei GW at Foster Irrigation Bore	1714633	6043629
30	Whatitiri GW at Tanekaha Partnership Irrigation Bore	1702715	6041675
31	GW Kai Iwi at Kai Iwi bore BH 8	1659694	6036653
32	Tauraroa GW at 88 Maungakaramea Road (Finlayson)	1708601	6031916
33	Managawhai GW at Mangawhai Golf Club (SOE Bore)	1742717	6004312
34	Tara GW at 551 Tara Road (Eran Orchards Ltd)	1736532	6003241
35	Mangawhai GW at Mangawhai Hideaway Camp bore	1742689	6002057
36	Mangawhai GW at Caravan Pk Bore Garden tap	1742621	6000376
37	Ruawai GW at Kaipara D/C Bore 5	1691998	6000192

5 Water Composition and General Characteristics

5.1 Redox Assignment

For those sites with the relevant water chemistry data, redox category and Terminal Electron Accepting Process (TEAP) were assigned using the Redox Assignment Workbook of Jürgen et al. (2009). The default redox thresholds are based on several assumptions and the authors recommend evaluation of the local suitability of the default threshold values for assignment of redox category and Terminal Electron Accepting Process (TEAP). Specifically, the default thresholds were developed for continental aquifer systems of the United States and are best suited for deep and relatively old groundwater systems that have more fully equilibrated with the aquifer system. To revise the default threshold relationships for Northland we use the raw groundwater dataset to plot cumulative probability graphs as they are a useful tool for differentiating different populations in geochemical data (Panno et al., 2006; Reimann and Garrett, 2005).

In a cumulative probability plot, significant inflections in the data indicate distinct populations. The cumulative probability plot of groundwater DO shows 4 key inflection points and 5 distinct populations in the data (Figure 5.1). By using oxidising surface waters (those with the lowest Mn^{II} and Fe^{II} and highest DO) as the initial DO (i.e. ≥10 mg/L) concentration starting point, we note a successive decline in DO concentration. Specifically, Population V is the most oxidising GW population with an inflection at c. 8 mg/L associated with a progressive decline in DO towards a 5 mg/L inflection point. Population IV waters have a median DO of 6.1 mg/L, indicating c. 4 mg/L of DO removal either within the soil zone or shallow aquifer.

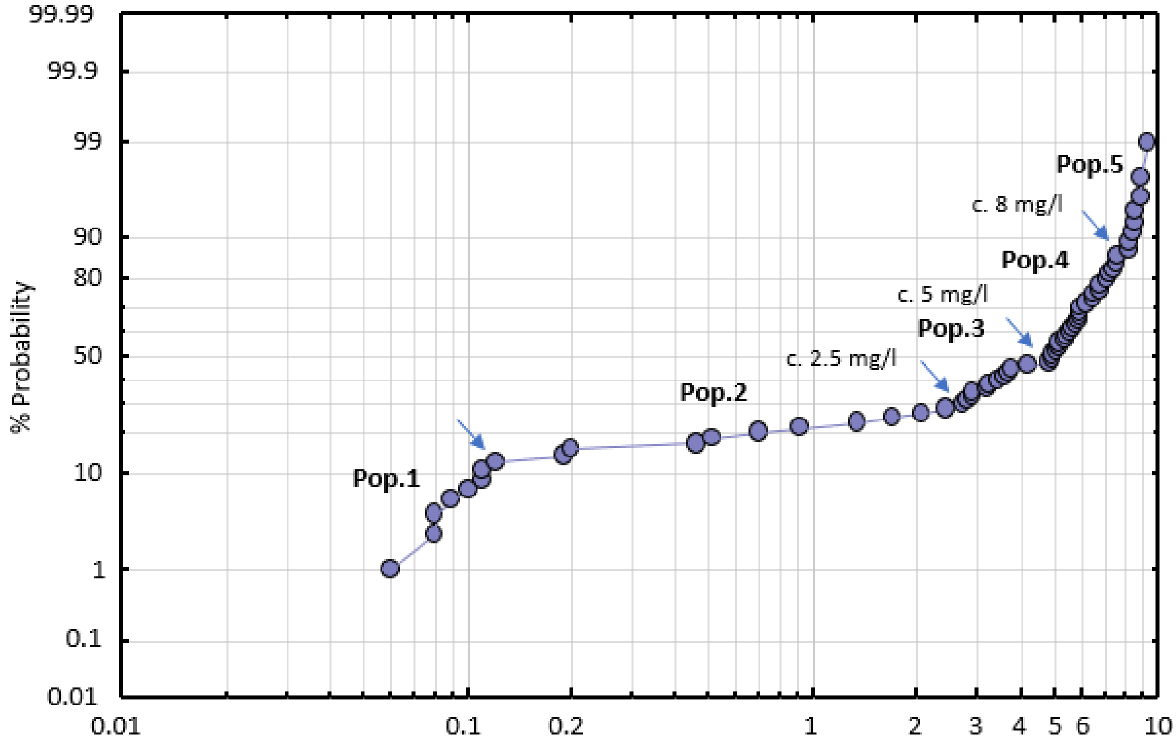

Figure 5.1. Cumulative probability plot of Dissolved Oxygen (DO, mg/L) for Northland groundwater. Four key inflection points (arrows) and five (V) DO populations are identified. Individual sample values, not site medians are used. DO measures are infrequent relative to NNN, dissolved Mn and Fe.

Nitrate, nitrite nitrogen (NNN) concentrations exhibit seven key populations (Figure 5.2). Above a concentration of 2.5 mg/L, median DO is at a maximum and dissolved Mn and Fe are at their lowest indicating more oxidising conditions.

Dissolved Mn shows three key inflection points with concentrations below 0.005 mg/L associated with the highest median NNN and lowest dissolved Fe concentrations (Figure 5.3). For concentrations >0.005, mg/L dissolved Fe concentrations increase and NNN concentrations decline.

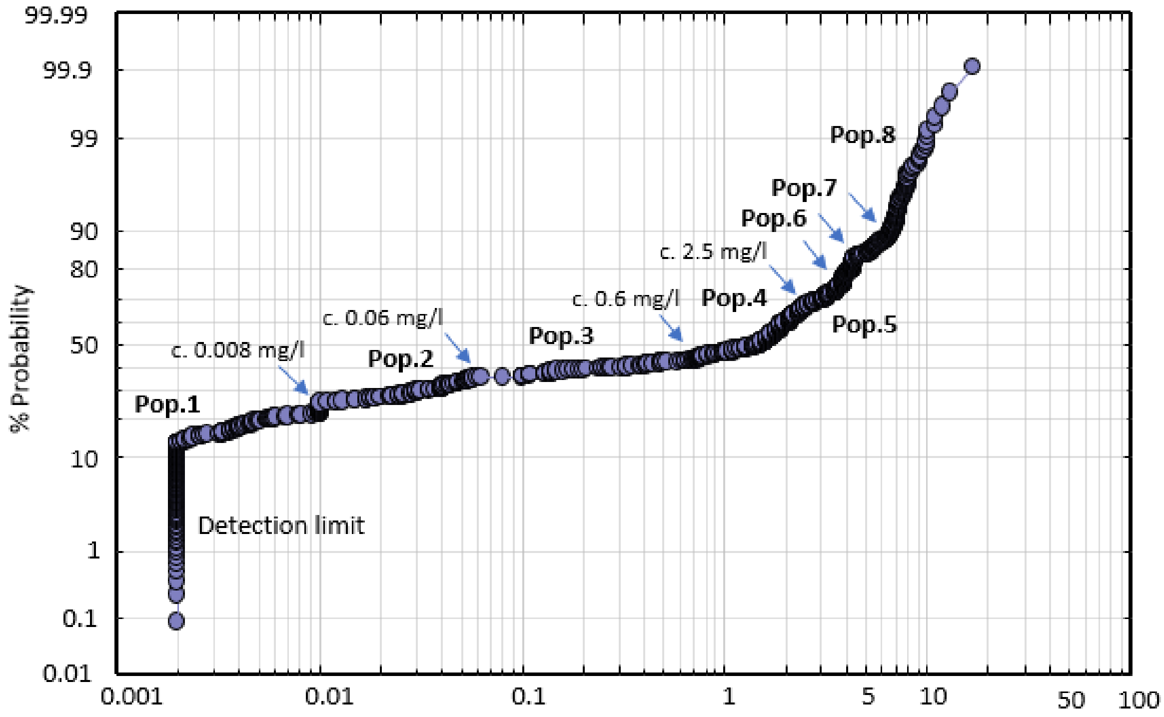

Figure 5. 2. Cumulative probability plot of NNN in mg/L for Northland groundwater. Seven key inflection points (arrows) and eight (VIII) NNN^{I} populations are identified. Individual site sample values, not site medians used.

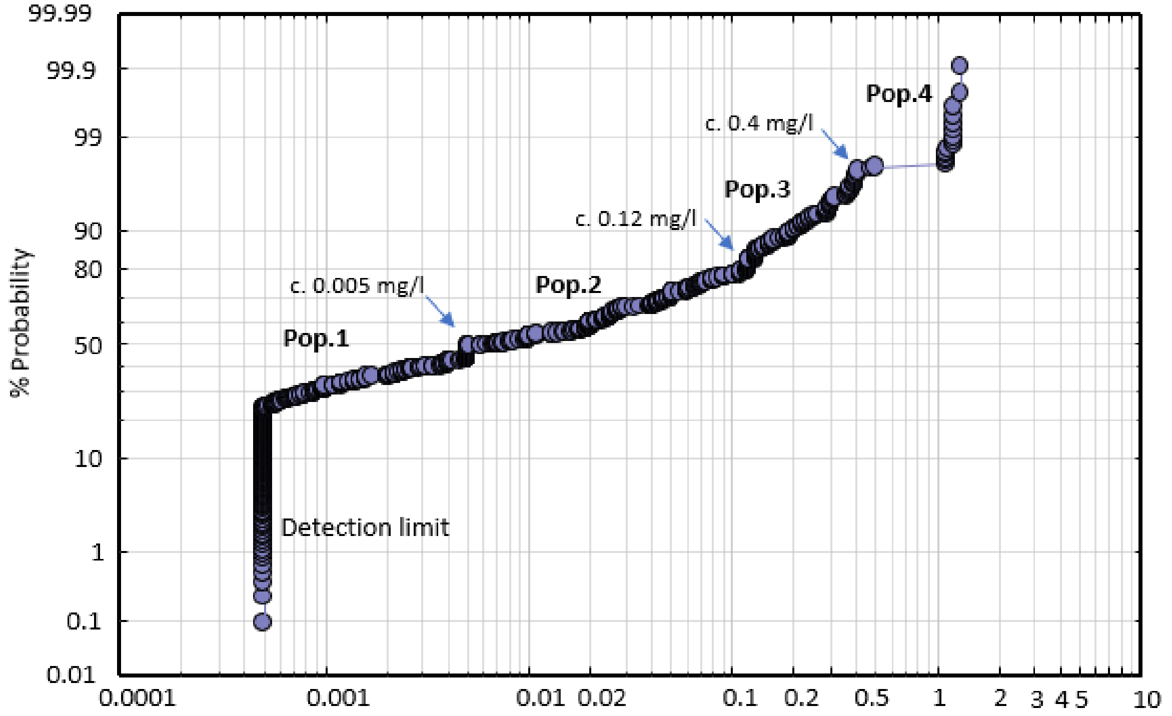

Figure 5. 3. Cumulative probability plot of dissolved Mn(II) in mg/L for Northland groundwater. Three key inflection points (arrows) and four (IV) Mn^{II} populations are identified. Individual site sample values, not site medians used.

Dissolved Fe concentrations also show 5 populations with key inflection points at 0.003 and 0.02 mg/L (Figure 5.4). Population III groundwaters have a median NNN of 0.005 mg/L. Population I and II have a combined median NNN concentration of 1.7 mg/L.

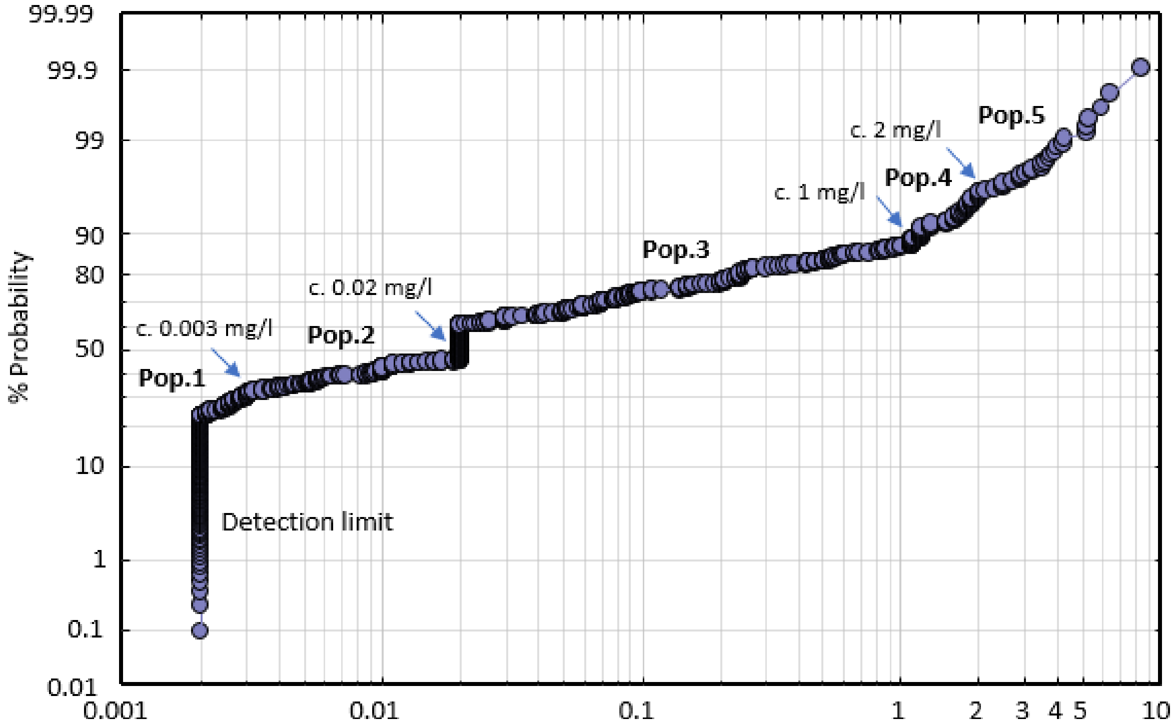

Figure 5. 4. Cumulative probability plot of dissolved iron (Fe^{II}) in mg/L for Northland groundwater. Four key inflection points (arrows) and five (V) Fe^{II} populations are identified. Individual site sample values, not site medians used.

On the basis of DO, NNN, Mn^{II} and Fe^{II} populations for Northland groundwaters, we replace the default threshold values within Redox Assignment Workbook of Jürgen et al. (2009) with 5, 2.5, 0.005 and 0.02 mg/L, respectively. The default value for SO_4 of 0.5 mg/L was not changed as it was consistent with local observations. Specifically, there is little evidence for SO_4-reduction in regional soils with only one groundwater site (i.e., Awanui GW at Vinac Farms) showing evidence for SO_4-reduction. The resulting redox assignment is designed to be more sensitive to regional conditions governing NNN and dissolved P concentrations and is applied to site median values for surface and groundwater datasets.

Based on water chemical composition and with a water quality focus, the new thresholds are considered more directly relevant to Northland's redox setting and associated water quality controls. Specifically, we propose that the TEAP is a more sensitive estimator of redox poise or buffering than general redox category. Overall, redox buffering with respects to nitrate increases across the $O_2 > NO_3 > Mn^{IV} > Fe^{III} > SO_4 > CO_2$ TEAP continuum. In other words, ground waters buffered at O_2 or NO_3 reduction are more susceptible to nitrate accumulation than waters buffered at Fe^{III}, SO_4 or CO_2 reduction. By revising the thresholds for Northland, prior to physiographic mapping, we attempt to ensure greater relevance to local conditions including greater sensitivity with regards to the role of nitrate removal under relatively weak reducing conditions. Redox assignments for surface waters are coarse and only able to discriminate between 'oxic' and 'mixed (oxic-anoxic)' redox categories. For a mixed redox category to be assigned dissolved Mn and Fe must be elevated above either the default or Northland specific thresholds[1]. Accordingly, absolute concentrations of redox sensitive species are considered a more sensitive indicator of redox succession in regional surface waters. The results of applying these regionally specific and nitrate centric thresholds are shown spatially in Figure 5.5 and in Table 5.3.

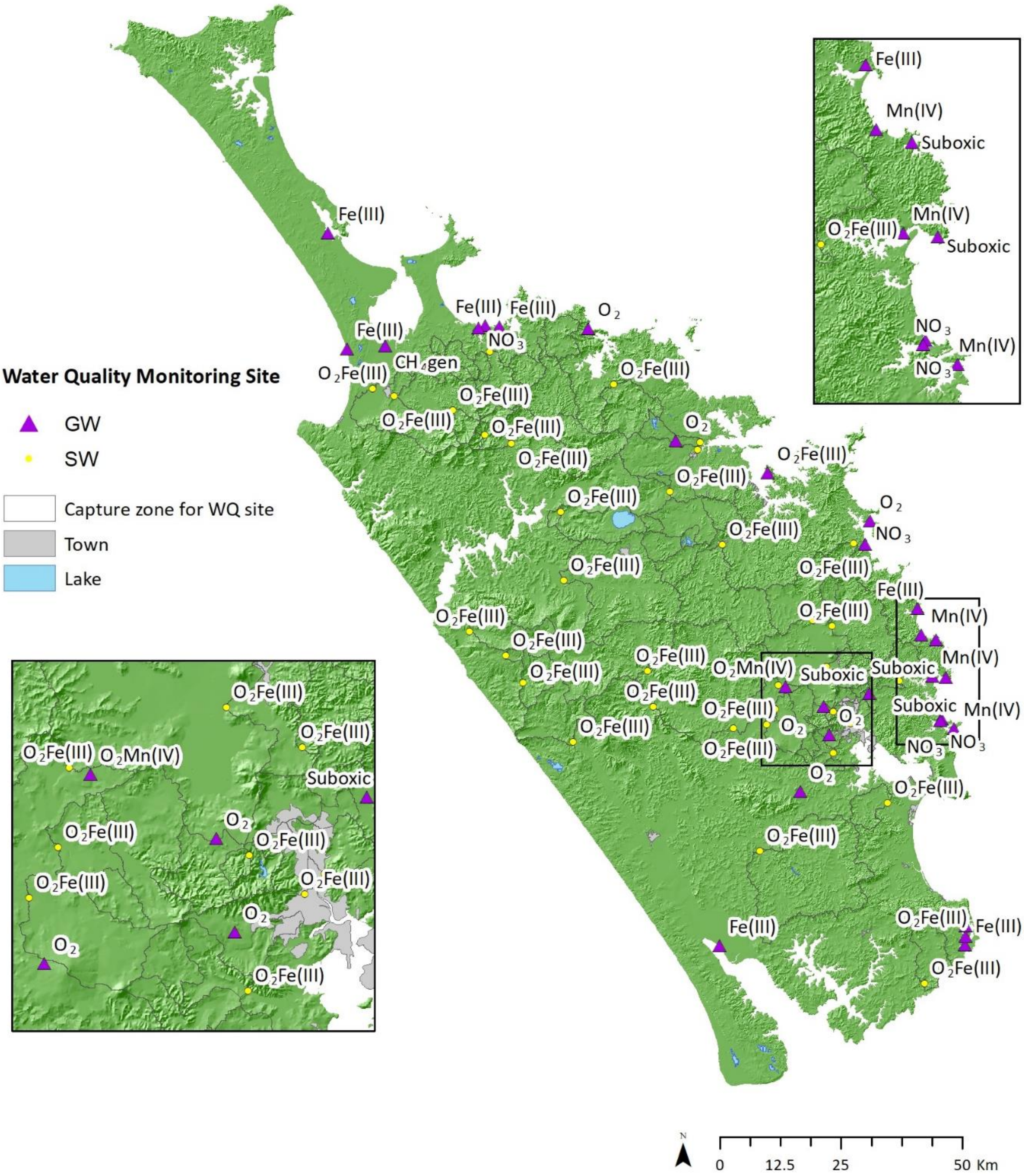

Figure 5.5: Terminal Electron Accepting Process for Northland surface water and groundwater.

---

[1] Overall, there is little difference in redox assignments using either the default or regionally specific thresholds.

Table 5. 1. Redox assignments for Northland surface water (SW) and groundwaters (GW) showing both the revised water quality specific and default outputs.

Site Name	Type	Water Quality Specific Redox Category	Water Quality Specific Redox Process	Default General Redox Category	Default Redox Process
Awanui at FNDC take	SW	Mixed(oxic-anoxic)	O_2-Fe(III)	Mixed(oxic-anoxic)	O_2-Fe(III)
Awanui at Waihue Channel	SW	Mixed(oxic-anoxic)	O_2-Fe(III)	Mixed(oxic-anoxic)	O_2-Fe(III)
Hakaru at Topuni	SW	Mixed(oxic-anoxic)	O_2-Fe(III)	Mixed(oxic-anoxic)	O_2-Fe(III)
Hatea at Mair Park	SW	Mixed(oxic-anoxic)	O_2-Fe(III)	Mixed(oxic-anoxic)	O_2-Fe(III)
Kaeo at Dip Road	SW	Mixed(oxic-anoxic)	O_2-Fe(III)	Mixed(oxic-anoxic)	O_2-Fe(III)
Kaihu at Gorge	SW	Mixed(oxic-anoxic)	O_2-Fe(III)	Mixed(oxic-anoxic)	O_2-Fe(III)
Kerikeri at Stone Store	SW	Mixed(oxic-anoxic)	O_2-Fe(III)	Mixed(oxic-anoxic)	O_2-Fe(III)
Mangahahuru at Apotu Road Bridge	SW	Mixed(oxic-anoxic)	O_2-Fe(III)	Mixed(oxic-anoxic)	O_2-Fe(III)
Mangahahuru at Main Road	SW	Mixed(oxic-anoxic)	O_2-Fe(III)	Mixed(oxic-anoxic)	O_2-Fe(III)
Mangakahia at Titoki	SW	Mixed(oxic-anoxic)	O_2-Fe(III)	Mixed(oxic-anoxic)	O_2-Fe(III)
Mangakahia at Twin Bridges	SW	Mixed(oxic-anoxic)	O_2-Fe(III)	Mixed(oxic-anoxic)	O_2-Fe(III)
Mangamuka at Iwitaua Road	SW	Mixed(oxic-anoxic)	O_2-Fe(III)	Mixed(oxic-anoxic)	O_2-Fe(III)
Manganui at Mitaitai Road	SW	Mixed(oxic-anoxic)	O_2-Fe(III)	Mixed(oxic-anoxic)	O_2-Fe(III)
Mangere at Knight Road	SW	Mixed(oxic-anoxic)	O_2-Fe(III)	Mixed(oxic-anoxic)	O_2-Fe(III)
Ngunguru at Coalhill Lane	SW	Mixed(oxic-anoxic)	O_2-Fe(III)	Mixed(oxic-anoxic)	O_2-Fe(III)
Opouteke at Suspension Bridge	SW	Mixed(oxic-anoxic)	O_2-Fe(III)	Mixed(oxic-anoxic)	O_2-Fe(III)
Oruru at Oruru Road	SW	Mixed(oxic-anoxic)	O_2-Fe(III)	Mixed(oxic-anoxic)	O_2-Fe(III)
Otaika at Otaika Valley Raod	SW	Mixed(oxic-anoxic)	O_2-Fe(III)	Mixed(oxic-anoxic)	O_2-Fe(III)
Pukenui at Kanehiana Drive	SW	Mixed(oxic-anoxic)	O_2-Fe(III)	Mixed(oxic-anoxic)	O_2-Fe(III)
Punakitere at Taheke	SW	Mixed(oxic-anoxic)	O_2-Fe(III)	Mixed(oxic-anoxic)	O_2-Fe(III)
Punaruku at Russell Road	SW	Mixed(oxic-anoxic)	O_2-Fe(III)	Mixed(oxic-anoxic)	O_2-Fe(III)
Ruakaka at Flyger Road	SW	Mixed(oxic-anoxic)	O_2-Fe(III)	Mixed(oxic-anoxic)	O_2-Fe(III)
Tapapa at SH1	SW	Mixed(oxic-anoxic)	O_2-Fe(III)	Oxic	O_2
Utakura at Okaka Road	SW	Mixed(oxic-anoxic)	O_2-Fe(III)	Mixed(oxic-anoxic)	O_2-Fe(III)
Victoria at Victoria Valley Road	SW	Mixed(oxic-anoxic)	O_2-Fe(III)	Oxic	O_2
Waiarohia at Second Avenue	SW	Mixed(oxic-anoxic)	O_2-Fe(III)	Mixed(oxic-anoxic)	O_2-Fe(III)
Waiharakeke at Stringers Road	SW	Mixed(oxic-anoxic)	O_2-Fe(III)	Mixed(oxic-anoxic)	O_2-Fe(III)
Waimamaku at SH12	SW	Mixed(oxic-anoxic)	O_2-Fe(III)	Mixed(oxic-anoxic)	O_2-Fe(III)
Waiotu at SH1	SW	Mixed(oxic-anoxic)	O_2-Fe(III)	Mixed(oxic-anoxic)	O_2-Fe(III)
Waipao at Draffin Road	SW	Mixed(oxic-anoxic)	O_2-Fe(III)	Mixed(oxic-anoxic)	O_2-Fe(III)
Waipapa at Landing	SW	Mixed(oxic-anoxic)	O_2-Fe(III)	Mixed(oxic-anoxic)	O_2-Fe(III)

Waipoua at SH12	SW	Mixed(oxic-anoxic)	O_2-Fe(III)	Mixed(oxic-anoxic)	O_2-Fe(III)
Wairau at SH12	SW	Mixed(oxic-anoxic)	O_2-Fe(III)	Mixed(oxic-anoxic)	O_2-Fe(III)
Wairua at Purua	SW	Mixed(oxic-anoxic)	O_2-Fe(III)	Mixed(oxic-anoxic)	O_2-Fe(III)
Waitangi at Waimate North Road	SW	Mixed(oxic-anoxic)	O_2-Fe(III)	Mixed(oxic-anoxic)	O_2-Fe(III)
Whakapara at Cableway	SW	Mixed(oxic-anoxic)	O_2-Fe(III)	Mixed(oxic-anoxic)	O_2-Fe(III)
Aupouri Groundwater at Houhora BG Fish Club	GW	Anoxic	Fe(III)	Suboxic	Suboxic
Awanui GW at Vinac Farms	GW	Anoxic	CH4gen	Mixed(oxic-anoxic)	O2-CH4gen
Cable Bay Groundwater at Croquet Club	GW	Anoxic	Fe(III)	Mixed(oxic-anoxic)	O_2-Fe(III)
Coopers Beach Ground Water at Youth Camp	GW	Anoxic	Fe(III)	Mixed(oxic-anoxic)	O_2-Fe(III)
Glenbervie GW at Barron's Property	GW	Suboxic	Suboxic	Oxic	O_2
GW Bland Bay at M/C Ngatiwai t/Board Camp	GW	Oxic	O_2	Oxic	O_2
Managawhai GW at Mangawhai Golf Club	GW	Mixed(oxic-anoxic)	O_2-Fe(III)	Oxic	O_2
Mangawhai GW at Caravan Pk	GW	Anoxic	Fe(III)	Suboxic	Suboxic
Mangawhai GW at Mangawhai Hideaway Camp	GW	Mixed(oxic-anoxic)	O_2-Fe(III)	Mixed(oxic-anoxic)	O_2-Fe(III)
Matapouri Groundwater at Smith	GW	Suboxic	Suboxic	Oxic	O_2
Matarau GW at Osbaldiston Bore	GW	Mixed(oxic-anoxic)	O_2-Mn(IV)	Oxic	O_2
Ngunguru Groundwater at Thompson	GW	Anoxic	Mn(IV)	Suboxic	Suboxic
Oakura GW at 3 Te Kapua Street	GW	Anoxic	NO_3	Oxic	O_2
Pataua North GW at WDC Toilets	GW	Anoxic	NO_3	Oxic	O_2
Pataua South GW at Pataua public toilets	GW	Anoxic	NO_3	Oxic	O_2
Ruawai GW at Kaipara D/C Bore 5	GW	Anoxic	Fe(III)	Anoxic	Fe(III)
Russell GW at 47 The Strand	GW	Mixed(oxic-anoxic)	O_2-Fe(III)	Mixed(oxic-anoxic)	O_2-Fe(III)
Sandy Bay GW at WDC Toilets	GW	Anoxic	Mn(IV)	Mixed(oxic-anoxic)	O_2-Mn(IV)
Taiharuru GW at WDC Toilets	GW	Anoxic	Mn(IV)	Mixed(anoxic)	NO_3-Mn(IV)
Taipa GW at Taipa High School	GW	Anoxic	NO3	Oxic	O_2
Taupo Bay GW at John Turner	GW	Oxic	O_2	Oxic	O_2
Tauraroa GW at 88 Maungakaramea	GW	Oxic	O_2	Oxic	O_2
Three Mile Bush GW at Wise Bore	GW	Oxic	O_2	Oxic	O_2
Waipapa GW at 10 Pungaere Rd	GW	Oxic	O_2	Oxic	O_2
Waipapakauri GW at Waipapakauri landing	GW	Anoxic	Fe(III)	Suboxic	Suboxic
WDC toilet at Whangaumu Bay	GW	Suboxic	Suboxic	Oxic	O_2
Whananaki North GW at WDC Toilets	GW	Anoxic	Fe(III)	Anoxic	Fe(III)
Whangarei GW at Foster Irrigation Bore	GW	Oxic	O_2	Oxic	O_2
Whatitiri GW at Tanekaha Partnership Irrigation	GW	Oxic	O_2	Oxic	O_2

5.2 Multivariate Analysis - Combined SW and GW

Multivariate analysis of Northland surface and ground waters was undertaken in order to provide a platform for understanding the drivers of spatial variability of Northland surface and ground waters. Processed surface and groundwater data sets were combined into one master data set of 115 sites. Hierarchal Cluster Analysis (HCA) followed by Principal Component Analysis (PCA) was undertaken for surface water only and a combined surface and groundwater dataset following the recommendations of Güler et al. (2002) for analysis of hydrochemical and water quality datasets[2]. Site median values were log transformed and z-scored. As pH is already in log form it was not transformed. The following subset of variables was used: Total alkalinity, pH, Ca, Mg, K, Si, Na, Cl, SO_4, Br, DRP, TAM, NNN, Fe^{II}, Mn^{II}, and Total Ammoniacal Nitrogen (TAN).

Of the 115 sites regionally, 65 had values for all 16 analytes - 35 surface water (SW) and 29 groundwater (GW). During HCA the single linkage dendrogram identified four key outliers: Kerikeri at Stone Store (SW) and Hatea and Mair Park (SW) both of which appear to be tidally influenced, and Mangawhai GW at Caravan Pk Bore and Three Mile Bush GW at Wise Bore. Neither of the GW sites seemed anomalous in terms of their local setting, with Mangawhai GW at Caravan Pk Bore characterised by elevated Na, Cl and Br and low DO suggesting a reducing aquifer influenced by seawater, and the Three Mile Bush GW at Wise Bore having low pH. As such, none of these sites were excluded from the dataset but the influence of seawater over Kerikeri at Stone Store (SW) and Hatea and Mair Park sites was noted. The resulting dendrogram can be subdivided into 3, 4 and 7 clusters (Figure 5.6, Table 5.4).

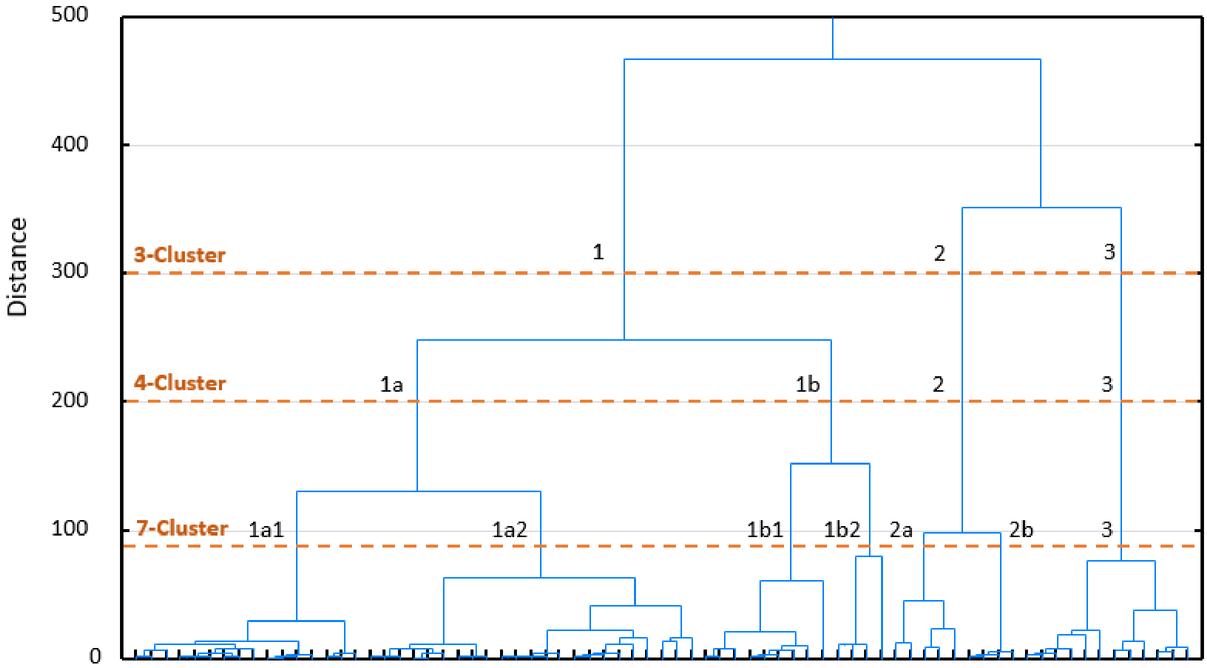

Figure 5. 6. Dendrogram using Ward's minimum variance method for Northland ground and surface waters. Variables Selected: Talk, TAN, Br, Ca, Cl, DRP, Fe, Mg, Mn, K, Si, Na, SO_4, pH. Distance measure = Squared Euclid. Three, 4 and 7 clusters are apparent at the 300, 200 and sub-100 phenon lines.

---

[2] HCA and PCA was also applied to the individual surface and ground water data sets to aid interpretation but is not reported here.

Table 5. 2: Cluster assignments of Northland's surface and groundwater sites at the 300, 200 and 90 phenon lines.

Type	Site Name	3-Cluster	4-Cluster	7-Cluster
SW	Kaeo at Dip Road	1	1a	1a1
SW	Kaihu at Gorge	1	1a	1a1
SW	Mangahahuru at Apotu Road Bridge	1	1a	1a1
SW	Mangahahuru at Main Road	1	1a	1a1
SW	Ngunguru at Coalhill Lane	1	1a	1a1
SW	Punaruku at Russell Road	1	1a	1a1
SW	Utakura at Okaka Road	1	1a	1a1
SW	Waiharakeke at Stringers Road	1	1a	1a1
SW	Waimamaku at SH12	1	1a	1a1
SW	Waiotu at SH1	1	1a	1a1
SW	Waipapa at Landing	1	1a	1a1
SW	Waipoua at SH12	1	1a	1a1
SW	Wairau at SH12	1	1a	1a1
SW	Wairua at Purua	1	1a	1a1
SW	Waitangi at Waimate North Road	1	1a	1a1
SW	Whakapara at Cableway	1	1a	1a1
SW	Awanui at FNDC take	1	1a	1a2
SW	Awanui at Waihue Channel	1	1a	1a2
SW	Hakaru at Topuni	1	1a	1a2
SW	Mangakahia at Titoki	1	1a	1a2
SW	Mangakahia at Twin Bridges	1	1a	1a2
SW	Mangamuka at Iwitaua Road	1	1a	1a2
SW	Manganui at Mitaitai Road	1	1a	1a2
SW	Mangere at Knight Road	1	1a	1a2
SW	Opouteke at Suspension Bridge	1	1a	1a2
SW	Oruru at Oruru Road	1	1a	1a2
SW	Otaika at Otaika Valley Raod	1	1a	1a2
SW	Pukenui at Kanehiana Drive	1	1a	1a2
SW	Punakitere at Taheke	1	1a	1a2
SW	Ruakaka at Flyger Road	1	1a	1a2
SW	Tapapa at SH1	1	1a	1a2
SW	Victoria at Victoria Valley Road	1	1a	1a2
SW	Waiarohia at Second Avenue	1	1a	1a2
SW	Waipao at Draffin Road	1	1a	1a2
GW	Ngunguru Groundwater at Thompson P/S	1	1a	1a2
GW	Russell GW at 47 The Strand (Dr Jack Phillips)	1	1a	1a2
GW	Waipapakauri GW at Waipapakauri landing	1	1a	1a2
GW	Glenbervie GW at Barron's Property, Ngunguru Road	1	1b	1b1
GW	Managawhai GW at Mangawhai Golf Club (SOE Bore)	1	1b	1b1
GW	Matarau GW at Osbaldiston Bore	1	1b	1b1
GW	Tauraroa GW at 88 Maungakaramea Road (Finlayson)	1	1b	1b1
GW	Three Mile Bush GW at Wise Bore	1	1b	1b1
GW	Waipapa GW at 10 Pungaere Rd (D Hop owner)	1	1b	1b1
GW	Whangarei GW at Foster Irrigation Bore	1	1b	1b1
GW	Whatitiri GW at Tanekaha Partnership Irrigation Bore	1	1b	1b1

GW	Sandy Bay GW at WDC Toilets	1	1b	1b2
GW	Taiharuru GW at WDC Toilets	1	1b	1b2
GW	WDC toilet at Whangaumu Bay	1	1b	1b2
SW	Hatea at Mair Park	2	2	2a
SW	Kerikeri at Stone Store	2	2	2a
GW	Matapouri Groundwater at Smith P/S Beside Road	2	2	2a
GW	Pataua North GW at WDC Toilets	2	2	2a
GW	Pataua South GW at Pataua public toilets	2	2	2a
GW	GW Bland Bay at M/C Ngatiwai t/Board Camp	2	2	2b
GW	Oakura GW at 3 Te Kapua Street (Patricia Wallis)	2	2	2b
GW	Taipa GW at Taipa High School	2	2	2b
GW	Taupo Bay GW at John Turner	2	2	2b
GW	Aupouri Groundwater at Houhora BG Fish Club	3	3	3
GW	Awanui GW at Vinac Farms	3	3	3
GW	Cable Bay Groundwater at Croquet Club by Stream	3	3	3
GW	Coopers Beach Ground Water at Youth Camp	3	3	3
GW	Mangawhai GW at Caravan Pk Bore Garden tap	3	3	3
GW	Mangawhai GW at Mangawhai Hideaway Camp bore	3	3	3
GW	Ruawai GW at Kaipara D/C Bore 5	3	3	3
GW	Whananaki North GW at WDC Toilets	3	3	3

5.2.1 3-Cluster waters

At the 300 phenon line the dataset is split into three clusters (Figure 5.6, Figure 5.7). Except for the tidally influenced Hatea at Mair Park and Kerikeri at Stone Store sites, all SW (n = 35) sites fall within cluster 1. Also occurring within cluster 1 are 14 GW sites. All other GW are separated into cluster 2 (n = 9 sites) and cluster 3 (n = 8 sites), with both the Hatea at Mair Park and Kerikeri at Stone Store sites included within cluster 2. Overall, cluster I SW, are by far the most dilute and exhibit the least variance in chemical composition. Median Na, Cl, Br and SO_4 concentrations all suggest a marine aerosolic origin (Table 5.5). Cluster 2 and Cluster 3 waters are more mineralised and primarily differentiated in terms of redox conditions - cluster 2 waters are more oxidising and cluster 3 are more reducing.

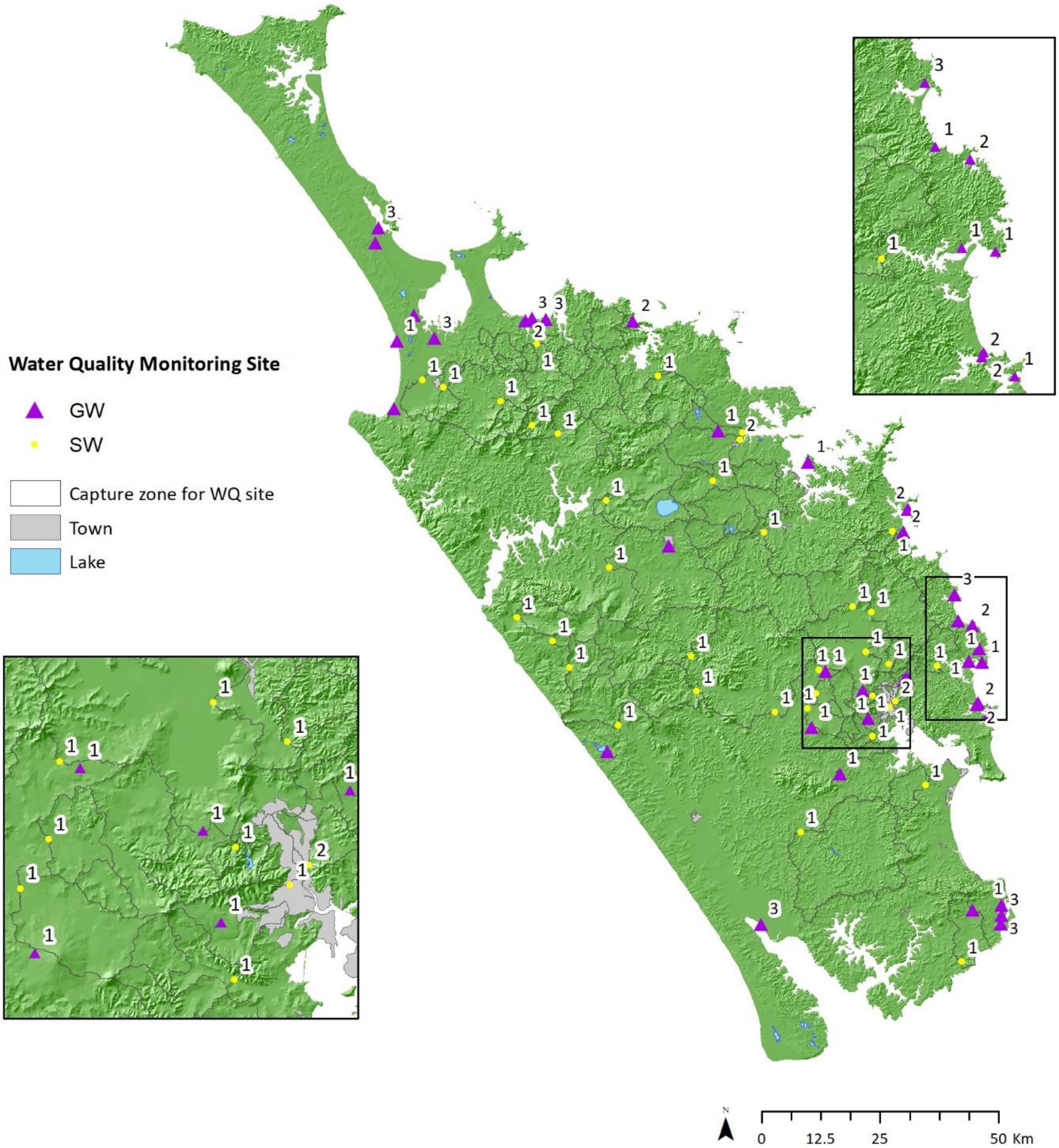

Figure 5. 7: Location of 3-cluster membership for surface (circles) and groundwater (triangles) sites.

5.2.2 4-Cluster waters

At the 4- cluster level, 200 phenon line cluster 1 is split into two subgroups (Figure 5.5). All SW sites fall into Cluster 1a along with 3 GW sites, Ngunguru Groundwater at Thompson P/S, Russell GW at 47 The Strand (Dr Jack Phillips), and Waipapakauri GW at Waipapakauri landing. The remaining GW sites comprise cluster 1b. More detail of these clusters is provided in the 7-cluster separation. Cluster 2 and 3 remain unchanged at this level of observation.

Table 5. 3. Summary of 3-cluster waters at the 300 phenon line.

	Cluster 1						**Cluster 2**						**Cluster 3**					
	n	**Mean**	**Median**	**C.V.**	**Min.**	**Max.**	**n**	**Mean**	**Median**	**C.V.**	**Min.**	**Max.**	**n**	**Mean**	**Median**	**C.V.**	**Min.**	**Max.**
WTemp	48	16.13	16.13	0.08	13.35	18.50	9	17.8	18.30	0.07	15.45	18.90	8	18.50	18.40	0.04	17.40	19.70
Condy	48	17.81	14.63	0.64	7.31	62.90	9	81.9	66.90	0.92	7.88	264.20	8	56.30	52.83	0.32	39.82	97.00
Talk	48	41.7	40.2	0.63	5.1	150.0	9	192.6	230.0	0.47	13.5	260.0	8	148.6	130.0	0.34	94.0	235.0
pH	48	7.02	7.15	0.10	4.89	8.13	9	7.5	7.43	0.03	7.18	7.70	8	7.33	7.52	0.09	6.01	7.93
DO	48	7.96	9.30	0.37	0.10	10.60	9	5.2	4.85	0.55	1.70	10.00	8	2.14	0.35	1.44	0.09	8.40
DO%	48	80.03	93.60	0.37	1.10	108.50	9	55.6	52.40	0.50	19.40	100.55	8	22.83	4.40	1.41	1.00	88.00
DOC	41	2.92	2.60	0.71	0.50	11.05	2	2.6	2.60	0.00	2.60	2.60	3	2.45	1.50	0.91	0.85	5.00
B	48	0.04	0.02	1.85	0.01	0.49	9	0.13	0.06	1.18	0.02	0.51	8	0.07	0.05	1.05	0.03	0.26
Br	48	0.10	0.07	0.86	0.03	0.47	9	0.83	0.18	1.22	0.08	2.70	8	0.30	0.26	0.61	0.11	0.69
Ca	48	10.08	8.95	0.68	0.30	38.00	9	67.91	79.00	0.48	8.20	98.00	8	25.31	26.00	0.46	9.50	45.00
Cl	48	23.74	17.00	0.79	11.00	100.00	9	162.17	53.00	1.32	26.00	640.00	8	82.63	67.50	0.58	31.00	181.00
Fe	48	0.30	0.25	1.02	0.00	1.53	9	0.08	0.00	1.89	0.00	0.36	8	1.09	0.83	1.10	0.06	3.60
Mg	48	4.41	4.05	0.54	0.50	10.50	9	19.94	17.00	0.68	5.40	51.00	8	8.16	6.93	0.54	3.00	15.70
Mn	48	0.04	0.02	1.86	0.00	0.40	9	<0.001	0.00	1.37	0.00	0.01	8	0.26	0.14	1.51	0.02	1.20
K	48	1.44	1.20	0.76	0.22	6.10	9	4.88	4.60	0.83	1.40	14.20	8	3.17	3.40	0.44	1.19	5.70
Si	48	23.43	21.00	0.50	5.80	60.00	9	11.86	11.50	0.34	6.70	20.00	8	52.94	50.50	0.41	20.50	86.00
Na	48	19.34	13.95	1.02	8.30	130.00	9	97.32	43.00	1.12	17.00	360.00	8	79.44	58.75	0.70	38.00	210.00
SO_4	48	8.20	5.00	1.35	1.60	56.00	9	36.95	32.00	0.86	7.90	110.00	8	13.23	13.98	0.65	0.45	25.00
NO_3-N	48	0.842	0.140	1.987	0.002	7.500	9	3.972	3.600	0.818	0.350	8.900	8	0.003	0.003	0.336	0.002	0.005
NO_2-N	48	0.002	0.002	0.442	0.002	0.007	9	0.007	0.004	1.263	0.002	0.030	8	0.002	0.002	0.166	0.002	0.003
NNN	48	0.836	0.141	2.001	0.003	7.502	9	3.978	3.606	0.817	0.350	8.904	8	0.005	0.005	0.227	0.004	0.007
TAM_pH	48	0.008	0.006	0.640	0.002	0.025	9	0.007	0.007	0.215	0.005	0.008	8	0.166	0.100	1.004	0.037	0.530
TKN	34	0.221	0.178	0.525	0.100	0.470	2	0.190	0.190	0.000	0.190	0.190	0	****	****	****	****	****
TN	34	0.478	0.398	1.050	0.100	2.800	2	0.565	0.565	0.113	0.520	0.610	0	****	****	****	****	****
TP	34	0.037	0.034	0.765	0.007	0.142	2	0.019	0.019	0.132	0.017	0.021	0	****	****	****	****	****
DRP	48	0.032	0.017	1.767	0.005	0.380	9	0.022	0.019	0.493	0.007	0.039	8	0.098	0.067	0.821	0.020	0.260
TSS	22	20.20	3.00	4.04	1.00	386.00	1	2.00	2.00	0.00	2.00	2.00	0	****	****	****	****	****

Turbidity	34	4.48	4.08	0.49	1.10	9.10	2	2.65	2.65	0.35	2.00	3.30	0	****	****	****	****	****
Secci	34	1.42	1.30	0.35	0.73	3.00	2	2.04	2.04	0.28	1.63	2.45	0	****	****	****	****	****
T. coli	48	4182	2993	1	1	24192	9	1225	42	2	1	6488	8	191	2	3	1	1414
E. coli	48	199	187	1	1	613	9	57	1	2	1	258	8	1	1	0	1	1
HCO_3	14	69.83	60.50	0.66	6.10	190.00	6	285.00	287.50	0.08	245.00	310.00	6	160.00	147.50	0.31	120.00	255.00
$CaCO_3$	14	1.01	1.00	0.05	1.00	1.20	6	2.37	2.00	0.61	1.00	5.20	6	1.35	1.00	0.64	1.00	3.10

5.2.3 7-Cluster waters

Below the 100 phenon line, Northland surface and groundwaters cluster into 7 subgroups (Figure 5.6). At the 7-cluster level, greater resolution of the spatial variance in Northland ground and surface waters is apparent with cluster 1 subdivided into 4 clusters and cluster 2 divided into 2 clusters (Figure 5.8). There is no change to cluster 3 (Table 5.5). Summary statistics for each cluster are shown in Table 5.6. Specifically, cluster 1a1 (n = 16) is comprised entirely of SWs whereas cluster 1a2 (n = 21) is a mix of 18 SW and 3 GW sites. The remaining clusters 1b1 (n = 8), 1b2 (n = 3), 2b (n = 4) and 3 (n= 8) are all GWs with the exception of both seawater influenced SW sites which fall within cluster 2a (n = 5). Once again both of the SW dominated clusters, 1a1 and 1a2 are the most dilute waters. However, the GW dominated cluster 1b1 SW does exhibit broadly similar major ion concentrations to both SW dominated clusters. Further, there is a strong spatial relationship between cluster 1a2 SW and cluster 1b1 GW with a number of the GW sites occurring within or close to the boundaries of the SW capture zones. Specifically, northwest of Whangarei and around Waipapa apparently in association with the geologically recent Kerikeri Volcanic Group.

Of note, all 1a2 SWs show some association with basaltic rock either Kerikeri or Tangihua basalts. Hydrochemically, 1a2 waters are characterised by elevated alkalinity, Ca and Si and show a similar composition to cluster 1b1 GWs which are predominantly hosted by fractured basalt aquifers. Both of these clusters exhibit marine aerosol concentrations consistent with a rainfall source. Despite similar lithological and aerosolic hydrochemical signatures the redox status of these two clusters are distinct, specifically cluster 1b1 GW are more strongly oxidising (mix of oxic and mixed(oxic-anoxic)) whereas all cluster 1a2 SW is of a mixed redox provenance (oxic-anoxic, O_2-Fe^{III}-reduction). The GW of cluster 1b1 are associated with the second highest median NNN within the data set. On the basis of local soil information, the mixed redox signatures of cluster 1a2 SW, including low median NNN concentrations, may reflect the mixing of oxic baseflow with a greater volume of reduced soil drainage waters. This could be verified by contrasting redox signatures against flow at these sites. If the oxidised base flow is important then dissolved Fe and Mn concentrations are likely to be low under low flows and DO and NNN elevated[3].

Given evidence for a hydrochemical and associated spatial relationship between 1a2 SW and 1b1 GW and fractured basalt aquifers it is likely that a similar spatial correlation exists for similar settings across the region. Discussion with NRC staff would further aid in refining evidence for GW-SW interaction across areas of fractured basalt. Additional insight over the redox signals of shallow aquifers and overlying soils can be derived from temporal analysis of SW data for those areas currently lacking local GW data (see Rissmann et al., 2018 TSF work).

Cluster 1a1 SW are the most dilute waters regionally and are characterised by the lowest pH and alkalinity along with the lowest median Na, Ca and Mg concentrations of regional waters. With the exception of Waimamaku at SH12, Wairau at SH12, Waipoua at SH12, Kaihu at Gorge and Waipapa at Landing sites, all occur in association with sedimentary mud or sandstones. A dominantly sedimentary association is consistent with the lower base cation concentrations, pH and alkalinity typical of the lower acid buffering capacity of Northland sedimentary rock. The Waimamaku at SH12, Wairau at SH12, Waipoua at SH12 and Kaihu at Gorge are all associated with relatively 'high-altitude' headwaters hosted by Tangihua Volcanics and a transport limited geomorphic setting. Despite a basaltic provenance, the hydrochemical signatures of these waters indicate a lesser opportunity for significant water-soil-rock interaction and attendant hydrochemically evolution typified by lower altitude waters hosted by basaltic volcanics (cluster 1a2).

Cluster 1a1 SW are hydrochemically most similar to cluster 1b2 GW, all of which are hosted by sedimentary aquifers including greywacke and argillite. For cluster 1a1 SW that do not have GW data

---

[3] NNN elevation is relative to land use intensity with cumulative probability plots in section 5 providing insight as to key thresholds.

within their capture zone, all but the western SW sites are associated with sedimentary sequences, in particular, mudstones. The lack of GW bores within mudstone aquifers is consistent with lower permeability although it is still likely that these aquifers contribute to baseflow during the drier times of the year. Cluster 1a1 SW are dominated by a mixed(oxic-anoxic) redox signature whereas GW associated with this cluster are all strongly anoxic e.g. median DO of <0.8 mg/L. A lack of GW samples from mudstone sequences precludes a redox assignment although given a high clay content, low permeability and an association with poorly drained (clay-rich) soils we anticipated a predominantly reducing aquifer system. Some discussion with local NRC staff regarding GW-SW interaction in areas of lowland sedimentary rock and in particular mudstones would aid in refining physiographic mapping of redox and hydrological controls. As noted above for basaltic volcanics, the temporal analysis of SW data could also be used to assess the character and likely origin of the shallow GW component supplying SW sites in areas of mudstone or mixed sedimentary sequences where groundwater data is lacking (see Rissmann et al., 2018).

Clusters 2a (n = 5), 2b (n = 4), and 3 (n= 8) and are all GWs with the exception of the tidally influenced Kerikeri at Stone Store and Hatea at Mair Park SW sites which fall within cluster 2a. Cluster 2a waters include Matapouri Groundwater at Smith P/S Beside Road, Pataua North GW at WDC Toilets and Pataua South GW at Pataua public toilets. Hydrochemically, these waters have the highest median Na, Cl, Br, Mg, K and SO_4 concentrations of all regional waters which is consistent with a strong seawater influence. The three GW sites are weakly anoxic (i.e., NO_3-reducing), whereas both SW sites are characterised by mixed(oxic-anoxic) conditions with median dissolved Fe and Mn concentrations that are at least 4.0 and 2.4 times higher, respectively than GW, indicating a shallow, likely soil zone reduction source. Spatially all of these waters occur in close proximity to the coast with Cl/Br, Cl/B ratios supporting a significant seawater influence.

Cluster 2b GW have lower Na, Cl and Br when contrast with seawater influence GW of cluster 2a. However, 2b GW contains a significantly higher median Ca concentration, a comparable Total Alkalinity and are at or slightly over saturated with respects to the carbonate minerals aragonite (median log Q/K = +0.15) and calcite (median log Q/K = +0.21). All of these GW are associated with shallow sandy coastal aquifers raising the possibility that shell beds are the carbonate source. In terms of redox, these GW are strongly oxidising to weakly reducing (i.e., NO_3-reduction) with the most elevated NNN concentrations of all GW within the data set (median = 4.85) and a peak value of 8.6 mg/L NO_3-N at the oxic, Bland Bay GW site. Importantly, soils surrounding these bores are predominantly well-drained making them more prone to nitrate leaching. Hydrochemically, these GW sites are compositionally distinct from any of the SW included in this analysis.

Finally, cluster 3 waters are dominated by anoxic redox signatures and are by far the most reduced ground waters in the regional data set. Awanui GW at Vinac Farms is the most reduced GW in the regional data set, specifically a TEAP consistent with CO_2-reduction and attendant methanogenesis. A SO_4 concentration of <0.5 mg/L for Awanui at Vinac Farms is consistent with the evolution of redox conditions beyond SO_4-reduction within an aquifer hosted by progradational estuarine sediments that include more recent Quaternary peat, alluvium sand and shell deposits. Other sites also exhibit evidence of strong reduction but are poised at Fe^{III}-reduction with some evidence of minor SO_4-depletion suggestive of SO_4-reduction. Given the evidence for strongly reducing conditions it is perhaps not surprising that cluster 3 is associated with the highest median DOC, Total Ammoniacal Nitrogen (TAM), DRP and dissolved Fe and the lowest median NNN concentrations of waters within the regional data set. Elevated TAM and DRP is to be expected under strongly reducing conditions due to the ammonification of naturally occurring organic matter within the aquifer and the instability of the oxides and oxyhydroxides of iron (Fe-III) under reducing conditions. Elevated DOC is the key electron donor driving the reduction processes and as noted is the most elevated in cluster 3 GW.

In terms of major ion concentrations, there is a considerable range reflecting variable redox buffering, the presence of carbonates (shell beds) and variable mixing with seawater, some of it potentially connate. Although these aquifers exhibit a wide range of lithologies all occur in close proximity to the coast or are hosted by marine influenced sediments suggesting a local shell-bed influence. For example, five of the sites are in equilibrium or saturated with respects to aragonite and calcite minerals suggesting a carbonate source (i.e., Aupouri Groundwater @ Far North Farms, Aupouri Groundwater at Houhora BG Fish Club, Awanui GW @ Vinac Farms, Coopers Beach Ground Water@Youth Camp and Mangawhai GW @ Caravan Pk Bore Garden tap). Mangawhai GW at Caravan Pk Bore Garden tap has the highest seawater component followed by Ruawai GW at Kaipara D/C Bore 5 and Whananaki North GW at WDC Toilets. Elevated seawater signatures at these localities is hardly surprising given their proximity at the coast. Aupouri Groundwater at Long Bore, Ahipara (NGMP site) is amongst the most intriguing site hydrochemically, with low Ca and pH, elevated dissolved Fe and a larger Cl/SO_4 ratio suggesting sulphur-reducing conditions within a relatively inert, base-poor aquifer. Bore log information and locational data indicate dune sands as the primary aquifer, which is consistent with the relatively low pH (6.05) and base cation concentrations. These GW are compositionally distinct from any of the SW included in this analysis.

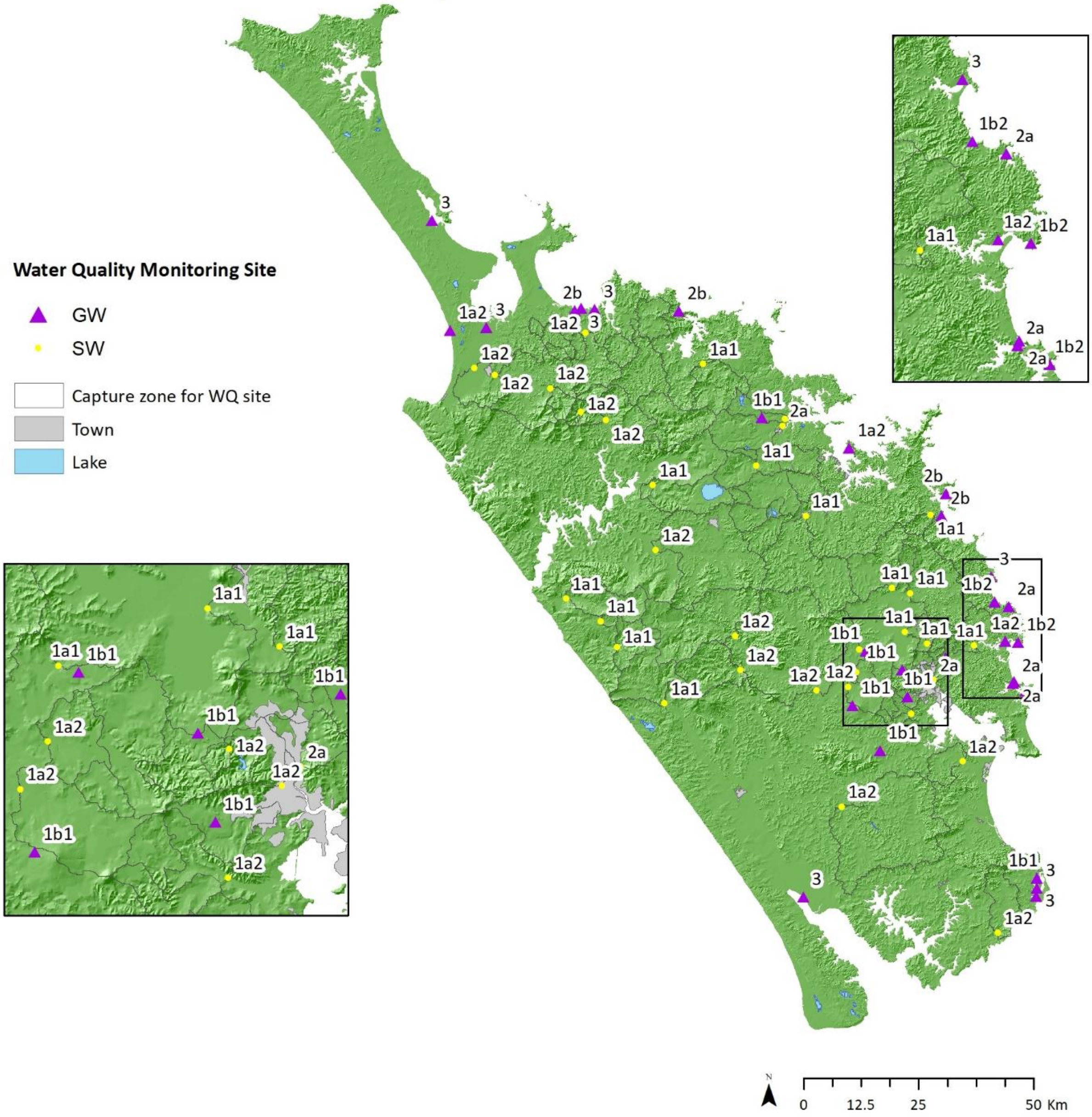

Figure 5. 8. Location of 7-cluster membership for surface (circles) and groundwater (triangles) sites.

Table 5. 4. Summary tables of 7-cluster waters below the 100 phenon line. As there is no change to cluster 3 at this level see Table 5.5 for Cluster 3 summary.

Cluster 1a

	Cluster1a1						Cluster1a2					
	n	Mean	Median	C.V.	Min.	Max.	n	Mean	Median	C.V.	Min.	Max.
WTemp	16	15.43	15.43	0.07	13.35	17.30	23	16.07	16.10	0.08	14.00	18.40
Condy	16	9.91	9.25	0.21	7.31	14.75	23	19.21	17.41	0.40	9.75	41.67
Talk	16	20.03	19.00	0.37	11.00	39.50	23	59.74	54.00	0.53	30.00	158.00
pH	16	7.07	7.04	0.03	6.64	7.40	23	7.39	7.40	0.06	6.00	8.13
DO	16	9.59	9.60	0.05	8.60	10.50	21	8.39	9.40	0.35	0.10	10.60
DO%	16	95.39	95.23	0.04	88.50	101.20	21	84.12	94.10	0.35	1.10	108.50
DOC	16	3.45	2.80	0.66	1.40	11.05	19	3.22	2.60	0.53	0.95	6.90
B	16	0.03	0.02	0.73	0.01	0.08	21	0.05	0.02	1.98	0.01	0.49
Br	16	0.07	0.07	0.23	0.05	0.10	23	0.09	0.08	0.52	0.04	0.23
Ca	16	5.52	4.90	0.61	2.40	15.00	23	15.50	13.00	0.56	6.60	42.00
Cl	16	16.03	16.00	0.13	13.00	20.00	23	22.49	19.00	0.50	13.00	64.00
Fe	16	0.51	0.38	0.68	0.16	1.53	23	0.28	0.26	0.75	0.00	0.72
Mg	16	2.18	2.20	0.17	1.60	2.85	23	5.08	5.15	0.26	3.40	9.40
Mn	16	0.04	0.03	1.79	0.00	0.31	23	0.03	0.02	0.65	0.00	0.08
K	16	1.23	1.25	0.44	0.53	2.60	23	1.61	1.30	0.65	0.53	4.80
Si	16	13.71	13.50	0.32	5.80	22.00	23	26.11	25.00	0.38	12.00	60.00
Na	16	11.35	11.00	0.19	8.30	16.00	23	17.47	15.00	0.41	11.00	40.50
SO_4	16	4.89	4.20	0.51	2.40	9.80	23	6.13	5.45	0.61	2.50	16.00
NO_3-N	16	0.163	0.140	0.797	0.003	0.395	23	0.374	0.072	1.743	0.002	2.600
NO_2-N	16	0.002	0.002	0.233	0.002	0.004	21	0.003	0.002	0.524	0.002	0.007
NNN	16	0.156	0.135	0.775	0.003	0.330	23	0.366	0.050	1.744	0.004	2.500
TAM_pH	16	0.005	0.005	0.430	0.002	0.009	23	0.010	0.008	0.601	0.003	0.025
TKN	16	0.201	0.158	0.475	0.100	0.390	18	0.238	0.203	0.554	0.100	0.470
TN	16	0.363	0.398	0.519	0.110	0.684	18	0.579	0.360	1.137	0.100	2.800
TP	16	0.026	0.018	0.675	0.007	0.057	18	0.048	0.039	0.694	0.013	0.142
DRP	16	0.011	0.011	0.561	0.005	0.024	23	0.034	0.025	0.916	0.006	0.138
TSS	10	2.85	2.50	0.55	1.00	6.00	12	34.67	3.00	3.19	1.00	386.00
Turbidity	16	4.60	4.09	0.48	1.10	8.85	18	4.37	3.93	0.50	1.25	9.10
Clarity	0	****	****	****	****	****	1	0.02	0.02	0.00	0.02	0.02
Secci	16	1.48	1.33	0.38	0.77	3.00	18	1.36	1.27	0.32	0.73	2.10
T.coli	16	3908	3818	1	703	7933	21	6414	4106	1	6	24192
E.coli	16	255	255	0	57	521	21	261	245	1	1	613
HCO_3	0	****	****	****	****	****	3	111.33	79.00	0.62	65.00	190.00
$CaCO_3$	0	****	****	****	****	****	3	1.07	1.00	0.11	1.00	1.20

Cluster 1b

	Cluster 1b1						Cluster 1b2					
	n	Mean	Median	C.V.	Min.	Max.	n	Mean	Median	C.V.	Min.	Max.
WTemp	9	17.39	17.10	0.04	16.40	18.60	4	18.19	18.18	0.01	17.90	18.50
Condy	9	18.18	19.67	0.25	10.60	22.49	4	57.87	56.23	0.25	43.61	75.40
Talk	9	45.18	44.00	0.48	5.10	74.00	4	54.50	46.50	0.74	15.00	110.00
pH	9	6.25	6.36	0.09	4.89	6.87	4	5.72	5.60	0.12	5.00	6.66
DO	8	6.25	6.42	0.26	3.04	8.86	3	0.77	0.51	0.65	0.46	1.35
DO%	8	65.48	66.98	0.25	32.20	91.30	3	8.27	5.40	0.64	5.00	14.40
DOC	6	0.57	0.55	0.13	0.50	0.65	0	****	****	****	****	****
B	8	0.01	0.01	0.55	0.01	0.03	3	0.11	0.06	0.76	0.06	0.20
Br	9	0.06	0.06	0.35	0.03	0.11	4	0.45	0.43	0.32	0.31	0.65
Ca	9	8.63	9.00	0.43	1.30	12.00	4	7.10	4.55	1.18	0.30	19.00
Cl	9	17.36	15.50	0.40	11.00	34.50	4	111.38	92.75	0.46	73.00	187.00
Fe	9	0.01	0.00	1.14	0.00	0.02	4	0.01	0.01	0.88	0.00	0.02
Mg	9	6.66	7.00	0.34	2.20	10.00	4	8.23	9.35	0.68	0.50	13.70
Mn	9	0.00	0.00	1.81	0.00	0.03	4	0.15	0.11	1.24	0.00	0.40
K	9	0.76	0.70	0.48	0.22	1.50	4	3.24	2.95	0.68	0.97	6.10
Si	9	34.14	39.00	0.35	9.80	46.00	4	30.83	34.00	0.33	16.30	39.00
Na	9	15.44	14.00	0.29	9.40	23.50	4	91.00	93.00	0.41	48.00	130.00
SO_4	9	4.86	3.10	0.85	1.10	14.00	4	43.25	44.50	0.27	28.00	56.00
NO_3-N	9	3.588	3.100	0.671	0.045	7.500	4	1.080	1.240	0.706	0.140	1.700
NO_2-N	8	0.002	0.002	0.000	0.002	0.002	3	0.002	0.002	0.000	0.002	0.002
NNN	9	3.590	3.100	0.670	0.047	7.502	4	1.082	1.241	0.704	0.142	1.702
TAM_pH	9	0.006	0.005	0.289	0.005	0.009	4	0.008	0.008	0.385	0.005	0.010
TKN	0	****	****	****	****	****	0	****	****	****	****	****
TN	0	****	****	****	****	****	0	****	****	****	****	****
TP	0	****	****	****	****	****	0	****	****	****	****	****
DRP	9	0.031	0.030	0.759	0.005	0.068	4	0.114	0.030	1.551	0.018	0.380
TSS	0	****	****	****	****	****	0	****	****	****	****	****
Turbidity	0	****	****	****	****	****	0	****	****	****	****	****
Clarity	0	****	****	****	****	****	0	****	****	****	****	****
Secci	0	****	****	****	****	****	0	****	****	****	****	****
T.coli	8	420	171	2	1	2419	3	53	14	1	1	144
E.coli	8	1	1	0	1	1	3	1	1	0	1	1
HCO_3	8	53.20	52.25	0.44	6.10	89.50	3	72.67	63.50	0.80	19.50	135.00
$CaCO_3$	8	1.00	1.00	0.00	1.00	1.00	3	1.00	1.00	0.00	1.00	1.00

Cluster 2

	Cluster 2a						Cluster 2b					
	n	Mean	Median	C.V.	Min.	Max.	n	Mean	Median	C.V.	Min.	Max.
WTemp	5	17.15	17.50	0.07	15.45	18.30	4	18.63	18.60	0.01	18.40	18.90
Condy	5	98.47	70.35	1.04	7.88	264.20	4	61.28	59.60	0.21	49.45	76.45
Talk	5	165.70	230.00	0.71	13.50	260.00	4	226.25	227.50	0.09	200.00	250.00
pH	5	7.48	7.43	0.02	7.30	7.68	4	7.47	7.51	0.03	7.18	7.70
DO	5	6.09	4.85	0.60	1.70	10.00	4	4.15	4.41	0.30	2.60	5.19
DO%	5	64.12	52.40	0.54	19.40	100.55	4	44.94	47.40	0.29	28.35	56.60
DOC	2	2.60	2.60	0.00	2.60	2.60	0	****	****	****	****	****
B	5	0.20	0.13	0.92	0.06	0.51	4	0.04	0.05	0.38	0.02	0.06
Br	5	1.40	1.33	0.76	0.17	2.70	4	0.12	0.10	0.38	0.08	0.18
Ca	5	55.84	58.00	0.72	8.20	98.00	4	83.00	86.00	0.15	67.00	93.00
Cl	5	261.20	180.00	0.97	47.00	640.00	4	38.38	34.25	0.40	26.00	59.00
Fe	5	0.14	0.01	1.32	0.00	0.36	4	0.00	0.00	0.43	0.00	0.00
Mg	5	27.35	22.00	0.51	15.75	51.00	4	10.68	10.15	0.47	5.40	17.00
Mn	5	0.00	0.00	0.97	0.00	0.01	4	0.00	0.00	0.18	0.00	0.00
K	5	7.35	5.60	0.54	4.60	14.20	4	1.80	1.65	0.29	1.40	2.50
Si	5	11.30	9.70	0.46	6.70	20.00	4	12.55	12.75	0.19	9.70	15.00
Na	5	154.37	118.85	0.78	43.00	360.00	4	26.00	24.50	0.41	17.00	38.00
SO_4	5	55.73	41.00	0.57	32.00	110.00	4	13.48	14.00	0.31	7.90	18.00
NO_3-N	5	2.869	1.100	1.263	0.350	8.900	4	5.350	4.850	0.462	3.100	8.600
NO_2-N	5	0.009	0.004	1.323	0.002	0.030	4	0.005	0.003	0.954	0.002	0.012
NNN	5	2.876	1.130	1.259	0.350	8.904	4	5.355	4.857	0.462	3.104	8.602
TAM_pH	5	0.007	0.008	0.246	0.005	0.008	4	0.007	0.007	0.199	0.005	0.008
TKN	2	0.190	0.190	0.000	0.190	0.190	0	****	****	****	****	****
TN	2	0.565	0.565	0.113	0.520	0.610	0	****	****	****	****	****
TP	2	0.019	0.019	0.132	0.017	0.021	0	****	****	****	****	****
DRP	5	0.021	0.019	0.614	0.007	0.038	4	0.024	0.020	0.406	0.019	0.039
TSS	1	2.00	2.00	0.00	2.00	2.00	0	****	****	****	****	****
Turbidity	2	2.65	2.65	0.35	2.00	3.30	0	****	****	****	****	****
Clarity	0	****	****	****	****	****	0	****	****	****	****	****
Secci	2	2.04	2.04	0.28	1.63	2.45	0	****	****	****	****	****
T.coli	5	2174	687	1	1	6488	4	39	9	2	1	135
E.coli	5	102	2	1	1	258	4	1	1	0	1	1
HCO_3	3	296.67	300.00	0.05	280.00	310.00	3	273.33	285.00	0.09	245.00	290.00
$CaCO_3$	3	2.00	2.00	0.00	2.00	2.00	3	2.73	2.00	0.80	1.00	5.20

5.2.4 Water Chemistry Summary

Overall, cluster analysis of Northland ground and surface waters indicate an association between fractured basalt and some sedimentary aquifers and stream flow. These waters tend to be characterised by meteoric signatures with little evidence of seawater or geothermal fluids. Major ion concentrations of these surface and ground waters show a distinct spatial correlation with lithology. Waters within basaltic areas, e.g. Kerikeri and Tangihua volcanics, exhibit elevated base cation concentrations and alkalinity whereas waters derived from clay-rich sedimentary rock are base-poor and of lower pH. Surface waters sourced from steep higher altitude catchments around Waipoua and Mataraua forests show less evolved signatures probably due to a greater proportion of quick flow and less time for soil-water-rock interaction with basaltic rock. Other groundwaters are more mineralised with strong evidence for a seawater influence and dissolution of shell-beds. There is little evidence for the contribution of water to streams from these marginal coastal aquifers.

Where isolated from the influence of active deposition, east coast aquifers hosted by fractured greywacke are predominantly oxidising. In comparison, reducing aquifers are associated with mixed-marine depositional facies, including estuarine sediments. However, shallow wells in dune sands, especially where the overlying soils are freely draining are strongly oxidising. Notably, although shallow aquifers are oxidising in areas of fractured basalts, surface waters show a mixed redox signature consistent with reducing soil water drainage derived from imperfectly to poorly drained soils. Although there are few wells in areas of mudstones, these rocks are likely to host reducing aquifers due to low permeability and a tendency to be capped by clay-rich and poorly drained soils.

In terms of surface waters, all surface water sites are dominated by mixed(oxic-anoxic) signatures, suggesting that shallow lateral and surficial (overland flow) flow pathways associated with imperfectly to poorly drained soils play an important role over surface water redox signatures in areas receiving oxidised base flow. The important role of soil hydrological properties in governing both the biogeochemistry and flow dynamics of streams across areas of imperfectly to poorly drained soils is well recognised (Katsuyama et al., 2001; Katsuyama and Ohte, 2002; Kasuyama et al., 2009; Inamdar, 2012; Rissmann et al., 2018). For stream capture zones associated with a greater area of well-drained soils or exposures of fracture bedrock the contribution of groundwater to stream is expected to be larger and the waters more oxidising. However, the recognition of the potential for larger areas of shallow oxidised aquifers, fractured basalt and greywacke, raises the question of an important groundwater control over in stream water quality during periods of low flow. Overall, the spatial variation in the redox signals necessitates the combination of both soil and aquifer reduction potential in order to make sense of the variation observed in Northland surface and ground waters.

The origin of and processes controlling the spatial variation in the constituents of regional surface waters and groundwater provides the foundation for subsequent analysis and mapping of the hydrological (H-PAL) and redox (R-PAL) layers for the Northland Region. The relationship between key process signals and landscape attributes are hypothesised on the basis of expert knowledge and statistical assessment. Expert knowledge is based on theoretical and empirical studies of the coupled relationship between landscape attributes and process signals (Rissmann et al., 2018). In terms of water quality, hydrological and redox processes are considered the main control over spatial variation in water quality outcomes in addition to land use pressure. These relationships are demonstrated in the following sections for each process-attribute layer.

5.3 Land Use

The degree to which the land has been modified, both chemically and physically, is an important factor to consider in every part of the physiographic application. As with landscape attributes, land use is a key determinant of water quality outcomes. To sustain agricultural production, lime and fertilisers are added to soils to amend acidity and increase the availability of plant available nutrients and trace elements for livestock, respectively (Rogers et al., 2017). Direct deposition and irrigation of animal wastes onto soils also modifies the nutrient and contaminant content of a soil. Addition of lime raises the pH of the soil and is an important tool for managing the acidity and adding base cations, especially across developed wetland areas. Potassium (K), nitrogen (N), phosphorus (P) and a range of other amendments modify but do not necessarily change the inherent properties of a soil. Subsurface drainage also plays a critical role in modifying the biogeochemical environment within the soil zone by increasing the supply of oxygen to the subsoil (Brady and Weil, 2007; Schoonover and Crim, 2015).

As with artificial drainage, the degree to which the chemical composition of a soil is modified depends upon the inherent properties of the soil. For example, large amendments of lime are required in areas of naturally acidic soils, higher P inputs are required for soils with very high or very low P-retention and trace element additions are also dependent on soil mineralogy and weathering status (McLaren and Cameron, 1996). Modification of the chemical environment of the soil in conjunction with the introduction of different plant and animal species has also changed the biological composition of the soil environment (Doran, 1979). However, as with artificial drainage, the type and intensity of land use is likely an additional driver over the chemical and biological modification of the soil.

Below we provide a simplified classification of land use for the Northland region produced using the Land Cover Database (LCDB4.1) (Table 5.8; Figure 5.9).

Table 5. 5: Simplified LCDB4.1 classification for use in the application of physiographics. Note not all land cover classes are present in Northland.

Land Cover Class	LCDB4.1 Classification
Indigenous forest	Indigenous forest; Broadleaved indigenous hardwoods
Indigenous scrub	Manuka and/or Kanuka; Matagouri or Grey scrub; Fernland; Flaxland; Sub-alpine shrubland; Mangrove
Exotic forest	Exotic forest; Forest – harvested; Deciduous hardwoods
Exotic scrub	Gorse and/or Broom; Mixed exotic shrubland
Exotic grass	High producing exotic grassland
Other grassland	Low producing grassland; Depleted grassland
Cropland	Short-rotation cropland, Orchards, vineyards or other perennial crops
Bare	Transport infrastructure; Surface mine or dump; Sand or gravel; Landslide; Gravel or rock; Permanent snow and ice
Wetland	Herbaceous freshwater vegetation; Herbaceous saline vegetation
Water bodies	Lake or pond; River; Estuarine open water

The land use of an area that contributes to a monitoring point can be used to inform the natural state or background concentrations across a region. An assessment of the relative area of natural state versus developed land is especially important when interpreting water quality signatures and to varying degrees hydrochemical signatures. Specifically, natural state areas tend to exhibit source limitation with respects to land use derived contaminants whereas developed systems are more often transport limited in terms of contaminants. Biogeochemical processes, such as redox evolution, also respond strongly to land use inputs, resulting in high rates of internal cycling than some natural state environments.

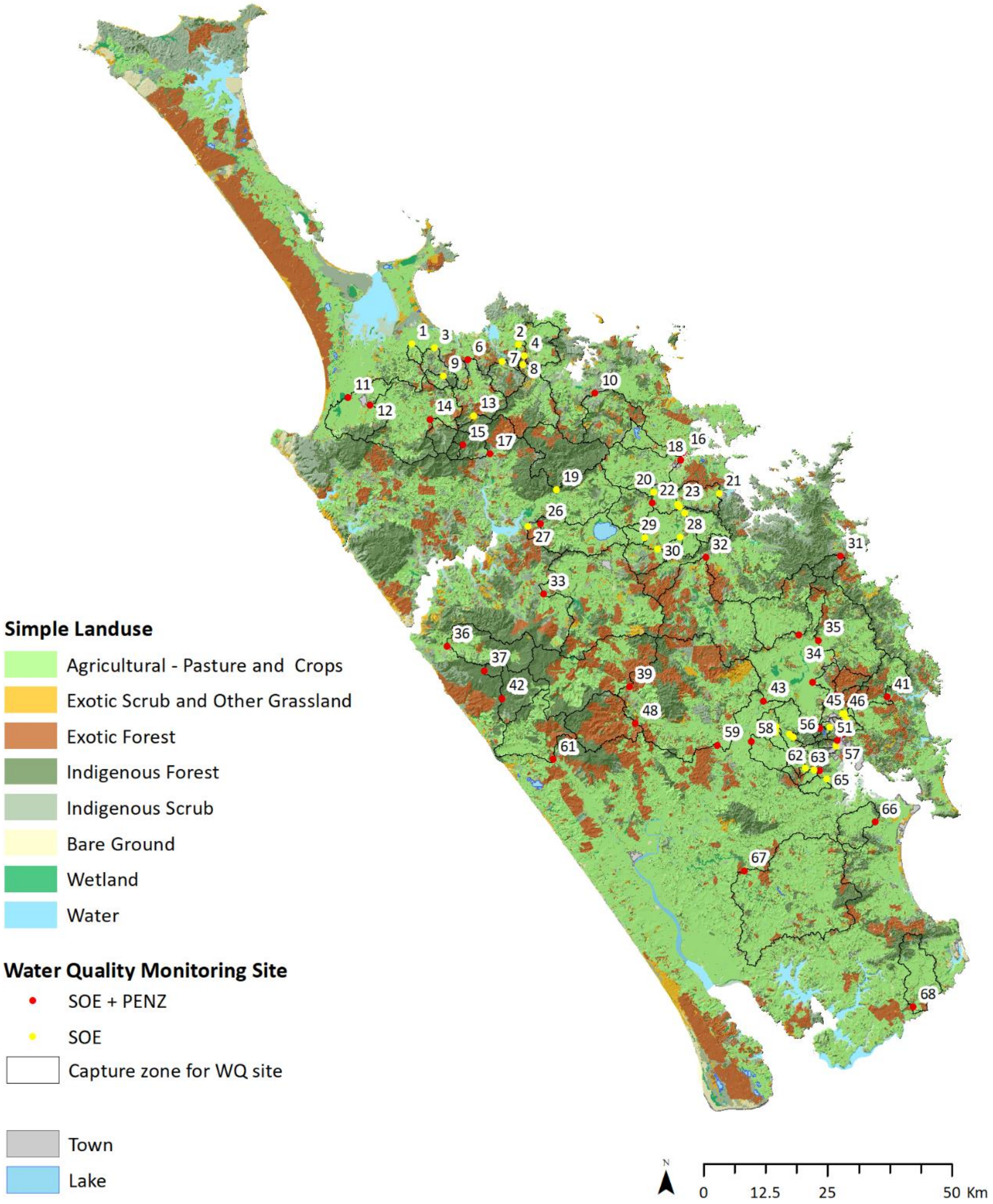

Figure 5. 9: Land cover as a proxy for land use in the Northland region.

Pukenui at Kenehiana Drive has the largest capture area of the surface water monitoring sites at 80,024 ha, however only 33% of the capture zone is in agricultural production (Figure 5.10). Mangahahuru at Main Road has the largest area of agricultural land but proportionally Pekepeka at Ohaeawai has the highest agricultural influence with over 98% of the capture zone under a pastoral land use (Figure 5.10 and 5.11). Waiharakeke at Stringers Road, Opouteke at Suspension Bridge, and Kaeo at Dip Road have entirely natural state catchments above the monitoring points.

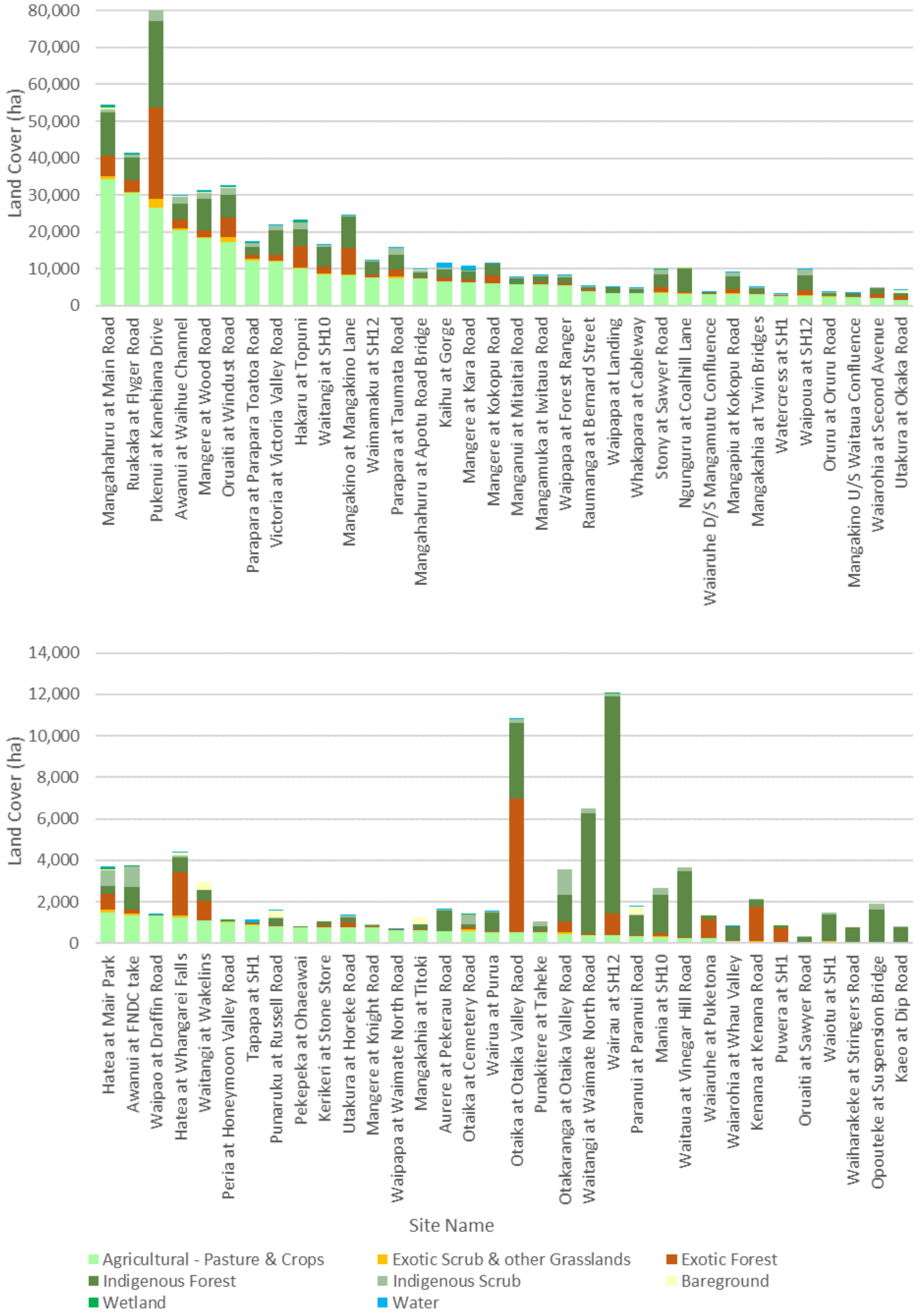

Figure 5. 10: Relative land cover by area of agricultural land within Northland surface water sites.

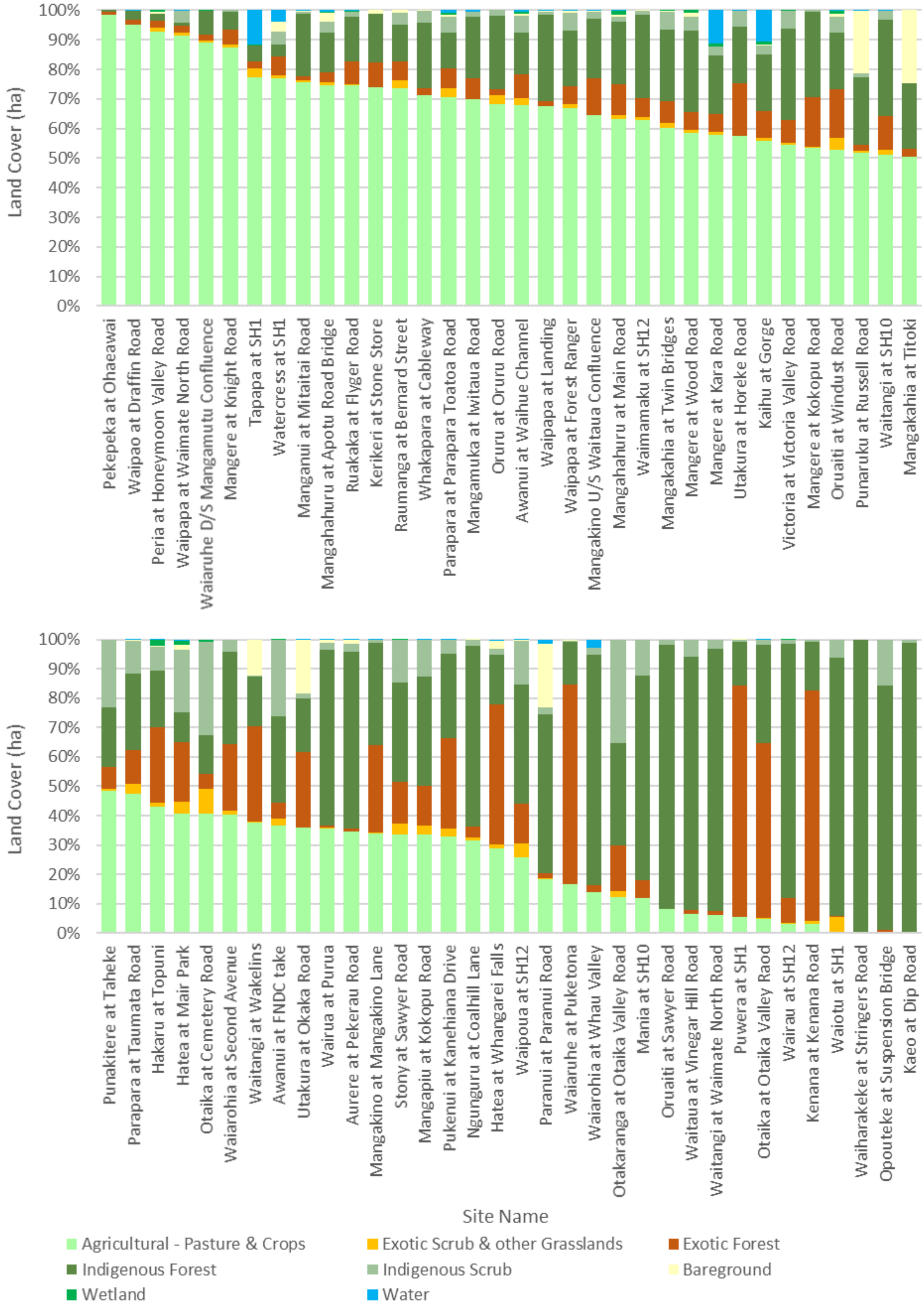

Figure 5. 11: Proportional land cover by area of agricultural land within Northland surface water sites.

6 Hydrological Process-Attribute Layer

6.1 Introduction

The purpose of the Hydrological PAL (H-PAL) is to characterise the source of surface and ground waters, which includes identification of the mechanism by which water is recharged, the degree of hydrological connectivity to the broader hydrological network and identification of smaller scale variation in the landscape attributes governing the likely path water takes across the landscape.

Water is the vehicle that transports land use derived contaminants from the land to water and the perennial hydrological network is the key distributor. Drainage from the northern portion of a catchment may be a key control over water composition and quality at its most distal sampling point. In addition to the perennial stream network, finer grained variation in topography and soil hydrological properties determine the pathway water takes to the stream channel (Figure 6.1). Specifically, deep drainage or 'vertical percolation' of water through the soil to underlying aquifers; lateral drainage, where water mainly moves horizontally through the soil zone, commonly in association with subsurface artificial drains to an open drain or surface water body, and; overland flow that results in water running off across the land surface directly to open ditches or natural waterways.

The pathway water takes from the land to stream is a strong influence over the type of water quality outcomes (e.g. sediment vs. nitrate) as well as the magnitude of export. Specifically, it is widely recognised that the export of sediment, nutrients and microbes generally increases across the soil permeability and drainage continuum (Rissmann et al., 2018). Therefore, when attempting to understand the spatial variation in water quality within a distributed hydrological network it is important to recognise the source of water and the probable hydrological pathways water has taken to the stream channel. The H-PAL layer produced here is designed to be used in conjunction with finer scale flow path mapping (i.e., paddock scale mapping of runoff pathways to identify discharge points).

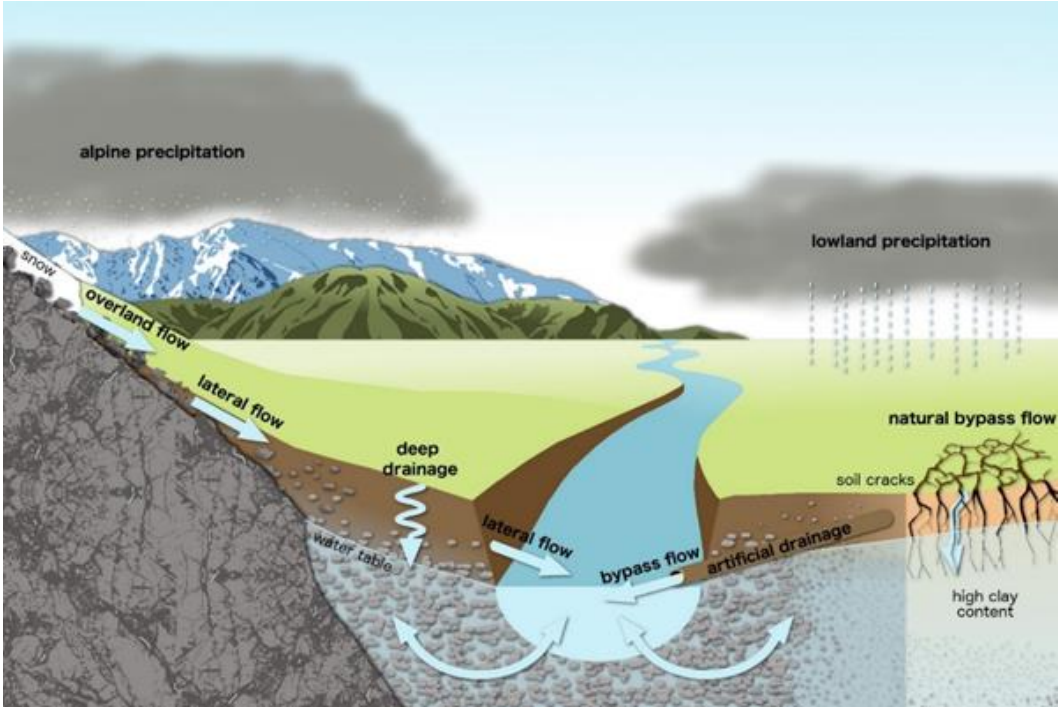

Figure 6. 1: Summary of water source and hydrological flow pathways.

6.2 Hydrological Domain: Water Source and Recharge Mechanism

The concentration of marine-derived salts in surface water and shallow groundwater is a powerful tool for understanding water source (where it is recharged). Importantly, gradients in these tracers of water are governed by the synoptic climatic setting and topography. Many studies, both nationally and internationally, have documented the spatial relationship between topography and both the stable isotopes of water (i.e., $\delta^{18}O$-H_2O and $\delta^{2}H$-H_2O, V-SMOW) and the concentration of marine aerosols (e.g. sodium (Na), chloride (Cl), and bromide (Br)) in precipitation (Nichol et al., 1997; Kendall and O'Donnell; Clark and Fritz, 1997; Baisden et al., 2016). These and other studies note that the concentration of marine aerosols in precipitation generally decline with altitude and distance from the coast and that the stable isotopes of water become increasingly negative with altitude. Importantly, recognising that topographic gradients play a key role in the variation of the signatures of stable isotopes and the concentration of marine aerosol concentrations in precipitation enables these measures to be used to constrain the source of water prior to its redistribution by the surface hydrological network.

For example, surface water and groundwater sourced from higher altitude catchments are often characterised by lower concentrations of marine aerosols such as sodium (Na), chloride (Cl), and bromide (Br) (Rodway et al., 2016). Whereas streams and shallow groundwater derived from low altitude precipitation, especially low altitude coastal areas, tend to show higher concentrations of marine aerosols. Using this information in conjunction with landscape attributes it is possible to discriminate between water source and associated mixing of waters from different altitudes or 'recharge domains'. This knowledge is important when attempting to understand 'how' and 'why' water quality varies between catchments, aquifers and monitoring sites. The dominant marine aerosols in precipitation are Cl and Na, although magnesium (Mg) and sulphate (SO_4) may be locally important. Bromide (Br) is also a marine aerosol but occurs in lower concentrations. Local deviation from a predominantly marine aerosol source for Cl, Br and Na may be associated with intrusion of seawater into coastal aquifers, potential connate seawater or due to geothermal activity (i.e., Ngawha). However, with the exception of coastal aquifers and recent marine sediments strong deviation from a marine aerosolic source for Cl and Br is unlikely although Na may be enriched in response to weathering of primary minerals (Rodway et al., 2016; Beyer et al., 2016).

6.2.1 Application to Northland

In order to better understand the general relationship between topography and the concentration of marine aerosols in Northland's ground and surface waters, correlation and Principal Component Analysis (PCA) was undertaken on log-transformed and z-scored median data following the recommendations of Güler et al. (2002) for hydrochemical datasets. The two main inputs for statistical analysis were: (i) conductivity, Na, Cl, Br, Mg, SO_4 concentrations from surface water monitoring sites, and; (ii) the landscape attributes altitude (m RSL), easting (m) and northing (m) for the capture zone of each respective monitoring site.

Correlation analysis on transformed data was undertaken prior to PCA to assess the representativeness of each analyte with regards to water source. The correlation matrix (i.e., Pearson, Spearman and Kendall matrix, Appendix 1) provides a measure of the strength of correlation (r) and the statistical significance between marine aerosols in water and the key landscape attributes. From the correlation matrix it is evident that Na, Cl, Br and to a lesser degree SO_4 are negatively correlated with northing and altitude and positively correlated with easting. Notably, conductivity is not correlated with easting or altitude and only weakly correlated with northing ($r = 22.0$, but not statistically significant at 0.05). Although conductivity is correlated with Cl ($r = 0.63$), its magnitude is influenced by a range of crustal processes and as such is not always a suitable tracer of hydrological water source and in particular altitude. Magnesium is also uncorrelated with northing and altitude yet exhibits a weak negative correlation with easting (r =

0.32), reflecting a likely geological control. As with conductivity, the concentration of Mg in precipitation is low, relative to the abundance of Mg in most soil and aquifer materials, with the marine-derived Mg component rapidly overwhelmed by crustal sources. Accordingly, correlation analysis reveals that Mg and conductivity are poor tracers of water source for the Northland data set and should not be used in PCA.

Principal Component Analysis was run on median surface water measures of Cl, Na, Br and SO_4 and attendant topographic measures (i.e. altitude, easting and northing) (Table 6.1). PCA identified 2 significant eigenvalues (>1.0) that collectively explain 74% of the variance. As with correlation analysis, PC-1 eigenvectors show negative weightings between marine aerosols and both altitude and northing and positive weightings for easting. PC-2 indicates a secondary control over variability associated with both northing and elevation with positive weightings for SO_4. Assuming the distribution of monitoring sites with aerosol data are broadly representative this suggests a primary altitudinal control and a secondary topographic control associated with an east-west gradient. As with other parts of New Zealand these findings are consistent with a generalised topographic control over the Na, Cl, Br and to a lesser degree SO_4 for Northland surface waters (Nichol et al., 1997; Rodway et al., 2016).

Table 6. 1: Principal Component Analysis of hydrological tracers for water source. Variables included are easting, northing, median elevation RSL, Na, Cl, Br, and SO_4.

Variance Table

Component No.	Eigenvalue	Cumulative Variance	Percent	Cumulative
1	4.13	4.13	0.59	0.59
2	1.04	5.16	0.15	0.74
3	0.78	5.94	0.11	0.85

Eigenvectors

	Component 1	Component 2	Component 3
Easting	0.33	-0.37	-0.59
Northing	-0.36	0.58	0.16
Median elevation RSL	-0.35	-0.58	0.20
Br	0.43	0.15	-0.00
Cl	0.43	-0.11	0.46
Na	0.41	-0.05	0.54
SO_4	0.33	0.40	-0.28

Regional median groundwater measures of Na, Cl, Mg and SO_4 concentrations are approximately 2 times the concentration of surface waters indicating a greater component of evaporative concentration in the soil zone prior to recharge and/or mixing with seawater (Table 6.2). An in-depth discussion of solute provenance in regional groundwaters is provided in section 5.2.

Table 6. 2: Median aerosol concentrations for Northland surface water and groundwater.

Groundwater	**Na**	**Cl**	**Br**	**Mg**	**SO_4**
Valid Cases	37	37	37	37	37
Mean	54.6	71.1	0.3	9.5	17.3
Median	36.0	43.0	0.1	7.0	9.9
Coefficient of Variation	1.2	1.5	1.5	0.9	1.2
Minimum	9.4	11	0.0	0.5	0.5
Maximum	360	640	2.2	51	110
Surface Water	**Na**	**Cl**	**Br**	**Mg**	**SO_4**
Valid Cases	36	36	36	36	36
Mean	19.9	29.2	0.2	4.4	7.4
Median	13	17	0.1	3.7	4.7
Coefficient of Variation	1.4	2.1	2.6	0.8	1.3
Minimum	8.3	13	0.0	1.6	2.4
Maximum	140	386	2.7	20	56.7

6.2.2 Hydrological Domain Map

Altitudinal variation across Northland is subdued relative to other parts of the country, and as such lesser contrast in marine aerosol concentrations are anticipated. Surface water monitoring sites are also predominantly at the distal end of the stream reach at which point recharge domain signals are mixed. Despite the current limitations in the data, a topographic control over marine aerosol concentration is still apparent within the monitoring data.

Hypothesise: Hydrological tracers of water source will vary according to the proportional area of different hydrological domains within the capture zone of a surface water monitoring site. Specifically, Na and Cl will decrease as the proportional area of ‘high-altitude’ land increases within the capture zone of a surface water monitoring site.

Inspection of plots of median altitude versus median Na, Cl, and SO_4 identify a distinct inflection at 180 – 200 m RSL below which marine aerosol concentrations increase within the surface water data (Figure 6.2). The preliminary classification of Northland into recharge domains according to altitude uses this inflection point to discriminate between high-altitude (≥200 m RSL) and low-altitude (<200 m RSL) recharge.

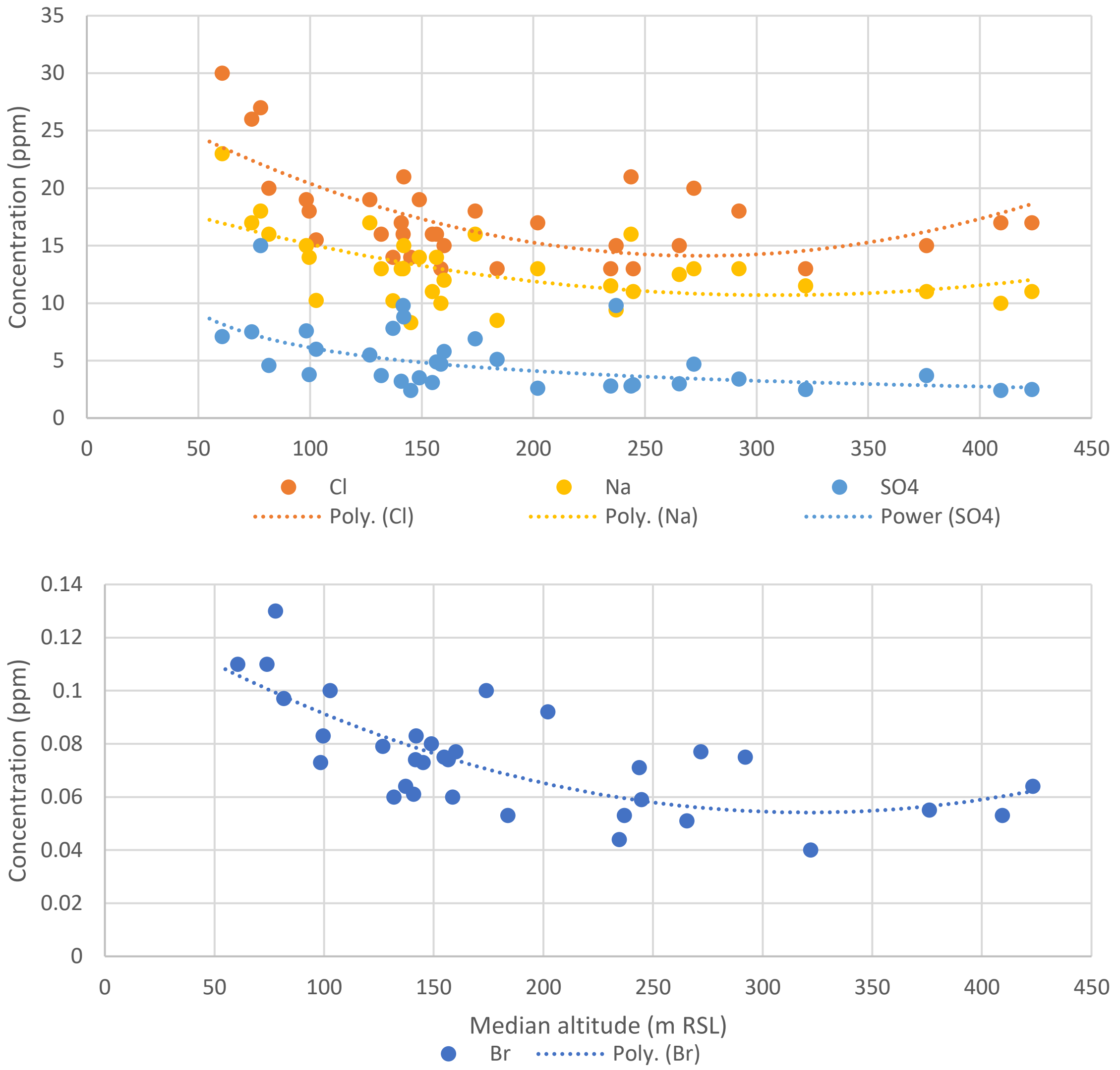

Figure 6. 2: Median altitude versus median Na, Cl, SO_4 and Br.

In ArcGIS, separation into high and low altitude recharge domains is spatially well correlated with annual average temperature, rainfall distributions for the region (Chappell, 2013) and modelled long-term average $\delta^{18}O$-H_2O (V-SMOW) and δ^2H-H_2O (V-SMOW) (Baisden et al., 2016). Figure 6.3 provides a preliminary map of Northland hydrological domains as defined by marine aerosol composition and geological substrate (Figure 6.3).

Within the domain recharge layer, the geological classification of rock type from the NZLRI was used to classify the underlying regolith into 3 classes: bedrock, weathered regolith, and unconsolidated. Unconsolidated materials have the highest aquifer potential to contribute to the surface water network. In this 3-tier classification, unconsolidated materials are assumed to have the highest aquifer potential and weathered regolith the lowest in terms of shallow groundwater contribution to the regional surface water network (Cameron et al., 2001). However, we stress that the magnitude of groundwater contribution is likely to be strongly controlled by soil hydrological properties (see Molenat et al., 2008; Wilson et al., 2014; Zomolt et al., 2015) and for this reason, the coarse aquifer potential classification should only be used in conjunction with soil hydrological information. Addition of the stream network (i.e. REC) to the spatial domain layer provides additional constraint over the likely hydrological connections between shallow aquifers and streams.

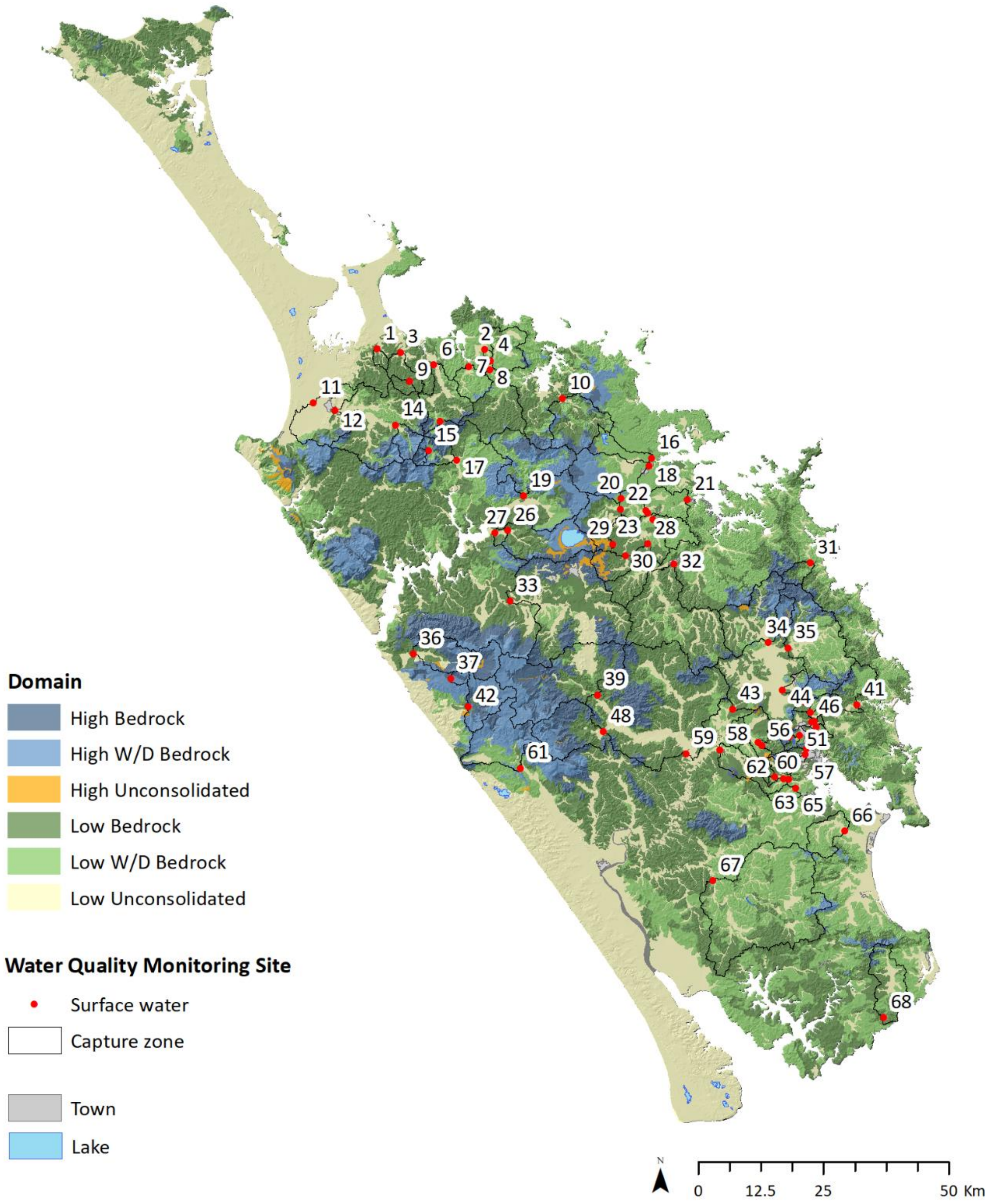

Figure 6. 3: Hydrological domain for Northland Region.

The area of each hydrological domain within a capture zone of a surface water monitoring site is shown in Figure 6.4, with the proportional area by high altitude recharge domain displayed in Figure 6.5. Sites with the largest areas of high altitude recharge areas will have a higher flushing and dilution potential, than those sites comprised of predominantly low altitude recharge domain. Wairua at SH12, Tapapa at SH1 and Pukenui at Kanehiana Drive have capture zones solely within the high-altitude domain. The median contribution of high altitude water source is 22%. Sites with a higher proportion of unconsolidated regolith will have a larger contribution to the stream network from aquifers for an equivalent soil hydrological composition. The capture zone of Wairua at Purua has the largest contributing area from unconsolidated regolith at 15,393 ha (28% of the capture zone), while Pekepeka at Ohaeawai has the largest proportional contribution from unconsolidated areas at 45% (490 ha).

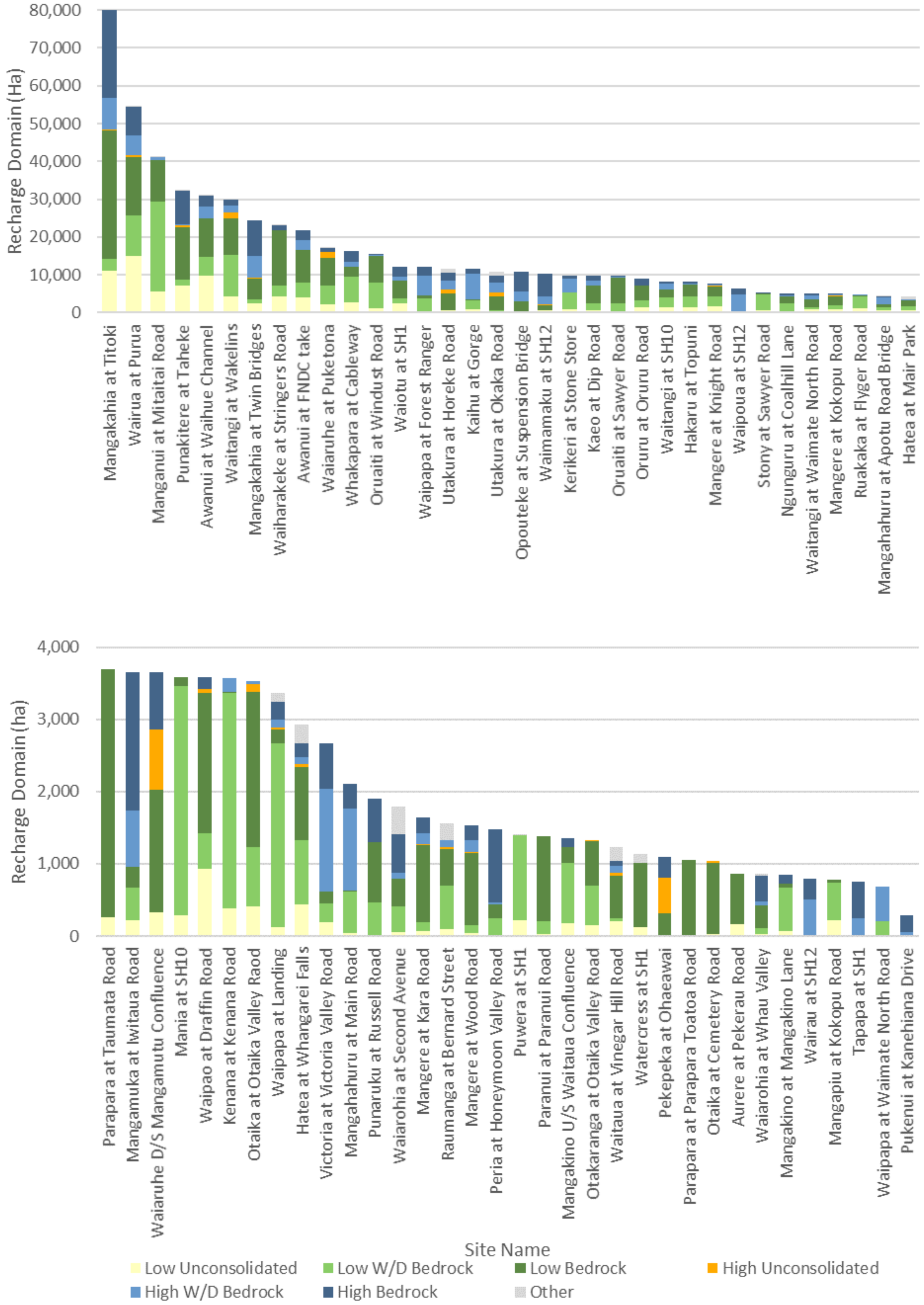

Figure 6. 4: Recharge domain area for Northland surface water sites (towns and lakes are shown as other).

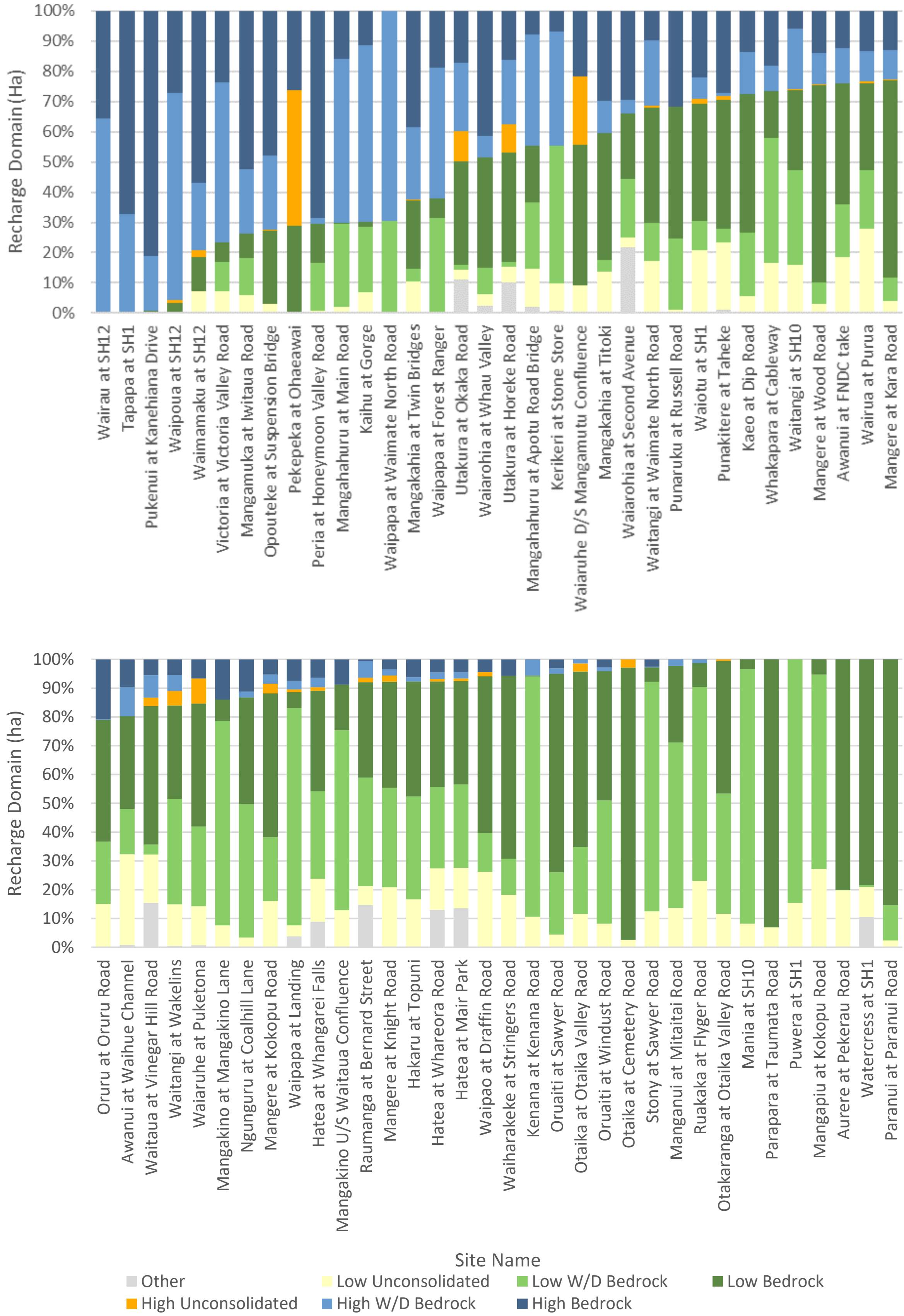

Figure 6. 5: Proportional domain area by high altitude recharge for Northland surface water monitoring sites (towns and lakes are shown as other).

We anticipate that this layer will be refined in response to additional regional sampling and the inclusion of data from other regions of New Zealand. Specifically, the recharge domain layer would benefit from isolated sampling of streams from the main 'high altitude' (>200 m RSL) areas of the region to provide additional contrast over the hydrological tracers of water source. Precipitation samples from both lowland coastal and high-altitude areas would also help better constrain the local topographic control over marine aerosol concentration, and as such, the source of waters supplying local streams and those shallow aquifers not influenced by seawater.

6.3 Flow Path Analysis

The pathway water takes across the landscape is strongly influenced by slope and soil hydrological properties. In conjunction with water source, the hydrological pathway is a key determinant of water composition and quality. The transport of water and contaminants to the surface water network is facilitated by baseflow from connected aquifers, lateral soil zone flow and overland flow (surficial runoff). For aquifers, soil drainage must percolate to depth through the subsoil and any undifferentiated sediments overlying the shallow water table aquifer. In some settings, stream flow may also infiltrate the shallow riparian aquifer. At certain times of the year and/or in response to the natural and modified properties of the surficial soil environment, water may bypass the soil matrix. Bypass flow via macropores may be associated with cracking soils, artificial drainage (both surficial open ditches, and subsurface mole-pipe drainage) and/or relic features such as root traces or burrows made by soil fauna. Within developed landscapes with slowly permeable and/or poorly drained soils, modification from artificial drainage as ditch or pipe and in cohesive soils as mole-pipe (tile) drainage is typically the most important bypass mechanism. This section investigates the relative proportions of the hydrological flow paths for the Northland Region and the development of GIS layers for overland flow, lateral drainage, artificial drainage, and deep drainage.

6.3.1 Application to Northland

The key controls over water pathway relate to climate, topography and soil hydrological properties (Pearson, 2015a, b). A simple assessment of the relationship between area weighted elevation and soil drainage class for Northland's surface water monitoring sites and key indicators of flow path (such as Total Coliforms, *E. coli*, K, ammoniacal and organic nitrogen and turbidity) is provided below prior to the development of a more evolved classification of hydrological pathway.

Areas of well-drained soils with a low % of precipitation occurring as overland flow (OLF) are dominated by deep vertical drainage ('profile drainage') to the underlying aquifer. In these locations, shallow flow paths associated with lateral drainage or surficial OLF are less important resulting in lower particulate export to streams (Katsuyama et al., 2001; Katsuyama and Ohte, 2002; Kasuyama et al., 2009; Inamdar , 2012; Rissmann and Beyer 2018; Rissmann and Pearson, 2018). On the other hand, areas or stream capture zones characterised by a larger proportion of poorly drained soils and steep slopes are associated with a greater quick flow response, and in areas of developed land a larger component of particulate transport to stream (Rissmann et al., 2018). Across areas of developed land discharge via subsurface artificial drainage ('mole-pipe') and surficial runoff (overland flow) is often associated with a greater colloidal type signal including larger *E. coli*, dissolved organic carbon (DOC), ammoniacal and organic nitrogen (TKN) concentrations.

A Spearman-Pearson-Kendall correlation matrix applied to log10 transformed and z-scored data shows a negative correlation (r = 0.67) between median (or mean) altitude and soil drainage class (DC), indicating a larger proportion of imperfectly to poorly drained soils across lowland areas. Total coliforms and *E. coli* versus soil DC, weighted by the area of developed land, are both positively correlated (r = 0.63 (T. coli) and 0.51 (*E. coli*)) indicating an increase in bacterial concentrations as the area of imperfectly to poor drained soils increases within the capture zone of a monitoring site.

Turbidity (r = 0.72) and measures of absorbance (r = 0.68 to 0.74, 330, 440 and 770 nm) versus soil DC also exhibit a positive correlation and Secchi disk is negatively correlated (0.66) with soil DC. Ammoniacal and organic (TKN) forms of nitrogen are strongly positively correlated (0.82) with soil DC weighted by the area of developed land. Notably, TP (0.61), relative to DRP (0.41), exhibits a stronger positive correlation with soil DC suggesting a greater component of Particulate Phosphorus (PP) export to streams for capture zones associated with a larger proportion of imperfectly to poorly drained soils. Finally, K, SO_4 and DOC all exhibit a positive correlation with soil DC indicating a greater proportion of shallow lateral and surficial flow path contributions to stream. Important here is the recognition that regional groundwaters with a clear meteoric signature are not associated with elevated *E. coli*, DOC and are unlikely to contain significant particulate P, or export appreciable ammoniacal or organic nitrogen to stream (Section 5). This and the knowledge that the volumetric contribution of soil water via shallow lateral and surficial runoff increases as soil drainage class decreases supports a strong soil hydrological control over water quality variation in addition to land use.

6.3.2 Overland Flow Layer

Overland flow (OLF, or surficial runoff) is cited as a key pathway for land-based contamination to enter waterways (Deakin et al., 2016; Goldsmith and Ryder, 2013; Orchiston et al., 2013; Curran Cournane et al., 2011; McKergow et al, 2007; McDowell, 2006; Smith and Monaghan, 2003). Where conventional hydrological assessments refer to overland flow as purely surface runoff we note a significant component of ‘A’ and/or ‘O’ horizon water in event runoff (Rissmann and Beyer, 2018; Rissmann and Pearson, 2018; Inamdar et al., 2011). Therefore, the contribution of overland flow commonly includes both surface and shallow ‘A’ and ‘O’ horizon waters under event conditions (see Inamdar et al., 2011 and references therein).

Overland flow is driven by two main mechanisms relating to the hydrological status and character of the soil. Specifically, saturation excess and infiltration excess OLF events. Saturation excess events occur when soils approach saturation and there is little capacity for precipitation to infiltrate the deeper soil zone (Srinivasan et al., 2002). The second type of OLF occurs when precipitation intensity exceeds the rate at which water can infiltrate the soil and is referred to as infiltration excess or Hortonian runoff (Horton, 1940). Infiltration excess OLF is difficult to predict as it can occur at any time of the year under varying soil moisture conditions. The likelihood of infiltration excess OLF occurring can be increased by animal treading damage, or heavy cultivation restricting soil permeability. On flat land, infiltration excess OLF will result in surface ponding (Needelman et al., 2004).

In reality, OLF may be driven by both permeability and saturation limitations, although it is apparent that the highest frequency of runoff events in general, occur during times when soil water content is elevated (Smith and Monaghan, 2003; McDowell et al. 2005; Monaghan et al, 2016). High densities of artificial drainage likely restrict the frequency and the duration of OLF by increasing the hydraulic conductivity and intrinsic permeability of the soil zone. However, bare paddocks associated with wintering by dense mobs of stock are known to reduce the permeability of soil thereby increasing the risk of surficial runoff and entrainment of contaminants (Drewry and Paton, 2000; Monaghan et al., 2016; Pearson et al., 2016).

The inherent susceptibility of the landscape to produce overland flow was assessed for the Northland region using a modified version of Pearson (2015a). The assessment uses soil (Fundamental Soils Layer, FSL) and topographical information (8 m Digital Elevation Model, DEM) in a GIS application to spatially depict saturation excess overland flow risk across the region as a percentage of annual rainfall. Overland flow risk is increased in areas where soils have poor internal drainage and are structurally vulnerable to slaking and dispersion, or in areas where there is sufficient slope to generate runoff.

The OLF assessment was developed by firstly combining soil texture, depth to slowly permeable layer and slaking/dispersion characteristics of the soil to calculate a hydrologic index, which was subsequently multiplied by a slope factor and expressed as a percentage of effective annual rainfall. Polygons with soil siblings were proportionally weighted to account for variation due to secondary soils. For each FSL soil polygon, the average slope was calculated using the national 8 m DEM. The hydrological index represents the likelihood of overland flow occurring due to the soil properties, while the slope index indicates whether the topography is a significant factor. The layer produced identifies the inherent risk and is independent of land use management practices or vegetation cover (Figure 6.6). It is important to note these factors can have a significant impact on the occurrence of overland flow (Pearson, 2015a).

The potential occurrence of overland flow by agricultural and non-agricultural land within each surface water monitoring site is shown in Figure 6.7 and sorted by proportion of agricultural land in Figure 6.8. Parapara at Parapara Toatoa Road has the highest potential for overland flow at 60.5% of annual rainfall and Pekepeka at Ohaeawai the lowest at 5.9%. Overland flow from land that is predominantly agricultural has a higher potential contaminant load, than overland flow originating in natural state areas. Therefore, Aurere at Pekerau Road, with a potential 31.2% from agricultural land may pose a greater risk to water quality than the sites with a larger proportion of non-agricultural land and yet a higher runoff potential (Figure 6.8).

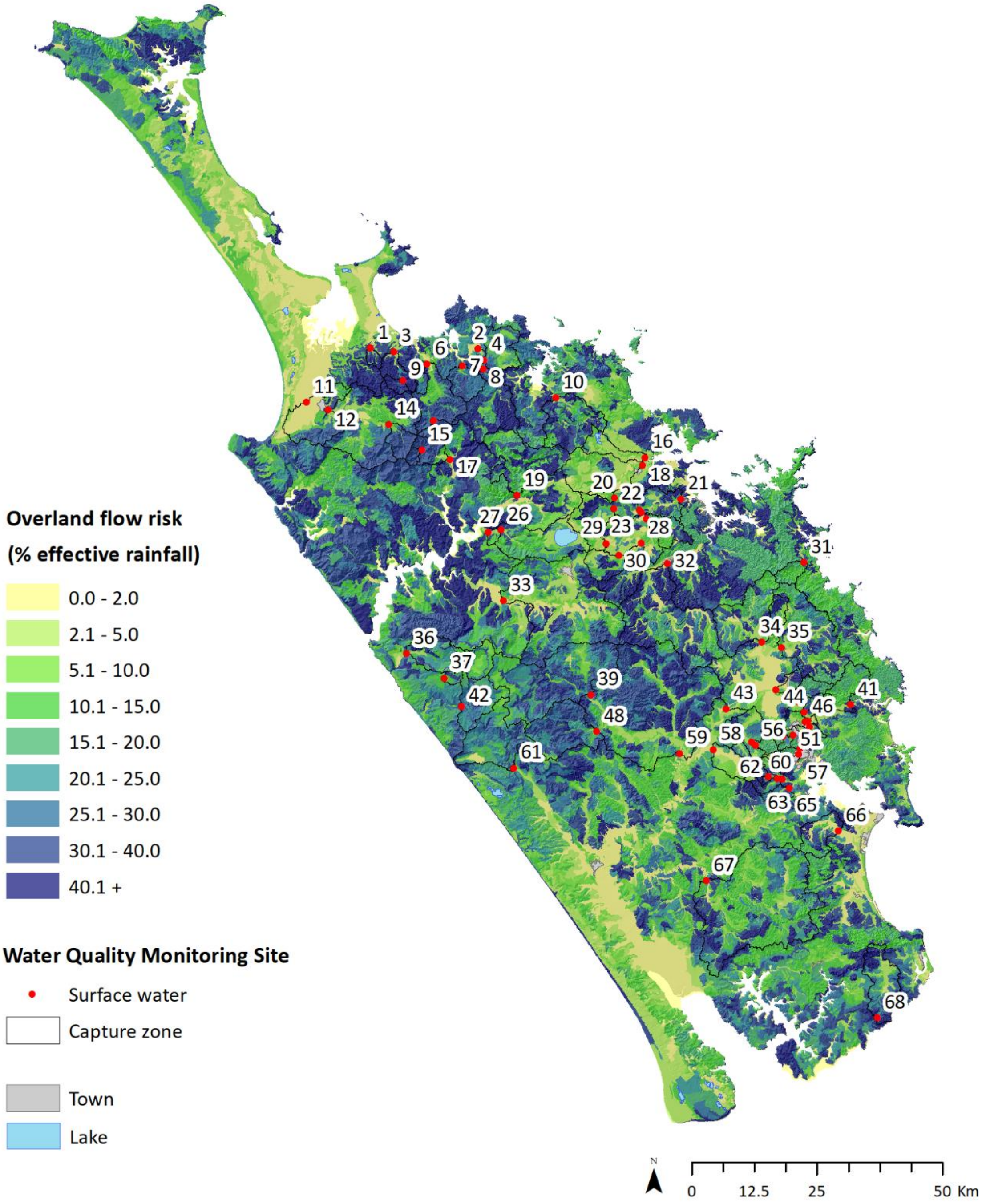

Figure 6. 6: Overland flow risk for the Northland Region expressed as a proportion of annual rainfall.

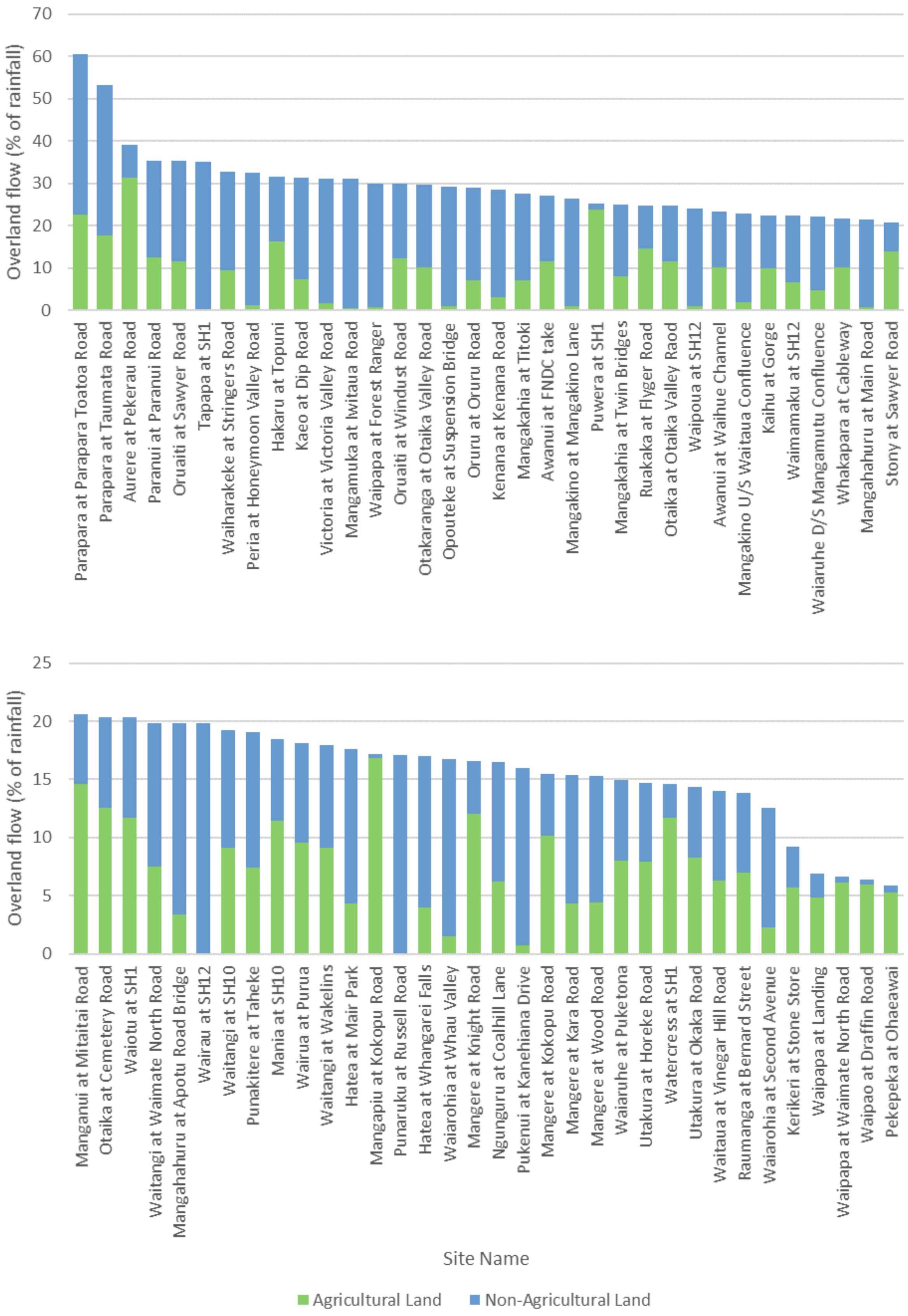

Figure 6.7: Overall overland flow risk for Northland surface water sites from agricultural and non-agricultural land.

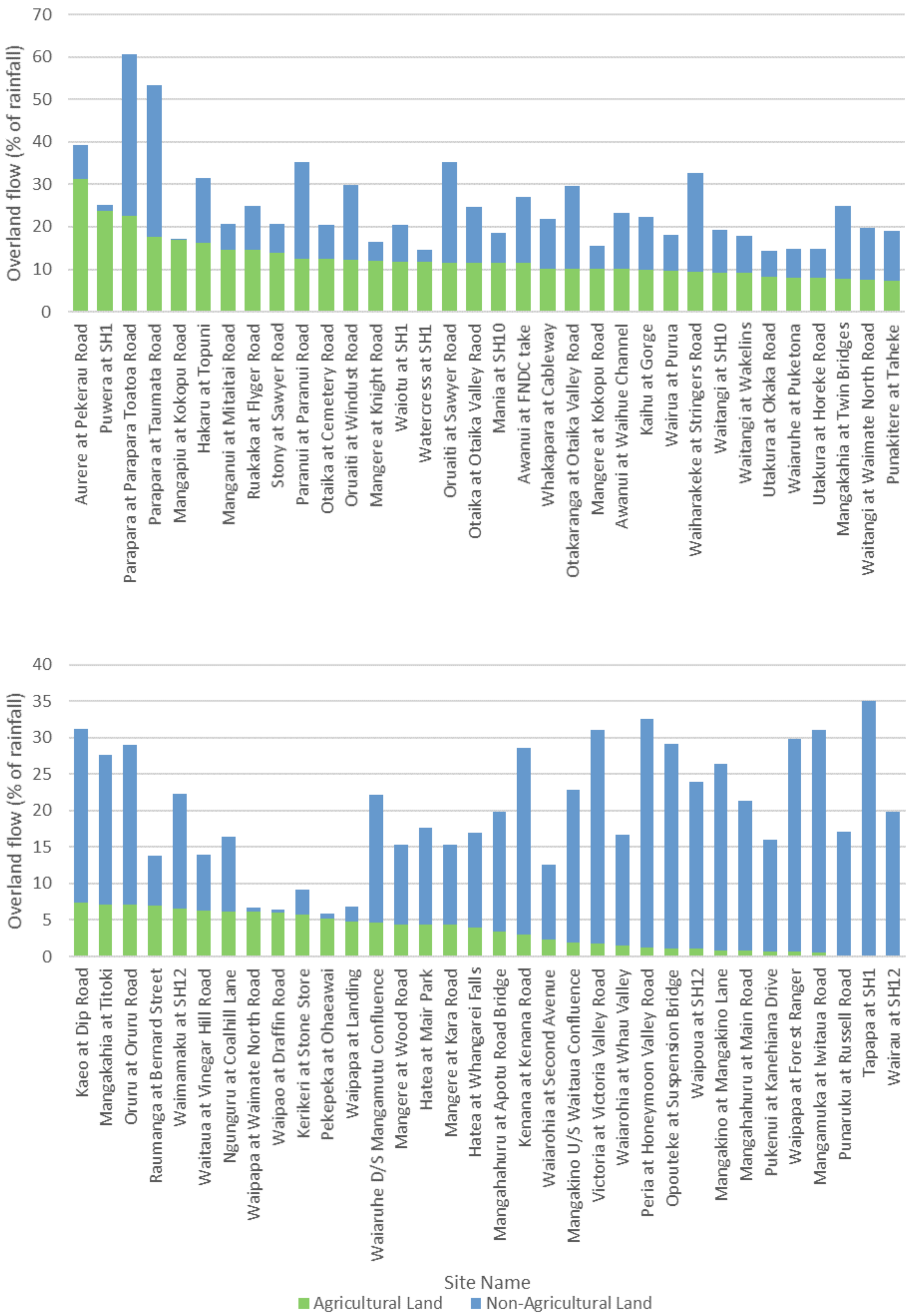

Figure 6.8: Overland flow risk for Northland surface water sites from agricultural and non-agricultural land.

6.3.3 Lateral and Artificial Drainage Layers

Lateral soil flow occurs when water infiltrating through the soil intersects a layer with lower vertical permeability. Water flows along the contact between the higher and lower permeability layers (e.g. within a permeable topsoil overlying a slowly permeable subsoil). In areas of low relief, water may accumulate to form a perched water table. Lateral flow is likely to be an important transport mechanism in hill country areas where thin sloping soils overlie slowly permeable bedrock, and in lowland areas identified as having moderate to highly permeable topsoil overlying a slowly permeable subsoil. This hydrological process is a critical consideration within the redox PAL as water can become reducing due to saturation above or at the contact with bedrock or slowly permeable layers.

An assessment of the potential lateral flow contribution was developed by modifying Pearson's (2015b) method for assessing areas modified by artificial drainage to focus on the soil attributes controlling lateral drainage. The lateral flow layer was created by firstly combining attributes of soil drainage class with permeability as in Pearson (2015b). Polygons with soil siblings were proportionally weighted to account for variation due to secondary soils. Lateral drainage is expressed as a 1 to 5 score, with 1 having a low proportion of soil zone drainage water moving laterally and 5 having a high proportion of lateral drainage.

The lateral flow layer produced for Northland includes areas of lateral flow occurring through artificially modified drainage networks (Figure 6.9). This is an assumed classification given it is not possible to map actual subsurface drainage density. Ground truthing of an equivalent estimation for the Southland Region showed a strong correlation between estimated and actual drainage densities (Pearson, 2015b).

To assess the proportion of potential modification to the drainage characteristics of the soil by artificial drainage, the lateral drainage assessment is combined with landscape attributes of slope and land cover as a proxy for land use. Artificial drainage occurs in areas used for agricultural production. The Land Cover Database (LCDB4.1) was used as a proxy for land use by selecting areas of high producing exotic grassland, short rotation cropland, and orchards, vineyards or other perennial crops. Discussion with NRC staff identified other land cover types that potentially could be included in the agricultural land classification as other grasslands and exotic scrub (Table 5.8), however their development for agriculture is likely limited even if the areas are used for grazing (pers. comm. D. Kervell, June 2018). Urban areas were not considered as part of this assessment. This area can be better refined through the addition of land use or drainage information. Artificial drainage, which occurs as both subsurface drains and/or open ditch drains, are typically used in areas of low relief. A threshold of <12 degrees was used for the Northland Region. This value was discussed with NRC and local experts with knowledge of drainage practices in the region. The resulting classification for 'None' was refined after these discussions to show areas with high deep drainage and those areas with slopes greater than 12 degrees. The resulting 'potential' artificial drainage layer is shown in Figure 6.10.

Of the surface water capture zones, Mangapiu at Kokopu Road has the largest proportional area which is artificially drained (Figure 6.11).

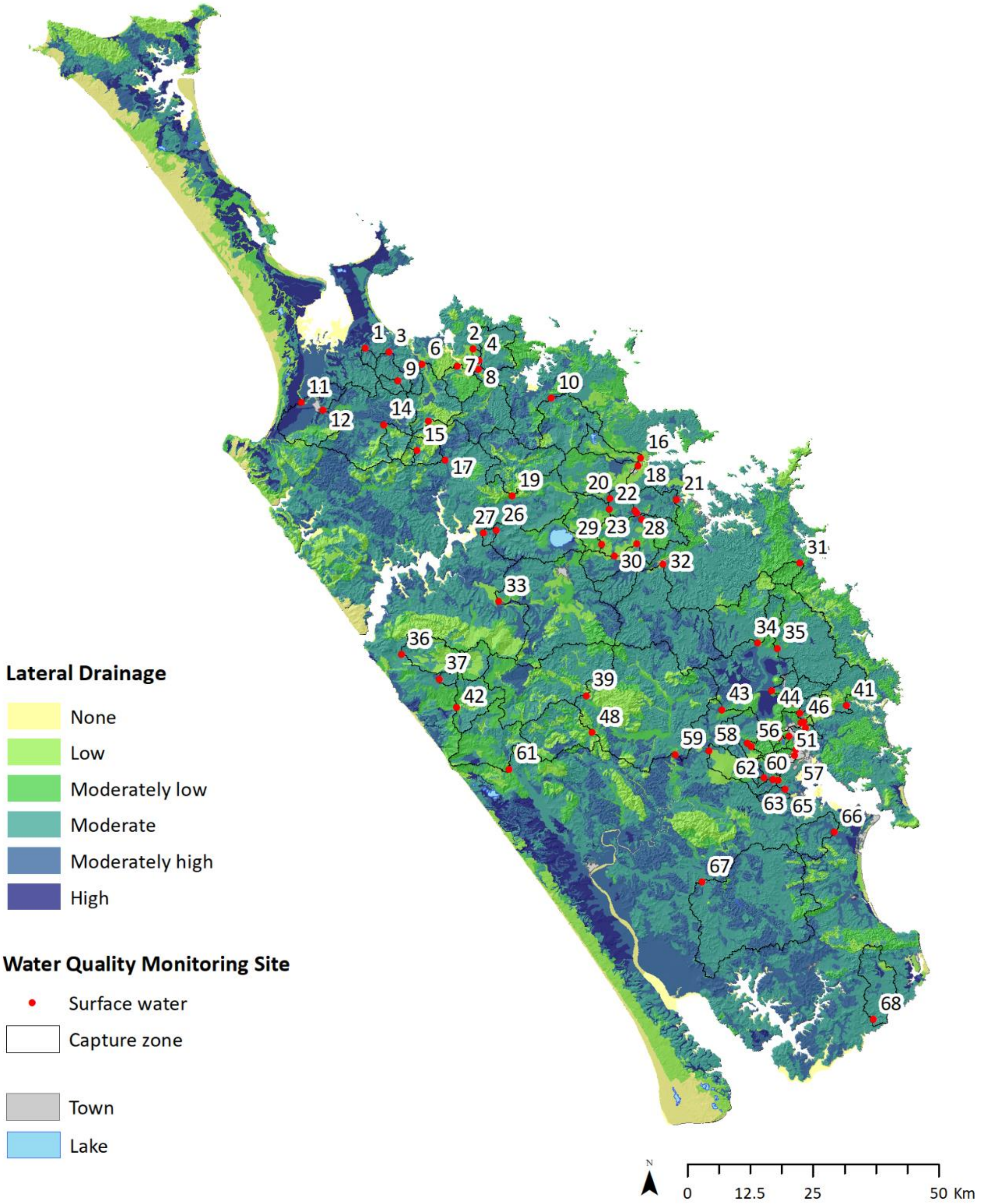

Figure 6. 9: Soil zone lateral drainage for the Northland Region. Lateral drainage includes the proportion of drainage water travelling laterally through artificial drainage networks.

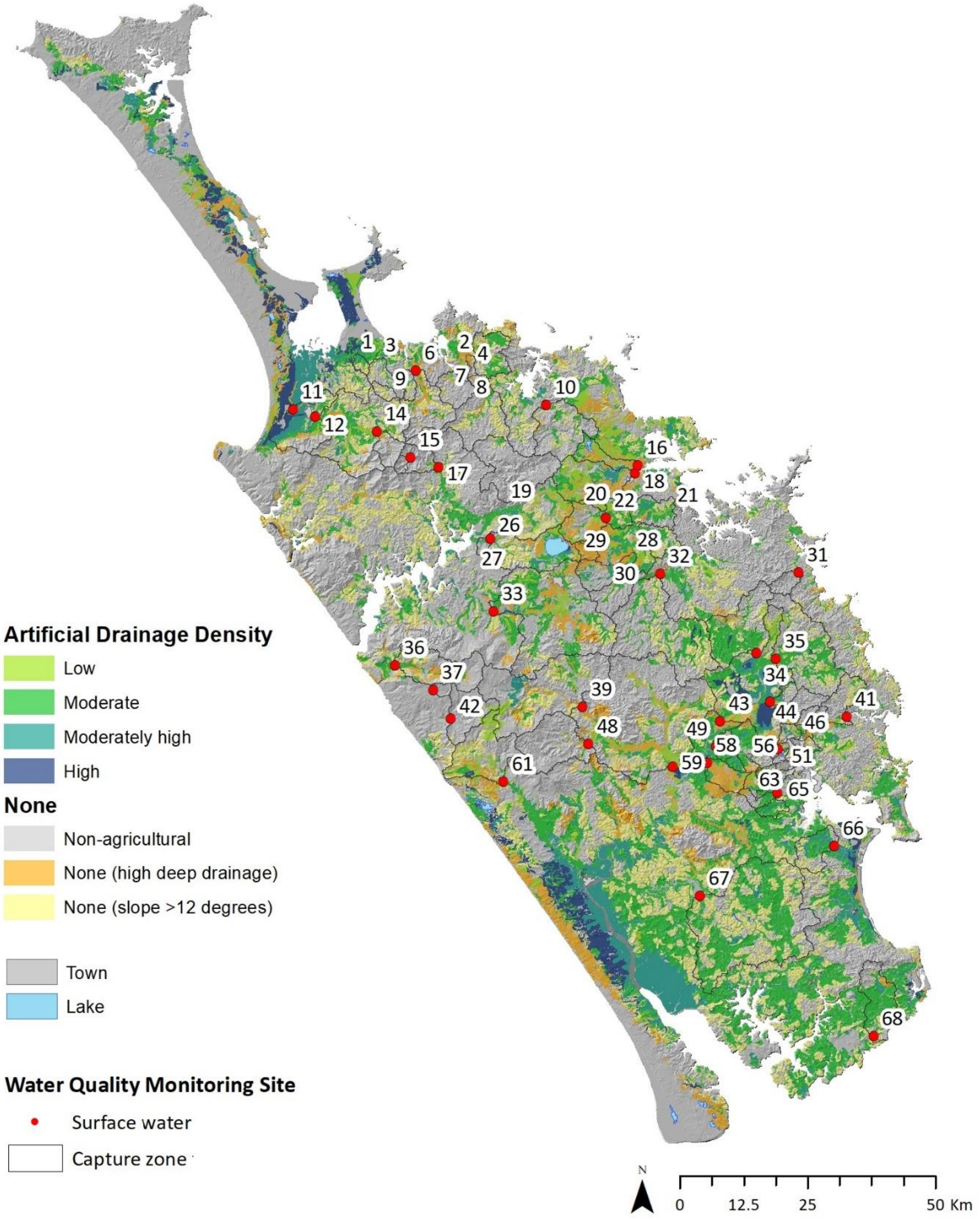

Figure 6. 10: Potential artificial drainage estimates for the Northland Region. Agricultural areas classified as having no artificial drainage are either non-agricultural, on sloping land greater than 12 degrees, or on well-drained soils with no slowly permeable horizons within 1m of the soil profile.

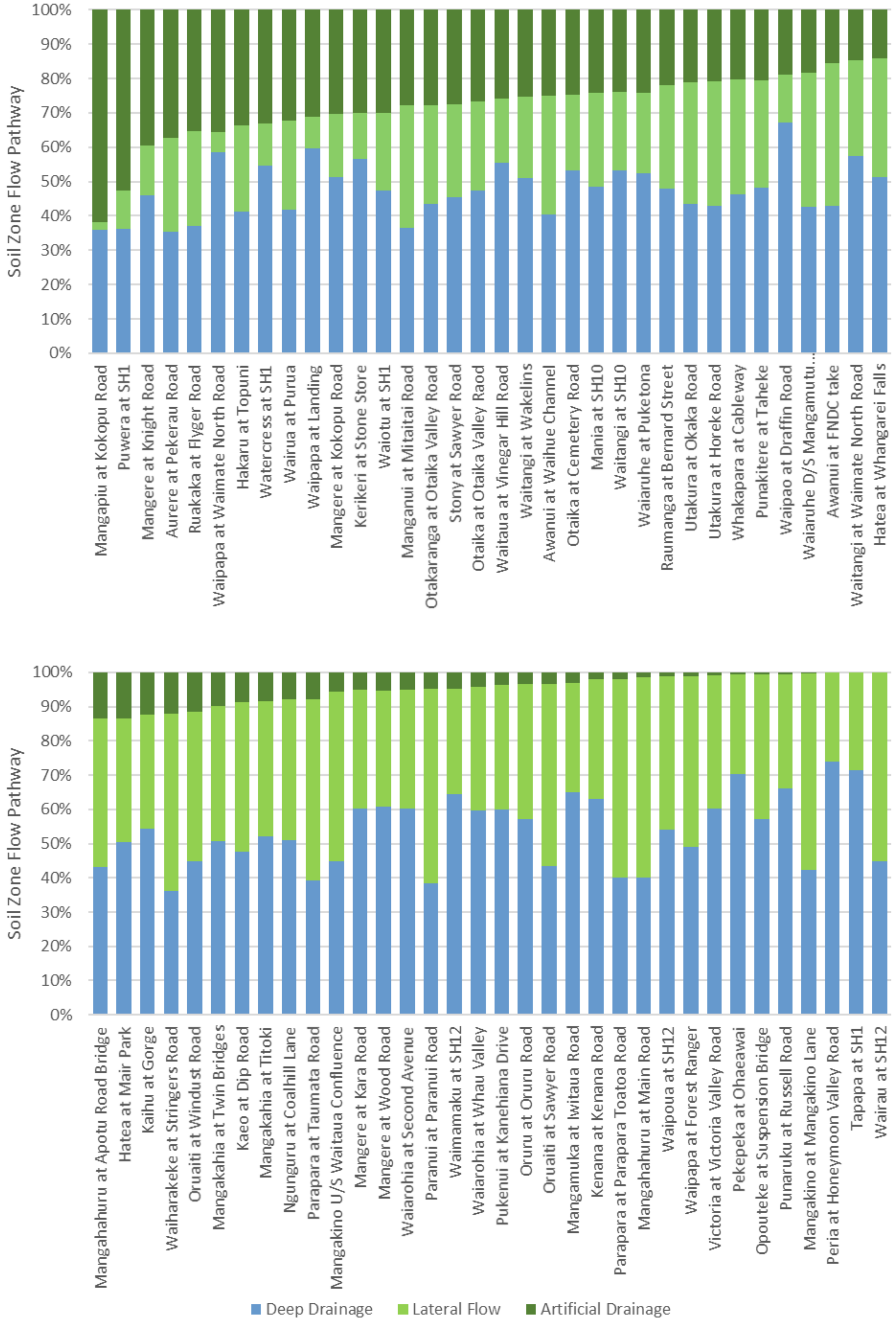

Figure 6. 11: Soil zone drainage pathways for Northland surface water sites sorted by artificial drainage.

6.3.4 Deep Drainage Layer

Deep drainage occurs from the percolation of rainfall through the soil zone to underlying aquifers. A qualitative indication of deep drainage can be derived from the inverse of the lateral flow assessment combined with the hydrological domain. Figure 6.12 provides a spatial model of the areas where deep drainage is likely to be occurring across the Northland Region. Areas of high deep drainage are associated with better-drained soils and unconsolidated recharge domains and to a lesser extent, areas of weathered regolith.

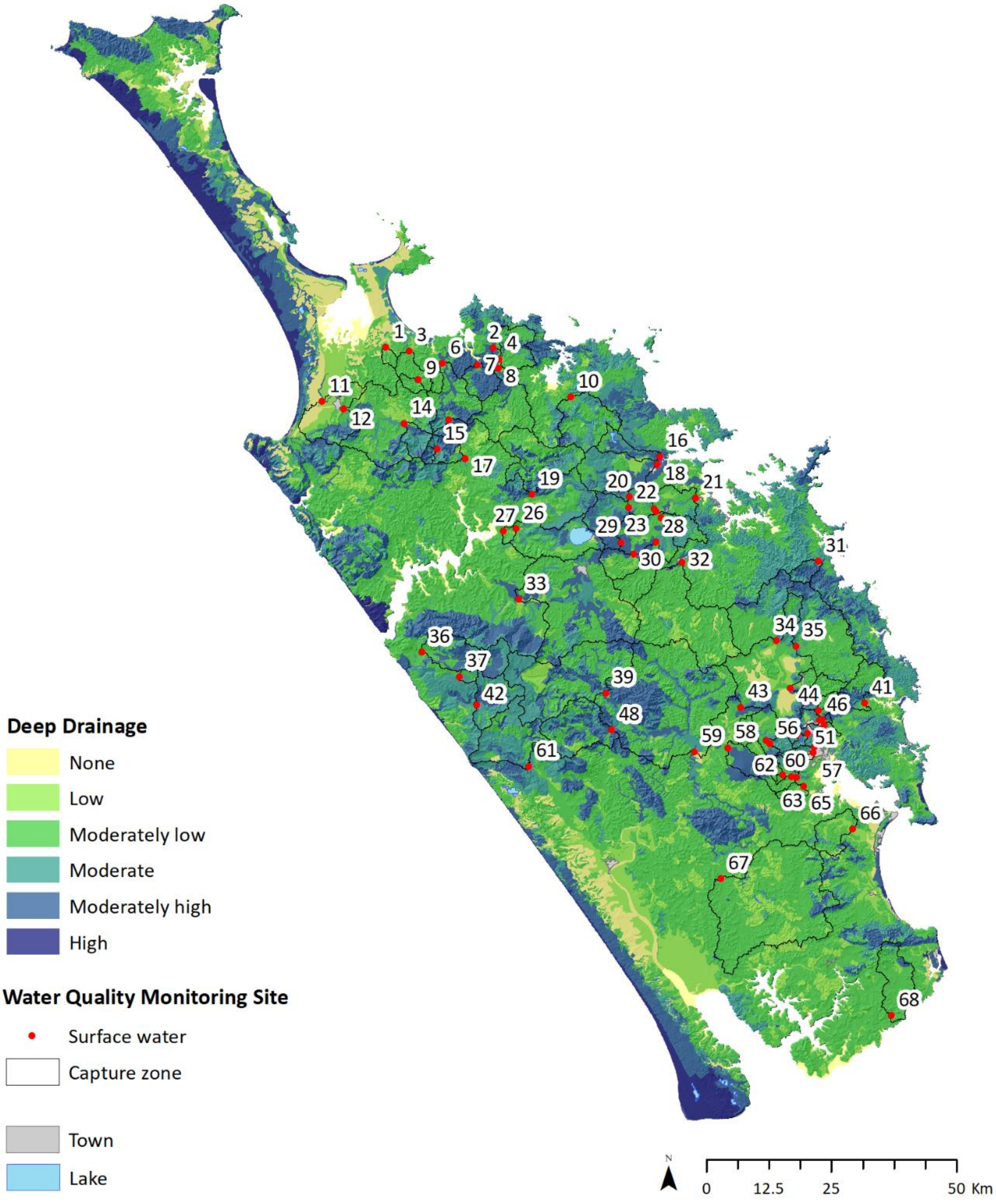

Figure 6. 12: Deep drainage for the Northland Region.

Departure from anticipated water flux pathway may occur seasonally where clay-rich soils comprised of expansive clays crack in response to soil moisture deficit. Under this scenario, instead of migrating laterally drainage waters may bypass the poorly permeable soil matrix, transporting contaminants to subsurface drainage networks and/or the under aquifer (Rissmann et al., 2016). These soils exhibit temporal variation in flow path, with the rehydration of desiccated clays driving the closure of cracks under cooler conditions and lower rates of evapotranspiration. Knowledge of the extent of shrink-swell soils is therefore critical to any understanding of spatial variation in water quality outcomes. We note this as a priority for future work for the Northland Region.

The soil zone proportional hydrological flow pathways for the surface water monitoring sites are shown in Figure 6.13. Peria at Honeymoon Valley Road has the highest proportion of water moving laterally as deep drainage. As demonstrated in the correlation matrix in Section 6.3.1, the pathway water takes to leave the land surface and the proportion of agricultural land are important factors controlling contaminant loss.

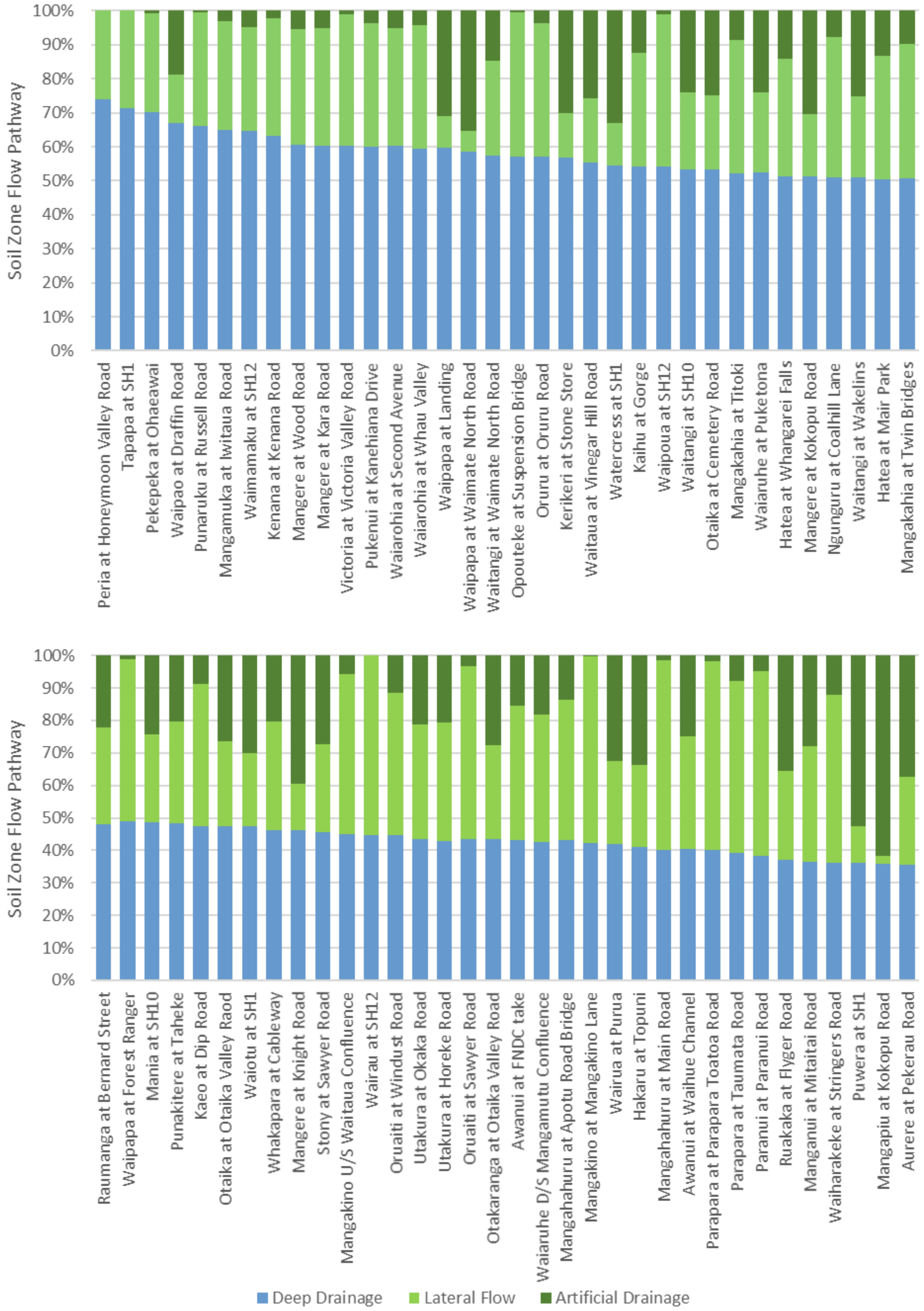

Figure 6.13: Soil zone drainage pathways for Northland surface water sites sorted by deep drainage.

6.4 Summary of Hydrological Layers (H-PAL) and Recommendations

An integrated picture of soil hydrological and aquifer relationships along with a clear understanding of hydrological water source is a necessary platform for estimating spatial variation in shallow groundwater and surface water quality across Northland. The preliminary H-PAL information also serves to highlight spatial variation in soil-aquifer-stream connectivity, which is critical to aquifer recharge and surface water hydrological response.

The recharge domain layer produced for Northland provides a reasonable platform for discriminating recharge source and can be used as preliminary water source layer for the Northland region. Water source information may be improved via sampling of headwater streams in the main high-altitude areas delineated by the Recharge Domain layer and where possible via collection of precipitation across altitudinal transects. In addition to refining water source estimates, such data can help to constrain the volumetric, solute and particulate mass flux from different recharge domains and its redistribution via the hydrological network (Rissmann et al., 2016b). The relative contribution of seawaters or geothermal fluids to shallow aquifers, springs or surface waters can also be constrained via the inclusion of relatively conservative tracers such as Cl, B and Br. Northland Regional Council staff are best placed to select sites of relevance for additional sampling of these key tracers of water and solute source.

In addition to water source and distribution via the hydrological network, the mapping of soil hydrology greatly refines the conceptual understanding of the hydrological pathways water and attendant contaminants take to stream and shallow aquifers across the region. For example, areas of high to moderately high deep drainage identify key areas of aquifer recharge and potentially elevated nitrate ingress (Figure 6.12). When used in conjunction with Domain and Domain Class (e.g. low unconsolidated, high unconsolidated) and aquifer lithology and type (e.g. permeable fractured basalt vs. poorly permeable mudstones) areas of higher groundwater recharge rates can be constrained. Importantly, soils with a high potential for aquifer recharge are associated with c. 16.4% of the Northland region, with the majority occurring in association with fractured basalts (both low and high altitude) and windblown coastal sands.

Development of a layer of soils prone to ‘shrink-swell’ behaviour may be an important qualifier of the spatiotemporal patterns in aquifer recharge dynamics with cracking soils facilitating bypass during the drier months of the year. Shallow aquifers that are overlain by shrink-swell soils tend to exhibit rapid recharge response followed by a dampened response to subsequent recharge as soils re-hydrate and cracks close in response to lower rates of evapotranspiration (Rissmann et al., 2016; Rissmann et al., 2018).

For regions such as Northland characterised by a large area of imperfectly to poorly drained soils overlying poorly permeable bedrock, the rapid decanting of shallow aquifers to stream is raised as a possible key hydrological mechanism (Katsuyama et al., 2001, 2009; Molenat et al., 2008; Inamdar, 2012 and references therein). Similar phenomena have been observed across Southland where the shallow alluvial aquifer is rapidly exhausted over the late spring and early summer with contributions from deeper fractured rock aquifers dominating during late summer and autumn (Rissmann and Beyer, 2018; Rissmann and Pearson, 2018). Age dating of baseflow under low aquifer levels is therefore likely to provide a maximum estimate of baseflow lags (Daughney et al., 2015) whereas much of the shallower groundwaters supplying stream, and the majority of contaminant load to streams, is likely to be much younger. Temporal stream flow analysis is likely to aid in the refinement of the conceptual understanding of aquifer lags across the region and provide important context to water quality management (see Molenat et al., 2008; Inamdar et al., 2012; Rissmann and Beyer, 2018, Rissmann and Pearson, 2018).

Although groundwater contributions to stream are likely an important control over in stream water quality during the summer months, it is considered likely that the relative volumetrically contribution to stream, and associated load, is likely to be small relative to that from soil and surficial layers across the majority of Northland. Specifically, the area of the region characterised by imperfectly to poorly drained soils (i.e., moderate, moderately low and low deep drainage) is large, comprising 83.6% of the total land area. Therefore, for the majority of the Northland area, lateral and surficial runoff paths are likely the dominant volumetric and contaminant (particulate and dissolved) export pathways to stream. A dominant soil zone influence over steady-state concentrations is consistent with the preliminary assessment of the relationship between surface water quality and soil hydrological properties in Section 6.3.1. In areas of developed land, characterised by imperfectly to poorly drained soils, artificial drainage either as subsurface mole-pipe or open ditch drainage is likely to be more common. Here, a much greater component of recharge is expected to move laterally to stream, or where the slope is not limiting, runoff in response to high-intensity rainfall. For the small area of Northland characterised by both permeable soils and aquifers, groundwater is expected to exert a greater influence over steady-state water quality signatures in the stream (Section 5.2).

Once again, the development of a layer of soils prone to ‘shrink-swell’ behaviour could be a potentially important qualifier of the spatiotemporal patterns of contaminant bypass to subsurface artificial drainage or in extreme instances the underlying water table aquifer. Green streams associated with Farm Dairy Effluent (FDE) irrigation over cracking soils that are artificially drained may be an important pathway of contaminant export to stream during the drier months of the year (Rissmann et al., 2016b).

In terms of future refinement of the H-PAL layers, there are a number of steps using existing data and or knowledge that could support additional refinement:

- Refinement of the soil hydrological flow pathways can be made through the inclusion of the following expert local knowledge:
    - Which soils series are prone to shrink-swell behaviour?
    - What are the local artificial drainage practices and where do they differ and why?
- Further resolution of sub-domains associated with marine aerosol gradients could be developed through:
    - Collection of high altitude stream samples (areas >200 m RSL) using the same physiographic sampling set. This would aid both in terms of water source but would also provide constrain over background concentrations of water quality measures from natural state areas. As with SOE sites we would 3 repeat measures at low, median and high flow to best constrain natural background levels.
    - Collection of precipitation samples across an elevation gradient, from sea level (or close) to highest rainfall gauge site. For precipitation data, we recommend analysis of Na, Cl, Br, SO_4, Mg and conductivity data.

7 Redox Process-Attribute Layer

7.1 Introduction

Redox is recognised as one of the most important processes controlling variation in water quality, both nationally and internationally (Moldan and Cerny, 1994; McMahon and Chapelle, 2008; Tratnyek et al., 2012). From studies of redox dynamics around the world, redox processes are known to control the form (speciation), and hence the mobility, of both N and P in addition to driving the process of denitrification through which NO_3 (nitrate) nitrogen is removed from water (Rissmann, 2011; Rissmann et al., 2012; Rissmann and Hodson, 2013; McMahon and Chapelle, 2008; Tratnyek et al., 2012)[4]. Redox processes also control the concentration of dissolved oxygen (DO), dissolved manganese (Mn^{2+}), dissolved iron (Fe^{2+}), sulphate (SO_4^{2-}) and the production of greenhouse gases such as the oxides of nitrogen (NOx), hydrogen sulphide (H_2S) and methane (CH_4). Ammoniacal forms of nitrogen are also produced under reducing conditions in areas with high organic carbon content (Ponnamperuma, 1972; Moldan and Cerny, 1994; McMahon and Chapelle, 2008; Tratnyek et al., 2012). Heavy metal solubility and mobility are also significantly influenced by redox processes.

In low temperature systems, redox evolution is mediated by bacteria and follows a successional sequence of Terminal Electron Accepting Processes (TEAPs): $O_2 > NO_3 > Mn^{4+} > Fe^{3+} > SO_4^{2-} > CO_2$ (Figure 7.1). Successional evolution of TEAP results in the transformation of O_2 to H_2O, NO_3 to gaseous N_XO (nitrous oxides) and/or N_2 (inert dinitrogen gas), Mn and Fe oxides and oxyhydroxides to dissolved Mn^{2+} and Fe^{2+}, and SO_4^- (sulphate) and CO_2 (carbon dioxide) to gaseous H_2S (hydrogen sulphide) and CH_4 (methane), respectively. The reduction of CO_2 to CH_4 represents the end point of the microbially mediated redox succession and is associated with the most reducing environments and subsequently waters. Peat aquifers are one example where the abundance of organic carbon and the absence of appreciable ferric oxides and oxyhydroxides results in the evolution of CO_2 reducing conditions (Ponnamperuma, 1972). Wetland soils are also known to produce CH_4 through redox succession. In other settings where electron donors are less abundant and/or drainage is good redox succession may be limited, with the system poised at O_2 reduction. In these systems, leached nitrate is able to accumulate without being removed. Across the Southland region the full range of TEAP is observed, however Fe^{III} reduction is by far the most common reflecting the large mass of iron in the earth's crust (Beyer and Rissmann, 2016; Rissmann et al., 2016).

Importantly, although an electron donor source is the primary control over redox succession, soils are not typically limited with respects to electron donors with an often-abundant supply of organic carbon from the upper horizons of the soil. Under these conditions, the frequency and duration of soil saturation is the key control over soil reduction potential (Seitzinger et al., 2006; Clough et al., 1998). As soil pores become saturated (at any level in the soil profile) the supply of meteoric oxygen is 'shut-off' kick-starting the chain of TEAP succession. The role of saturation of the soil over redox progression reflects the c. 10,000-fold reduction in the diffusivity of molecular O_2 through water relative to air-filled pores. Accordingly, the degree and duration of soil saturation exerts a key control over soil zone reduction with the indicators of soil reduction including low chroma colours, 'gleying' and 'percent mottling,' increasing along the soil drainage continuum (Ernstsen et al., 2006; Beyer et al., 2016; Webb et al., 2010). Due to the strong correlation between soil saturation and soil colour (chroma), percent mottling and iron pan formation these visual indicators of redox evolution are often used to assess soil drainage class (Milne et al., 1995). As organic soils are the result of organic matter accumulation under saturated conditions, redox succession is often advanced. Therefore, for regions characterised by larger areas of imperfectly to poorly drained soils, soil reduction process are often the dominant control, on an areal basis, over surface and groundwater

---

[4] It is important to note that whilst redox processes influence the mobility and form of P, they do not result in the removal of P.

redox signatures (Rissmann et al., 2016; Beyer et al., 2016; Beyer and Rissmann, 2016; Wilson et al., 2018).

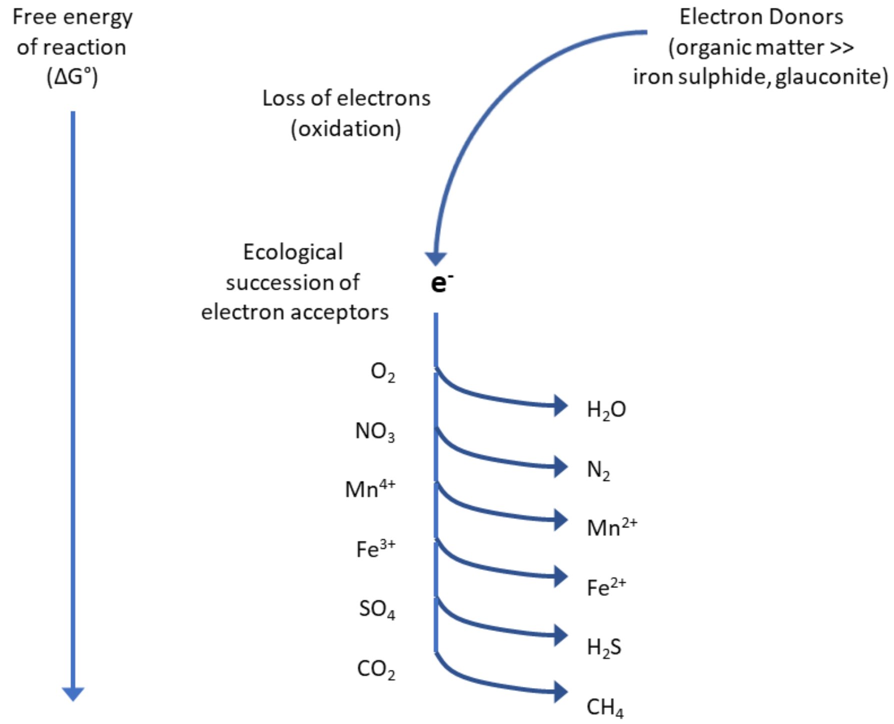

Figure 7.1: an Ecological succession of terminal electron acceptors in natural waters (modified from McMahon and Chapelle, 2009).

7.2 Application to Northland

7.2.1 Redox State

A summary of the General Redox Category, Terminal Electron Accepting Process (TEAP) and redox-sensitive species are provided in Table 7.1. All of Northland's surface waters, with the full suite of redox-sensitive species, are designated as Mixed (oxic-anoxic) and O_2- Fe^{III} reducing (TEAP) (see section 5.1). Given the importance of marine aerosol deposition over SO_4 and little evidence for the evolution of SO_4-reduction in regional soils, it is reasonable to assume that most of these waters appeared to be buffered by Fe^{III}-reduction.

As surface water median values are a measure of the integrated water source, their signature includes that of the shallow groundwater supplying stream. However, the volumetric contribution of shallow groundwater to the stream may be low in areas of imperfectly to poorly drained soils, especially those that are clay-rich. For this reason, temporal analysis of variation in surface water composition is recommended in order to isolate the relative volumetric and contaminant contribution from the three main compartments supplying a stream (Rissmann and Beyer, 2018; Rissmann and Pearson, 2018). For now, we proceed with evaluating the relationship between signatures of redox and landscape attributes.

Table 7. 1: Redox assignment and median concentrations of redox sensitive species

Type	Site_Name	Cluster	Redox Category	TEAP	DO	DOC	Fe	Mn	NNN	SO4	TKN	TN	TP
SW	Kaeo at Dip Road	1a1	Mixed(oxic-anoxic)	O_2-Fe(III)	9.3	2.80	0.310	0.042	0.030	7.80	0.14	0.18	0.01
SW	Kaihu at Gorge	1a1	Mixed(oxic-anoxic)	O_2-Fe(III)	10.3	1.90	0.240	0.013	0.200	4.70	0.15	0.36	0.01
SW	Mangahahuru at Apotu Road Bridge	1a1	Mixed(oxic-anoxic)	O_2-Fe(III)	9.3	3.60	0.850	0.031	0.310	6.90	0.24	0.54	0.05
SW	Mangahahuru at Main Road	1a1	Mixed(oxic-anoxic)	O_2-Fe(III)	9.9	2.50	0.430	0.031	0.130	2.60	0.14	0.28	0.02
SW	Ngunguru at Coalhill Lane	1a1	Mixed(oxic-anoxic)	O_2-Fe(III)	9.9	2.00	0.330	0.013	0.125	3.50	0.15	0.27	0.02
SW	Punaruku at Russell Road	1a1	Mixed(oxic-anoxic)	O_2-Fe(III)	9.8	1.40	0.300	0.038	0.015	3.20	0.11	0.12	0.01
SW	Utakura at Okaka Road	1a1	Mixed(oxic-anoxic)	O_2-Fe(III)	8.6	6.00	0.570	0.038	0.140	9.80	0.34	0.48	0.04
SW	Waiharakeke at Stringers Road	1a1	Mixed(oxic-anoxic)	O_2-Fe(III)	9.7	11.05	1.525	0.310	0.110	6.00	0.39	0.50	0.04
SW	Waimamaku at SH12	1a1	Mixed(oxic-anoxic)	O_2-Fe(III)	10.1	2.60	0.160	0.005	0.004	3.70	0.12	0.14	0.01
SW	Waiotu at SH1	1a1	Mixed(oxic-anoxic)	O_2-Fe(III)	9.3	3.50	0.560	0.037	0.255	4.70	0.25	0.62	0.05
SW	Waipapa at Landing	1a1	Mixed(oxic-anoxic)	O_2-Fe(III)	9.3	2.80	0.330	0.012	0.270	2.40	0.20	0.44	0.01
SW	Waipoua at SH12	1a1	Mixed(oxic-anoxic)	O_2-Fe(III)	10.5	2.10	0.180	0.004	0.013	2.40	0.10	0.11	0.01
SW	Wairau at SH12	1a1	Mixed(oxic-anoxic)	O_2-Fe(III)	9.4	3.00	0.360	0.011	0.003	2.50	0.15	0.15	0.01
SW	Wairua at Purua	1a1	Mixed(oxic-anoxic)	O_2-Fe(III)	9.2	4.20	0.800	0.021	0.313	9.80	0.39	0.68	0.06
SW	Waitangi at Waimate North Road	1a1	Mixed(oxic-anoxic)	O_2-Fe(III)	9.6	2.80	0.390	0.030	0.330	5.10	0.17	0.50	0.02
SW	Whakapara at Cableway	1a1	Mixed(oxic-anoxic)	O_2-Fe(III)	9.6	2.90	0.770	0.014	0.250	3.10	0.19	0.45	0.04
GW	Ngunguru Groundwater at Thompson P/S	1a2	Anoxic	Mn(IV)	0.1		0.002	0.045	0.008	16.00			
GW	Russell GW at 47 The Strand (Dr Jack Phillips)	1a2	Mixed(oxic-anoxic)	O_2-Fe(III)	6.8	1.40	0.130	0.080	0.050	6.75			
GW	Waipapakauri GW at Waipapakauri landing	1a2	Anoxic	Fe(III)	0.1		0.020	0.006	0.004	5.45			
SW	Awanui at FNDC take	1a2	Mixed(oxic-anoxic)	O_2-Fe(III)	8.3	3.25	0.385	0.030	0.017	3.80	0.21	0.24	0.03
SW	Awanui at Waihue Channel	1a2	Mixed(oxic-anoxic)	O_2-Fe(III)	8.1	4.45	0.545	0.049	0.035	4.60	0.41	0.48	0.09
SW	Hakaru at Topuni	1a2	Mixed(oxic-anoxic)	O_2-Fe(III)	10.2	5.20	0.490	0.021	0.180	7.50	0.37	0.60	0.08
SW	Mangakahia at Titoki	1a2	Mixed(oxic-anoxic)	O_2-Fe(III)	9.3	2.80	0.370	0.028	0.049	4.90	0.20	0.24	0.02
SW	Mangakahia at Twin Bridges	1a2	Mixed(oxic-anoxic)	O_2-Fe(III)	10.6	2.60	0.230	0.018	0.035	2.90	0.14	0.19	0.01
SW	Mangamuka at Iwitaua Road	1a2	Mixed(oxic-anoxic)	O_2-Fe(III)	9.4	1.50	0.126	0.035	0.004	2.80	0.10	0.10	0.04
SW	Manganui at Mitaitai Road	1a2	Mixed(oxic-anoxic)	O_2-Fe(III)	8.3	6.90	0.500	0.055	0.102	15.00	0.45	0.63	0.07
SW	Mangere at Knight Road	1a2	Mixed(oxic-anoxic)	O_2-Fe(III)	8.5	4.95	0.610	0.034	0.475	8.80	0.41	0.92	0.08
SW	Opouteke at Suspension Bridge	1a2	Mixed(oxic-anoxic)	O_2-Fe(III)	10.4	2.10	0.132	0.024	0.035	3.40	0.14	0.19	0.01
SW	Oruru at Oruru Road	1a2	Mixed(oxic-anoxic)	O_2-Fe(III)	8.1	1.80	0.305	0.039	0.020	3.70	0.13	0.17	0.04
SW	Otaika at Otaika Valley Raod	1a2	Mixed(oxic-anoxic)	O_2-Fe(III)	9.7	4.00	0.410	0.018	1.100	7.60	0.24	1.40	0.04
SW	Pukenui at Kanehiana Drive	1a2	Mixed(oxic-anoxic)	O_2-Fe(III)	10.3	2.20	0.260	0.022	0.099	2.80	0.11	0.21	0.03
SW	Punakitere at Taheke	1a2	Mixed(oxic-anoxic)	O_2-Fe(III)	9.9	5.30	0.720	0.025	0.380	5.80	0.30	0.69	0.04

SW	Ruakaka at Flyger Road	1a2	Mixed(oxic-anoxic)	O_2-Fe(III)	8.5	5.40	0.400	0.045	0.340	7.10	0.47	0.89	0.14
SW	Tapapa at SH1	1a2	Mixed(oxic-anoxic)	O_2-Fe(III)	9.6	0.95	0.027	0.003	0.018	2.50	0.10	0.10	0.05
SW	Victoria at Victoria Valley Road	1a2	Mixed(oxic-anoxic)	O_2-Fe(III)	9.6	1.40	0.087	0.014	0.004	3.00	0.10	0.10	0.02
SW	Waiarohia at Second Avenue	1a2	Mixed(oxic-anoxic)	O_2-Fe(III)	10.1	2.40	0.160	0.024	0.332	7.70	0.14	0.49	0.02
SW	Waipao at Draffin Road	1a2	Mixed(oxic-anoxic)	O_2-Fe(III)	10.4	2.60	0.150	0.006	2.500	5.50	0.27	2.80	0.04
GW	Glenbervie GW at Barron's Property, Ngunguru Rd	1b1	Suboxic	Suboxic	3.0	0.60	0.002	0.001	1.902	6.70			
GW	Managawhai GW at Mangawhai Golf Club	1b1	Mixed(oxic-anoxic)	O_2-Fe(III)	6.7	0.50	0.020	0.005	2.352	14.00			
GW	Matarau GW at Osbaldiston Bore	1b1	Mixed(oxic-anoxic)	O_2-Mn(IV)	6.1	0.65	0.002	0.026	4.302	1.60			
GW	Tauraroa GW at 88 Maungakaramea Road	1b1	Oxic	O_2	6.8	0.50	0.006	0.002	7.502	6.70			
GW	Three Mile Bush GW at Wise Bore	1b1	Oxic	O_2	6.1		0.002	0.001	2.302	6.40			
GW	Waipapa GW at 10 Pungaere Rd (D Hop owner)	1b1	Oxic	O_2	5.5	0.50	0.002	0.001	0.047	1.80			
GW	Whangarei GW at Foster Irrigation Bore	1b1	Oxic	O_2	6.9		0.005	0.001	3.802	3.10			
GW	Whatitiri GW at Tanekaha Partnership Irrigation	1b1	Oxic	O_2	8.9	0.65	0.002	0.001	7.002	2.30			
GW	Sandy Bay GW at WDC Toilets	1b2	Anoxic	Mn(IV)	0.5		0.003	0.400	1.702	47.00			
GW	Taiharuru GW at WDC Toilets	1b2	Anoxic	Mn(IV)	0.5		0.018	0.200	0.782	42.00			
GW	WDC toilet at Whangaumu Bay	1b2	Suboxic	Suboxic	1.4		0.002	0.001	0.142	56.00			
GW	Matapouri Groundwater at Smith P/S Beside Road	2a	Suboxic	Suboxic	4.9		0.003	0.004	1.130	41.00			
GW	Pataua North GW at WDC Toilets	2a	Anoxic	NO_3	4.2		0.009	0.001	8.904	39.00			
GW	Pataua South GW at Pataua public toilets	2a	Anoxic	NO_3	1.7		0.005	0.001	3.606	110.0			
SW	Hatea at Mair Park	2a	Mixed(oxic-anoxic)	O_2-Fe(III)	9.7	2.60	0.320	0.011	0.390	32.00	0.19	0.61	0.02
SW	Kerikeri at Stone Store	2a	Mixed(oxic-anoxic)	O_2-Fe(III)	10.0	2.60	0.355	0.008	0.350	56.65	0.19	0.52	0.02
GW	GW Bland Bay at M/C Ngatiwai t/Board Camp	2b	Oxic	O_2	5.1		0.002	0.001	8.602	14.00			
GW	Oakura GW at 3 Te Kapua Street (Patricia Wallis)	2b	Anoxic	NO_3	3.7		0.002	0.001	5.912	18.00			
GW	Taipa GW at Taipa High School	2b	Anoxic	NO_3	2.6		0.004	0.001	3.104	14.00			
GW	Taupo Bay GW at John Turner	2b	Oxic	O_2	5.2		0.002	0.001	3.802	7.90			
GW	Aupouri Groundwater at Houhora BG Fish Club	3	Anoxic	Fe(III)	0.1		0.094	0.019	0.004	15.00			
GW	Awanui GW at Vinac Farms	3	Anoxic	CH4gen	4.9		0.540	0.045	0.004	0.45			
GW	Cable Bay Groundwater at Croquet Club by Stream	3	Anoxic	Fe(III)	0.5		3.600	0.220	0.005	25.00			
GW	Coopers Beach Ground Water at Youth Camp	3	Anoxic	Fe(III)	2.8	5.00	1.120	0.300	0.005	21.00			
GW	Mangawhai GW at Caravan Pk Bore Garden tap	3	Anoxic	Fe(III)	0.1		0.056	0.023	0.007	12.95			
GW	Mangawhai GW at Mangawhai Hideaway Camp	3	Mixed(oxic-anoxic)	O_2-Fe(III)	8.4		1.200	0.150	0.004	5.60			
GW	Ruawai GW at Kaipara D/C Bore 5	3	Anoxic	Fe(III)	0.2	0.85	0.240	0.120	0.004	5.80			
GW	Whananaki North GW at WDC Toilets	3	Anoxic	Fe(III)	0.1	1.50	1.900	1.200	0.007	20.00			

If surface water monitoring sites are considered representative of the broader Northland region, a dominance by mixed(oxic-anoxic) redox assignments indicates all surface water sites are influenced to varying degrees by reduction. Regional GW shows a wider range of redox conditions and attendant TEAP from O_2 (oxic) through to CO_2-reduction (anoxic). Even in areas of oxidising aquifers, surface waters contain signatures of soil zone reduction suggesting either hyporheic and/or reduced soil zone drainage. Given the ubiquity of imperfectly to poorly drained soils across the region a significant soil zone role over SW reduction signals are not unexpected (see also Beyer and Rissmann et al., 2016a,b; Rissmann et al., 2018a,b). Despite the predominance of a mixed redox category for regional SW, there is still evidence for a redox continuum within the data, which we consider most likely to be associated with the relative proportion of reducing soils within the capture zone of a site in addition to land use intensity.

Table 7. 2: Summary of median concentrations for redox-sensitive species in Northland surface waters. Valid case = number of monitoring sites; C.V. = coefficient of variation.

Redox-Sensitive Measures	Valid Cases	Mean	Median	C.V.	Minimum	Maximum
DO (Field)	37	9.3	9.4	0.1	7.2	10.8
DO (Lab)	67	9.0	9.3	0.1	5.6	10.6
DO%	67	90.2	93.2	0.1	55.1	108.5
NNN	67	0.27	0.18	1.42	0.003	2.50
Fe^{II}	36	0.41	0.36	0.69	0.027	1.53
Mn^{II}	36	0.03	0.02	1.54	0.003	0.31
DOC	36	3.3	2.8	0.6	1.0	11.1

Specifically, correlation analysis performed on log-transformed and z-scored redox-sensitive species show that DOC concentration, a key electron donor, is positively correlated with Fe^{II} concentration (0.83) and Mn^{II} (0.63). We also note positive correlations between DOC and both ammoniacal nitrogen (0.76) and Total Nitrogen (TN: 0.75) and Total Phosphorus (TP: 0.53), suggesting that reducing conditions play an important role over spatial variation in the concentration of these important water quality measures. Importantly, the positive correlation between DOC and TN and TAM and the low concentration of NNN in Northland surface waters suggest that organic and ammoniacal forms of nitrogen are the most important source of nitrogen to regional river networks. 2018).

The role of redox over the speciation (forms) of N and P is well recognised. The different forms of N and P may behave significantly differently and exhibit distinctly different process-attribute relationships. For example, organic and ammoniacal nitrogen (TKN) tends to increase as soil and geological (shallow aquifer) reduction increases whereas nitrate typically exhibits the opposite behaviour. Nitrate is also more mobile that organic and ammoniacal forms of nitrogen due to its negative charge and relatively large hydrated radius. In comparison, ammoniacal forms of nitrogen, especially at the circum-neutral pH range of most natural waters, is positively charged and strongly retained by most soil and aquifer materials. Phosphorus both as orthophosphate and inositol hexaphosphate (an important organic form) is highly surface reactive forming electrostatic and ultimately chemical bonds between the oxides and oxyhydroxides of iron and aluminium. Accordingly, both P forms tend to be relatively immobile and often transported as attached load to soil (sediment) particles. However, P can be highly mobile in soils and aquifers dominated by organic carbon and/or that have moved beyond Fe^{III}-reduction (see Rissmann and Lovett, 2016 and references therein). In these settings P may behave much more like nitrate.

The relationship between DOC concentration and redox-sensitive species for Northland surface waters is once again consistent with theoretical and empirical knowledge regarding redox systematics (Rissmann, 2011; McMahon and Chappelle, 2009; Tratnyek et al., 2012; Beyer and Rissmann, 2016). However, temporal analysis of variation in surface water composition is recommended in order to isolate the relative volumetric and contaminant contribution from shallow aquifers supplying stream (Rissmann and Beyer, 2018; Rissmann and Pearson, 2018). For now, we proceed with evaluating the relationship between signatures of redox and key landscape attributes.

7.2.2 Correlation

Soil drainage class exerts a significant control over the concentration of redox-sensitive species such as DO, NO_3, Mn^{II}, Fe^{II} and ammoniacal and organic forms of nitrogen (Ernsten, 2006; Beyer and Rissmann, 2016). Soil zone redox also influences P retention and mobility via the reductive dissolution of the oxides and oxyhydroxides of Fe. As soil drainage status declines organic carbon contents also tend to increase reflecting longer periods of saturated conditions. As organic carbon increases so does soil acidity which can influence the stability of aluminium oxides and oxyhydroxides that also contribute to P retention.

A correlation matrix of log10 transformed and z-scored data shows a negative correlation ($r = 0.6$) between DO and soil Drainage Class (DC), indicating that DO declines as the area of imperfectly to poorly drained soils increases within the capture zone of a surface water monitoring site. Dissolved Fe (Fe^{II}), shows a strong positive (0.76) correlation with DC, indicating that Fe^{II} concentration increases as the area of imperfectly to poorly drained soils increase within the capture zone of a surface water monitoring site. The relationship between DO and Fe^{II} and soil DC is an important indicator of redox control given that neither species is associated with a land use gradient. For example, iron is the 4th most abundant element in the earth’s crust and is strongly correlated with soil DC irrespective of the proportion of developed land within the capture zone of a monitoring point. Evidence for reducing soil profile forms is evident in the field via the observations of low chroma colours and mottling (Milne et al., 1995).

Ammoniacal and organic nitrogen (TKN) is also strongly positively correlated (0.82) with soil DC weighted by the area of developed land. This relationship is not unexpected with the production of ammoniacal and organic nitrogen in anaerobic soils (poorly drained) occurring via several mechanisms: organic nitrogen mineralisation (ONM); dissimilatory nitrate reduction to ammonium (DNRA), and; the release of adsorbed ammonium during microbial reduction of iron oxides (MRFeO) (Mengel, 1996; Tratnyek et al., 2012; Richard et al., 2014; Chacón et al., 2017). Direct deposition of animal wastes, if not rapidly mobilised to stream, are subject to these same processes resulting in greater relative export of TKN than equivalent natural state settings (Ladd and Jackson, 1982; Coyne, 2009; Paul, 2013; Rissmann et al., 2018). The latter is consistent with a weaker correlation between TKN and soil DC for surface water captures zones for which the area of developed land is not used as a weighting measure. Recognising the important role of soil DC over TKN export is of particular relevance to Northland for which TKN on a median basis makes up 2/3rds of the regional median and mean Total Nitrogen (TN) concentration for the 67 regional streams analysed here. By comparison, NNN makes up 1/3rd of the TN and has a regional median and mean concentration of 0.17 and 0.27 ppm, respectively. The relatively low NNN concentration is perhaps not surprising given the ubiquity of imperfectly to poorly drained soils and the important role of redox processes such as denitrification. As expected, DOC concentrations and measures of absorbance are highly correlated, with organic carbon widely recognised as the dominant electron donor driving redox evolution in natural (low temperature) waters. DOC is significantly correlated with all key redox indicators sampled for Northland waters and is also strongly positively correlated with soil DC (0.75), irrespective of whether weighted or unweighted by the area of developed land.

Principal Component Analysis was run of redox-sensitive species that showed a similar correlation strength for soil DC weighted or unweighted by the area of developed land (Table 7.3). The outputs identify one main Eigenvalue that explains 66% of the variance in redox-sensitive species. Eigenvectors for Component 1 indicate positive weightings between soil DC, DOC and each redox species, supporting the general interpretation that soil DC, in addition to land use, exerts an important control over the concentration of redox-sensitive species and associated nutrients in Northland surface waters.

Table 7. 3: Principal Component Analysis of redox-sensitive species. Variables included are soil drainage class (wDC), soil drainage class of developed land (wDC_DL), and surface water measures for DOC, Fe, Mn, TAM and TKN.

Variance Table

Component No	Eigenvalue	Cumulative Variance	Percent	Cumulative
1	4.65	4.65	0.66	0.66
2	0.91	5.56	0.13	0.79
3	0.58	6.13	0.08	0.88

Eigenvectors

	Component 1	Component 2	Component 3
wDC	0.37	-0.37	-0.34
wDC_DL	0.31	0.54	0.56
DOC	0.43	-0.07	-0.19
Fe^{II}	0.40	-0.37	0.12
Mn^{II}	0.33	-0.38	0.61
TAM (Lab)	0.37	0.50	-0.21
TKN	0.42	0.20	-0.33

7.3 Soil Reduction Potential Map

The R-PAL for the Northland Region was developed by classifying the soil (FSL; NZLRI, DSIR, 1968) and geological (QMAP; Turnbull and Allibone, 2003) layers to produce two sperate layers, one of Soil Reduction Potential (SRP) and another of Geological Reduction Potential (GRP). The GRP layer is used to estimate shallow aquifer redox conditions although where bedrock outcrops and there is no soil zone GRP dominates. In order to explain spatial variation in the regional surface water and groundwater redox both layers must be combined. The SRP and GRP layer are subsequently combined to produce a combined reduction potential layer or redox process-attribute layer (R-PAL).

The soil reduction potential (SRP) is primarily influenced by soil drainage class (DC) as organic carbon, the key electron donor driving reduction, is seldom limiting. Further, soil DC, soil organic carbon and DOC are all strongly positively correlated indicating that soil organic carbon content increases as soil DC shifts from well (score of 1) to poorly drained (5). The soil reduction potential was therefore assigned a score of 1 to 5 (low to high) according to soil drainage class. For mixed soil polygons, at the soil series level, the SRP was proportionally weighted by the extent of each soil series within the polygon.

The SRP scores were classed into 5 classes (low <1.5, moderately low 1.51-2.5, moderate 2.51-3.5, moderately high 3.51-4.5, and high >4.5) according to expert judgement. We anticipate these thresholds will be revised as part of the national classification. The soil reduction potential layer produced for the Northland Region is shown in Figure 7.2. A summary of the surface water capture zones and SRP are presented in Figure 7.3. For each surface water capture zone, sites have been proportionally weighted by the SRP score for each polygon which enables a direct comparison between sites. It is important to note that mapping of the spatial extent of cracking soils is likely to be an important modifier of this layer. This reflects the effect of recharge bypassing the reducing soil matrix. Under these conditions removal of nitrate or other oxidising species is lessened or negated and the redox properties of the shallow aquifer become more critical.

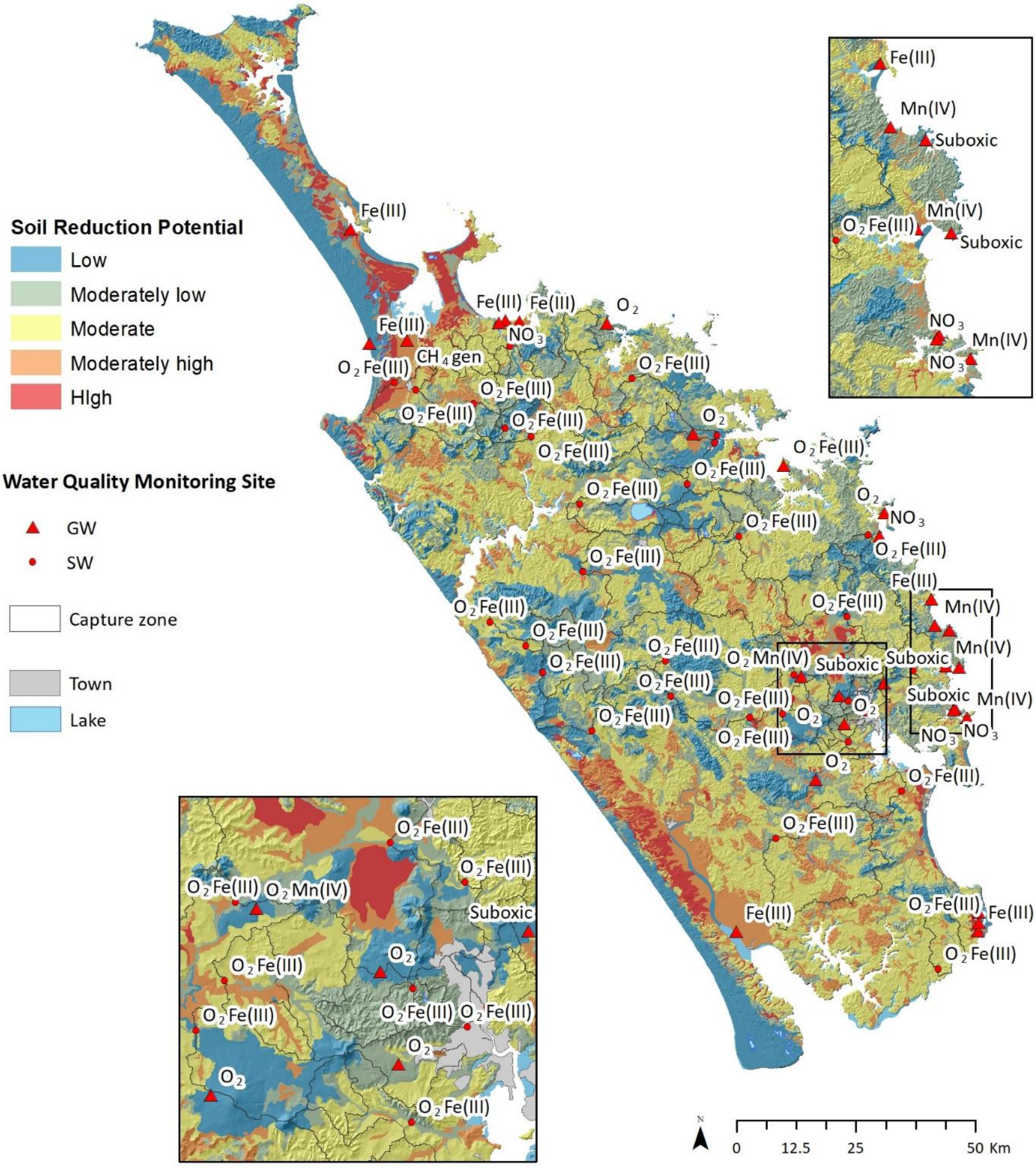

Figure 7. 2: Soil reduction potential for the Northland Region.

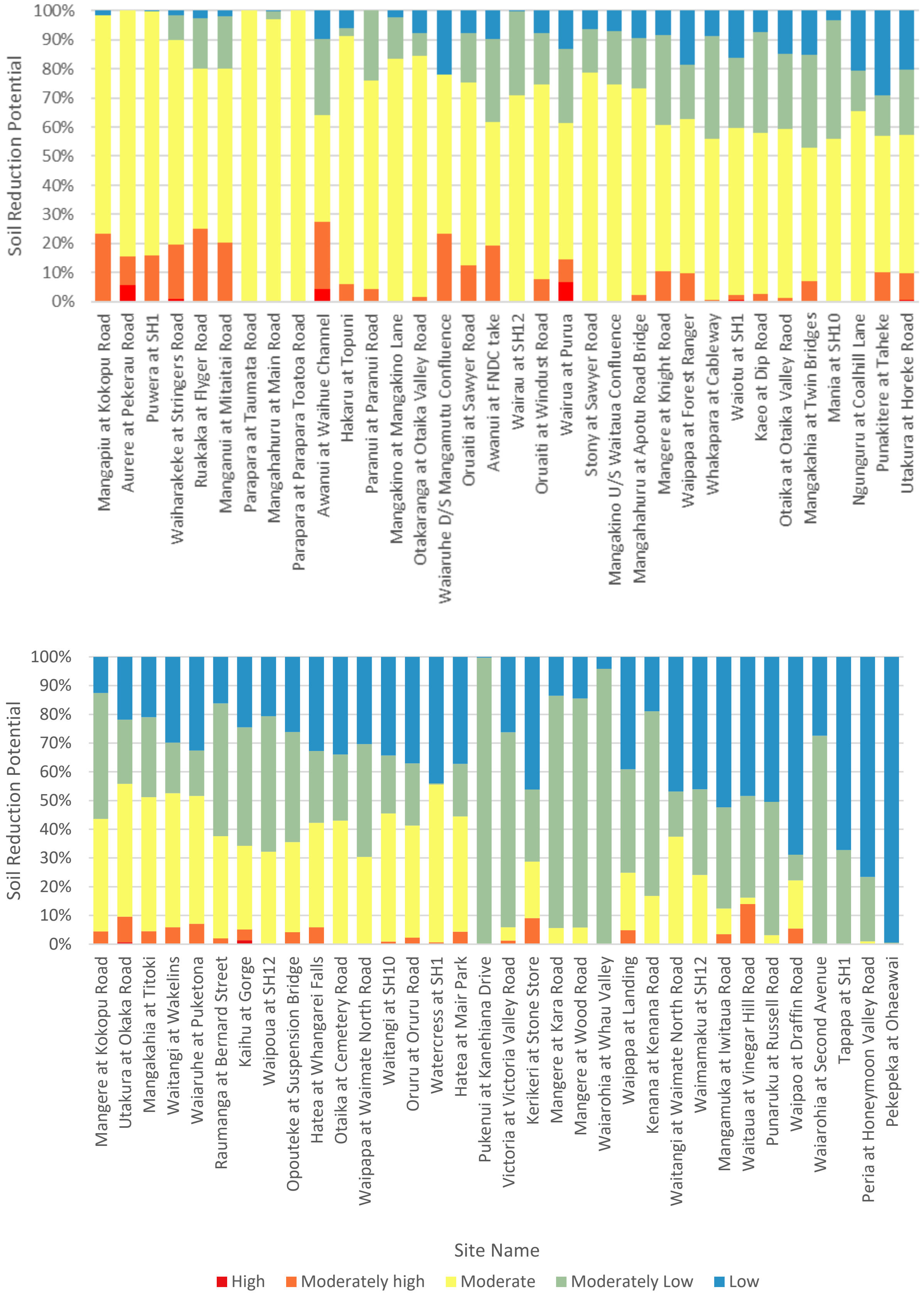

Figure 7. 3: Proportional soil reduction potential for Northland surface water capture zones.

In addition to cracking soils, it is apparent that a large number of smaller swamp and wetland deposits are not represented by the NZLRI (see also Rissmann et al., 2017). Organic carbon-rich deposits are a key driver of redox succession and can exert a strong control over peripheral and downgradient water composition (Rissmann et al., 2018b). An assessment of radiometric (50 m^2 pixel resolution) and sentinel satellite imagery (c. 10 m^2 pixel resolution) indicates much greater spatial constraint over smaller scale wetland deposits including dune lake systems. This data could be used in combination to further refine the resolution of both the soil and geological redox potential layers and associated redox gradients for the region.

7.4 Geological Reduction Potential Map

An assessment of the geological reduction potential (GRP) of an area is primarily designed to assess the redox setting of shallow unconfined aquifer systems that are directly linked to stream or shallow coastal margins. However, where bare rock outcrops especially in high-altitude areas, GRP is also an important determinant over the redox status of recharge waters. The redox potential of shallow aquifers is determined by a range of factors, of which the abundance of organic carbon is key (McMahon and Chapelle, 2009; Rissmann, 2011; Rissmann et al., 2012; Beyer et al., 2016). Aquifers hosted in materials containing a significant proportion of organic carbon tend to be strongly reducing, whereas aquifers with little organic carbon tend to be oxidising. However, other factors such as aquifer permeability, groundwater residence time and coupling to the atmosphere are also important controls over redox evolution (see Rissmann, 2011). In the following, regional groundwater signatures are used to guide the redox categorisation of shallow geological units. The focus on shallow geology reflects the greater connectivity of surficial geological units with the surface water network. Q-MAP was preferred over the NZLRI for the geological classification after an assessment of data sources relative to direct radiometric measures for the Northland Region was undertaken by the authors (Rissmann et al., 2017).

The assessment of the redox signatures of Northland aquifers in section 5.1 revealed some key relationships between lithological assemblages and redox signals, specifically:

1. Although there are few wells in areas of mudstones, these rocks are likely to host reducing aquifers due to low permeability and a tendency to be capped by clay-rich and poorly drained soils.
2. Where isolated from the influence of coastal-marine sediment deposition, coastal aquifers formed in fractured rock (esp. greywacke but not mudstones) are oxidising to weakly reducing (i.e. O_2 to Mn^{IV}-reduction).
3. The most reduced aquifers are associated with geologically recent coastal-marine sediments, including estuarine sediments. Bore depth and associated aquifer confinement are also relevant here with shallower bores expected to be more oxidising (see discussion below).
4. Well sorted and winnowed dune sand aquifers, especially where the overlying soils are freely draining are strongly oxidising. Bore depth and associated aquifer confinement are also relevant here with deeper bores expected to be more reducing (see discussion below).
5. Where aquifers are hosted by fractured basalt they are predominantly oxidising.

On the basis of these findings, the classification of GRP by Rissmann (2011) was modified for the Northland Region by extending the 3-class classification to a 5-class classification on the basis of regional differences in the geological properties of surficial aquifers pertinent to redox control. The geological composition was scored 1 to 5 (low to high) based on organic carbon of the substrate and likely permeability. Our estimate of aquifer permeability was visually compared against the aquifer potential layer of GNS Science (Tschritter et al., 2017).

The output of this classification was reviewed by staff at Northland Regional Council whom also consulted with local experts. Subsequent refinement of the GRP classification was made in response to feedback from NRC. The resulting QMAP classification was aggregated into the NZLRI polygons to combine the classification (section 7.5). The GRP scores were classed into 5 classes (low <1.5, moderately low 1.51 - 2.5, moderate 2.51 - 3.5, moderately high 3.51 - 4.5, and high >4.5). We anticipate these thresholds to be revised as part of the national classification. The resulting GRP classification is shown in Figure 7.4 and proportionally by surface water capture zone in Figure 7.5 in the same manner as the SRP layer.

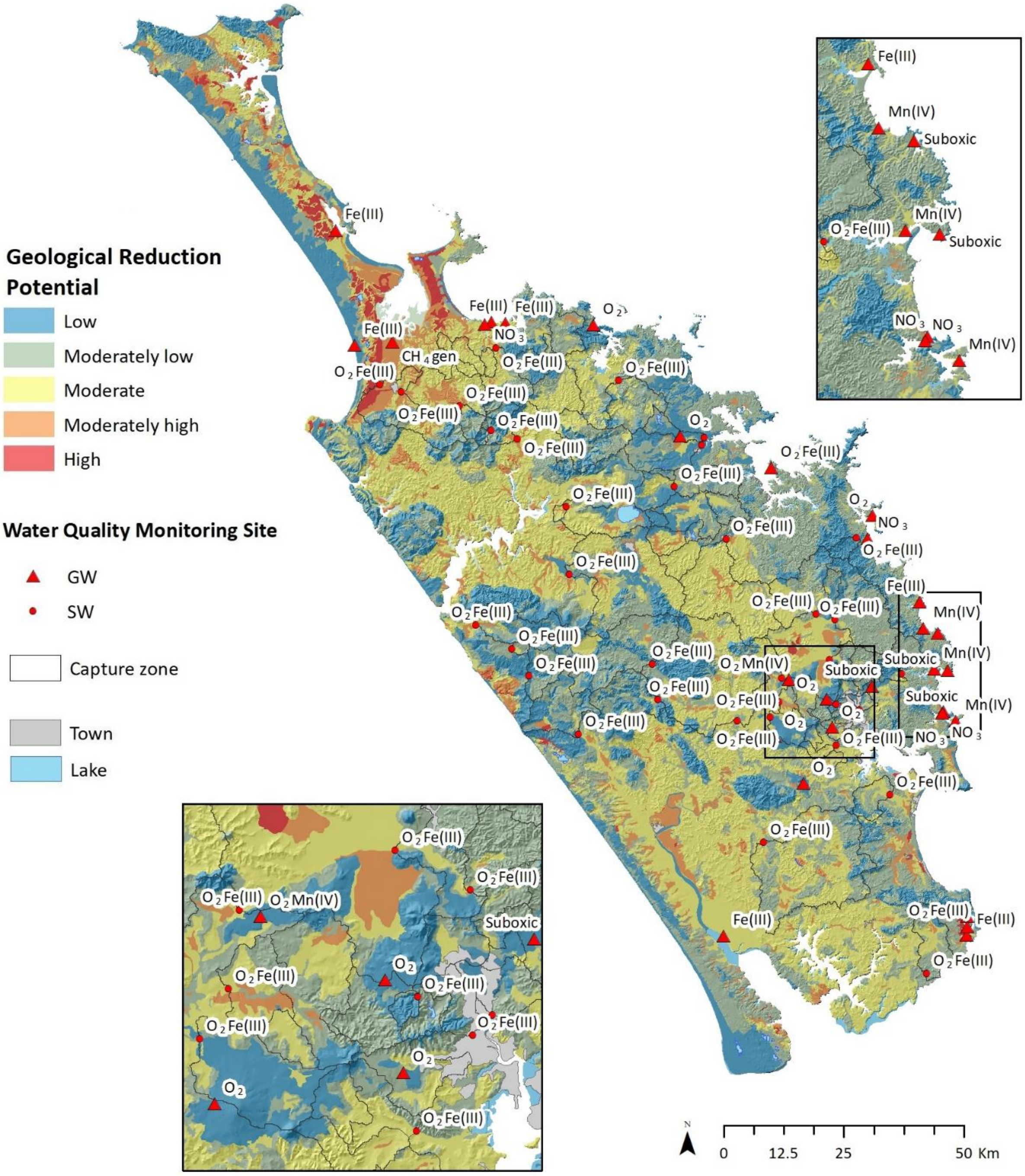

Figure 7. 4: Geological reduction potential for the Northland Region.

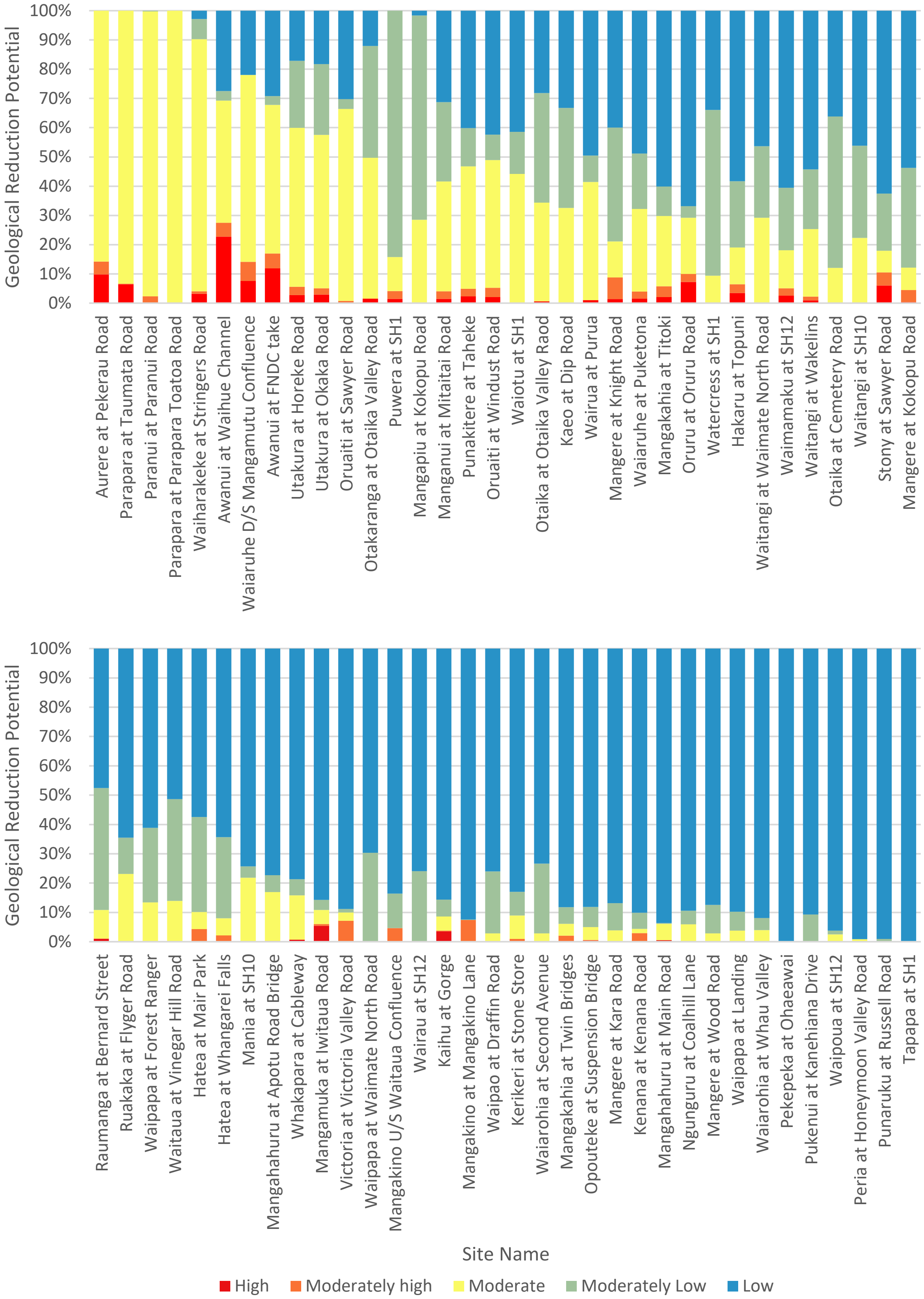

Figure 7. 5: Proportional geological reduction potential for Northland surface water capture zones.

Overall the spatial relationship between the preliminary GRP layer and groundwater redox signatures is consistent with theoretical and empirical data. Although the GRP layer presented here is developed for shallow unconfined aquifers it is important to note that for deeper aquifers, and especially semi-confined and confined aquifers, there is currently a lack of vertical resolution over rock and sediment heterogeneity as it pertains to redox. The latter is especially true of deeper bores (>30 m bgl) that tap unconsolidated sediments associated with dynamic landscape environments such as stream floodplains, estuaries, and coastal dune systems where intercalation of organic matter with inorganic sediments is commonly responsible for considerable heterogeneity in subsurface redox gradients. Bore log information reveals this heterogeneity is most pronounced in unconsolidated Quaternary deposits associated with coastal sand dune systems, deltaic systems, and estuarine deposits. Geomorphic knowledge of the aquifer setting could be used to better constrain vertical gradients in aquifer redox potential.

The Waipapakauri GW at Waipapakauri landing bore is the only site where there is a significant departure from the estimated redox potential and the actual. This site provides a good example of the complexity as the bore is relatively deep (57 m bgl) and designated as being hosted by windblown sand with a GRP classification of O_2-reduction for the unconfined (shallow) aquifer. However, the groundwaters from this bore are anoxic and buffered at Fe^{III}-reduction. Northland Regional Council bore log data indicates a semi-confined aquifer hosted by peat, Quaternary dune sand, and shell fragments as is consistent with the location of this aquifer at the coastal margin. In comparison, shallow bores (<10 m bgl) hosted by equivalent sediments at GW Bland Bay @ M/C Ngatiwai t/Board Camp new bore and Oakura GW @ 3 Te Kapua Street (Patricia Wallis) are both oxidising and classified as such by the GRP layer. Well depth and the dynamic nature of the landscape setting is, therefore, an important consideration of the likely redox signature of the groundwater sampled.

With regards to the redox gradients of the shallow, unconfined aquifer system the current GRP layer could be improved via finer-grained mapping of large number of smaller swamp and wetland deposits that are not represented by the NZLRI (see also Rissmann et al., 2017). Organic carbon-rich deposits are a key driver of redox succession and can exert a strong control over downgradient groundwater redox conditions (Rissmann et al., 2018b). An assessment of radiometric (50 m^2 pixel resolution) and sentinel satellite imagery (c. 10 m^2 pixel resolution) indicates much greater spatial constraint over smaller scale wetland deposits including dune lake systems. These data could be used in combination to further refine the resolution of both the soil and geological redox potential layers and associated redox gradients for the region.

7.5 Combined Redox Process Attribute Layer (R-PAL)

To combine the soil and aquifer redox potential into a single classification the scores were averaged and ranked. Importantly, the Combined Reduction Potential (CRP) layer represents the maximum reduction potential for waters that have percolated through the soil and unsaturated zone and into the underlying aquifer (Figure 7.6). Accordingly, water bypassing the soil matrix through artificial drainage and overland flow has not interacted with the redox environment of the shallow aquifer. Accordingly, steady-state signatures for surface waters dominated by shallow soil zone runoff are not expected to show a correlation with the GRP and as such may depart significantly from the CRP layer. The CRP layer is most relevant to shallow unconfined aquifers that are hydrologically connected to the stream network and to streams during periods of baseflow dominance.

The resulting CRP classification (or R-PAL) is shown in Figure 7.6 and proportionally by surface water capture zone in Figure 7.7. Proportionally the Aurere at Pekerau Road monitoring point is the most reducing while Pekepeka at Ohaeawai monitoring point is the most oxidising. To understand potential impacts on water quality this assessment needs to be combined with land use information, especially, areas used for the grazing of livestock.

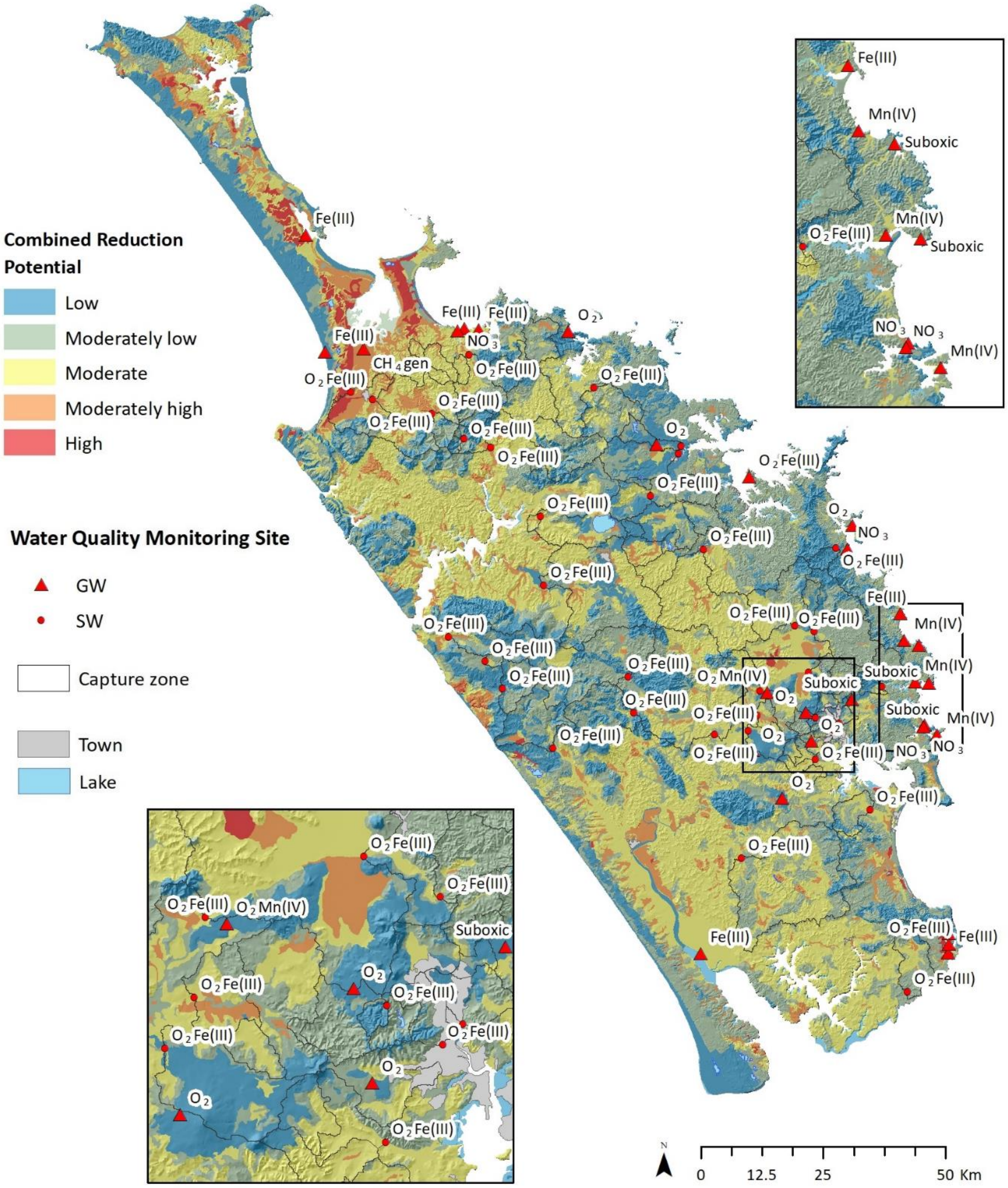

Figure 7. 6: Combined soil and geological reduction potential process-attribute layer (R-PAL) for the Northland Region.

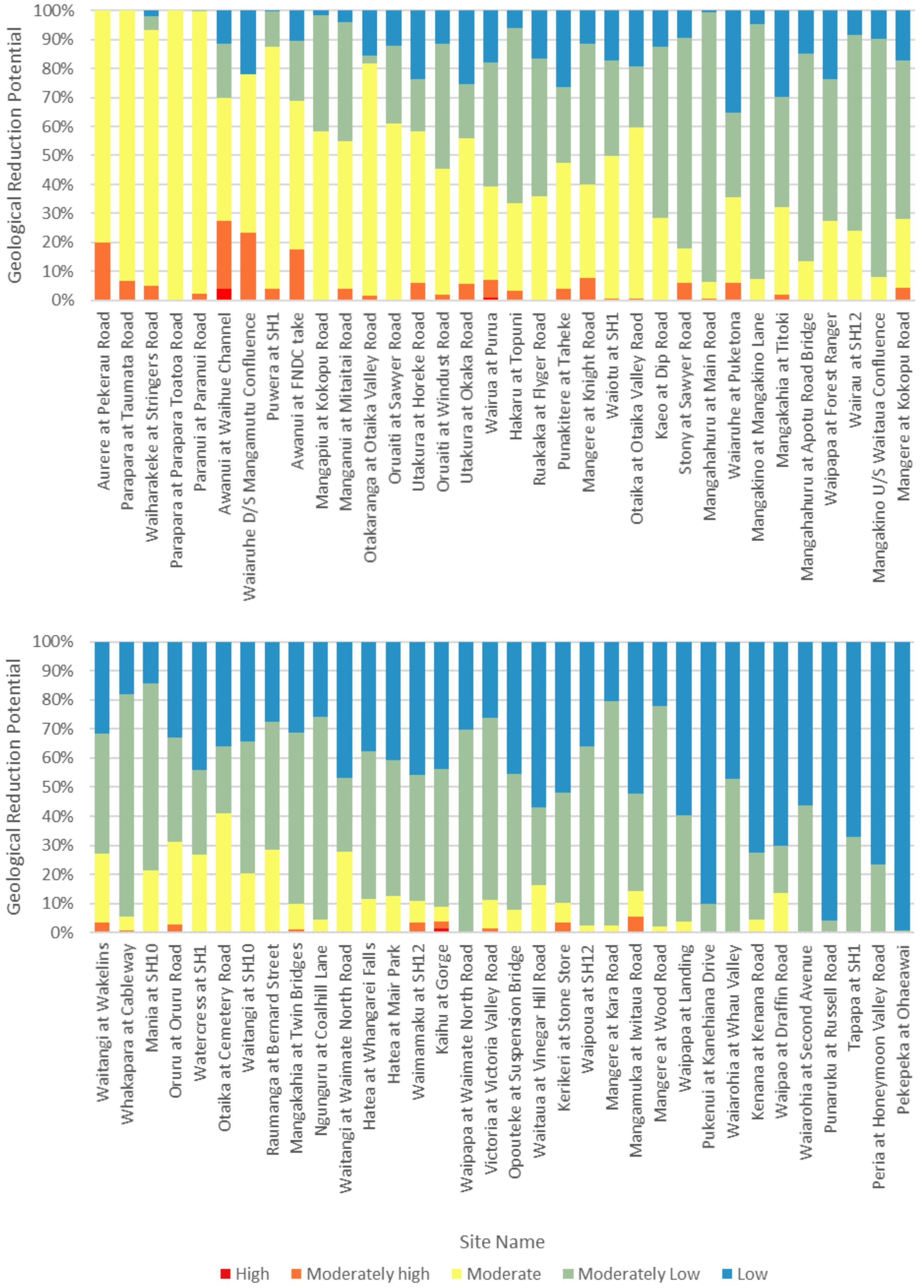

Figure 7. 7: Proportional combined soil and geological reduction potential for Northland surface water capture zones.

7.6 Summary of Redox Layer (R-PAL) and Recommendations

The redox layer (R-PAL) is based on two key layers, the soil zone and geological layer that hosts the shallow groundwater that is highly coupled to stream. The Soil Reduction Potential (SRP) layer depicts the likely spatial coupling between soil reduction potential and soil water reduction. The Geological Reduction Potential (GRP) layer depicts the likely spatial coupling between geological reduction potential of rock and sediment and shallow groundwater reduction signals. In areas of rock outcrop, the GRP layer is considered a key determinant over the ensuing redox evolution of recharge waters.

The combination of the SRP and GRP layers to produce a Combined Reduction Potential (CRP) layer The CRP layer represents the maximum reduction potential and is most relevant to waters that have percolated through the soil and unsaturated zone and into the underlying aquifer. The CRP layer is most relevant to shallow unconfined aquifers that are hydrologically connected to the stream network and to streams during periods of baseflow dominance (see section 6).

Although the spatial relationships between surface and groundwater signatures and both SRP and GRP layers appear reasonable calibration of these preliminary layers is subject to further refinement associated with physiographic mapping of other regions, especially Auckland, Bay of Plenty and Waikato. Future works that could improve the resolution and accuracy of these layers could include:

- High-resolution mapping of wetland areas using a combination of radiometric and satellite imagery (Sentinel). This has been discussed with NRC.
- Characterisation of the geomorphic setting of Quaternary aquifer systems could be used to refine the likely vertical (and lateral) gradients in redox signatures for deeper bores and semi-confined/confined aquifers.
- For groundwater monitoring sites that do not directly sample the bore, a lack of DO measures is a limiting factor in better understanding redox dynamics. An effort to shift to direct sampling of bores and field measurement of DO would add considerable value to the current monitoring programme given the critical role of redox over N and P concentrations and mobility.
- Samples of stream flow in groundwater recharge areas, areas of well-drained soils and permeable fractured rock aquifers (both low and high altitude) may help better constrain water origins in downgradient aquifers.
- As noted in the H-PAL summary and recommendations section, the development of a map of shrink-swell soil is potentially an important hydrological component influencing shallow groundwater redox signatures and that of artificial drainage to streams.

8 Concluding Comments

The H-PAL and R-PAL layers produced in this document represent a preliminary assessment of the key Process-Attribute Gradients, that in conjunction with land use, are thought to control spatial variation in surface water and shallow groundwater quality. The emphasis on landscape gradients reflects the important role of spatial variation in landscape attributes over the key processes that govern variation water composition and hence quality.

The basis for physiographic mapping is the understanding that natural gradients in landscape attributes have long been recognised as the governing controls over spatial and temporal variation in both hydrochemical and hydrological signatures. We note that where there is a similar assemblage of landscape attributes, a similar 'physiographic setting,' that the processes governing hydrochemical and hydrological signatures are often similar. As such, for a broadly equivalent land use pressure we would expect to see distinctly different outcomes between physiographic settings.

Knowledge of how and why water quality outcomes vary in space, and ultimately in time, is a powerful basis for more effective and targeted management of natural resource use including the identification of what mitigations are likely to be best suited to a particular setting to improve water quality.

The next steps for this work subject to approval by NRC and Our Land and Water National Science Challenge Funding (or other) include:

1. Refinement of the layers in light of new information and works provided by NRC
2. Addition of a sediment specific layer for the Northland Region, contracted by NRC and via Waterways Centre and for delivery by Land and Water Science due 31st January 2019
3. Quantitative validation of the performance of the Hydrological and Redox (also potentially the Sediment) Process Attribute Layers to estimate spatial variation in the key water quality measures Nitrogen, Phosphorus, Sediment(?) and Microbes.
4. Production of 'Physiographic Environments'
5. Consideration of farm extension opportunities offered by physiographic mapping and the Farmer Interface for Physiographic Environments funded by the Ministry for Primary and driven by co-innovation with Primary Industry Groups including Fonterra, Beef & Lamb, Foundation of Arable Research, Deer New Zealand, the New Zealand Landcare Trust, Living Water, Ravensdown and Balance.

9 Acknowledgments

We acknowledge the contribution from Our Land and Water National Science Challenges research funding under the Physiographic Environments of New Zealand project. We thank Northland Regional Council staff for their interest and significant contribution in terms of time and local knowledge that has greatly aided and improved the accuracy of this work. In particular, we thank Susie Osbaldiston, Jean-Charles Perquin and Duncan Kervell. We also thank colleagues at GNS Science, NIWA, AgResearch, Waikato University, University of Canterbury and Lincoln University for helpful discussion regarding soil, geological, hydrological, biogeochemical and geomorphic influences over the hydrochemical and hydrological response.

10 References

Baisden, W.T., Keller, E.D., Van Hale, R., Frew, R.D., Wassenaar, L.I. (2016). Precipitation isoscapes for New Zealand: enhanced temporal detail using precipitation-weighted daily climatology. Isotopes in environmental and health studies, 52(4-5): 343-352

Ballinger, J., Nicholson, C., Perquin, J-C., Simpson, E. (2014). River water quality and ecology in Northland- State and trends 2007-2011.

Becker, J. C., Rodibaugh, K. J., Labay, B. J., Bonner, T. H., Zhang, Y., and Nowlin, W. H. (2014). Physiographic gradients determine nutrient concentrations more than land use in a Gulf Slope (USA) river system. Freshwater Science, 33(3): 731–744.

Beyer, M., and Rissmann, C. (2016). Tile drain and soil water sample assessment: relationships between soil denitrification potential and redox processes. Lower Hutt, N.Z.: GNS Science. GNS Science report 2016/60 ii.

Beyer, M., Rissmann, C., Rodway, E., Killick, M., and Pearson, L. (2016a). Technical Chapter 6: Influence of Soil and Geological Composition over Redox conditions for Southland groundwater and surface waters. Environment Southland. Technical Report. No: 2016/3. Invercargill, New Zealand

Beyer, M., Rissmann, C., Rodway, E., Marapara, T. R., and Hodgetts, J. (2016b) Technical Chapter 2: Discrimination of recharge mechanism and vulnerability to bypass flow. Environment Southland. Technical Report. No: 2016/3. Invercargill, New Zealand

Brady, N.C., and Weil, R.R., (2007). The nature and properties of soils. 14th edition. Prentice-Hall Upper Saddle River, New Jersey.

Cameron, S., Osbaldiston, S., Skuse, G., Revfem, C. (2001). Chapter 12 Northland, Part II - Regional Groundwater Summaries, In: Groundwaters of New Zealand, Michael R. Rosen and Paul A. White, editors, New Zealand Hydrological Society Inc; Wellington North, New Zealand; ISBN0-473-07816-3; 498 pp; 2001.

Chappell, P.R. (2013). The climate and weather of Northland. NIWA Science and Technology Series, 59 (3rd edition).

Chiodini, G., Frondini, F., Kerrick, D. M., Rogie, J., Parello, F., Peruzzi, L., and Zanzari, A. R. (1999). Quantification of deep CO2 fluxes from Central Italy. Examples of carbon balance for regional aquifers and of soil diffuse degassing. Chemical Geology, 159(1–4), 205–222.

Clark, I. and Fritz, P. 1997. Environmental Isotopes in Hydrogeology (2nd edition). CRC Press ISBN: 1-56670-249-6

Clough, T.J., Jarvis, S.C., Dixon, E.R., Stevens, R.J., Laughlin, R.J., and Hatch, D.J. (1998) Carbon induced subsoil denitrification of 15N-labelled nitrate in 1m deep soil columns. Soil Biology and Biochemistry 31(1): 31-41

Cooper, A.B., Thomsen, C.E. (1988). Nitrogen and phosphorus in stream waters from adjacent pasture, pine and native forest catchments. N.Z. J. Mar. Freshwater Res. 22, 279–291.

Cox, M and Browne, P. (1991). Geochemistry of ground and thermal waters in the Ngawha area and elsewhere n Northland, New Zealand. Proceedings 13th New Zealand Geothermal Workshop 271 - 277.

Curran Cournane, F., McDowell, R., Littlejohn, R., and Condron, L. (2011). Effects of cattle, sheep and deer grazing on soil physical quality and losses of phosphorus and suspended sediment losses in surface runoff. Agriculture, ecosystems and environment, 140(1): 264- 272.

Daughney, C.J., Rissmann, C., Friedel, M.J., Morgenstern, U., Hodson, R., van der Raaij, R.W., Rodway, E., Martindale, H., Pearson, L., Townsend, D.B., Kees, L., Moreau, M., Millar, R., and Horton, T. 2015 Hydrochemistry of the Southland region. Lower Hutt, N.Z.: GNS Science. GNS Science report 2015/24 202 p

Day, R.W. (1994). Swell–shrink behaviour of expansive compacted clay. Journal of Geotechnical Engineering, ASCE, 120(3): 618-623.

Deakin, J., Flynn, R., Archbold, M., Daly, D., O'Brien, R., Orr, A., and Misstear, B. (2016). Understanding pathways transferring nutrients to streams - Review of a major Irish study and its implications for determining water quality management strategies. Proceedings of the Royal Irish Academy: Biology and Environment, 116B(3): 233 - 243.

Dif, A.F., and Blumel, W.F. (1991). Expansive soils with cyclic drying and wetting. ASTM, Geotechnical Testing Journal, 14(1): 96-102.

Donovan, C., and Donovan, W. (2003). Environment Bay of Plenty estimate of the geothermal nutrient inputs to twelve Rotorua lakes. Bioresources Consulting.

Doran, J.W. (1978). Soil microbial and biogeochemical changes associated with reduced tillage. Soil Science Society of America Journal 44(4): 765-771.

Dow, C. L., Arscott, D. B., and Newbold, J. D. (2006). Relating major ions and nutrients to watershed conditions across a mixed-use, water-supply watershed. Journal of the North American Benthological Society, 25(4): 887–911.

Drewry, J. J., and Paton, R. J. (2000). Effects of cattle treading and natural amelioration on soil physical properties and pasture under dairy farming in Southland, New Zealand. New Zealand Journal of Agricultural Research, 43(3): 377-386.

Edbrooke, S.W., and Brook, F.J. (compilers) (2009). Geology of the Whangarei area. Institute of Geological and Nuclear Sciences 1:250 000 geological map 2. 1 sheet + 68 p. Lower Hutt, New Zealand. GNS Science. QMAP Whangarei

Eriksson, E. (2012). Principles and Applications of Hydrochemistry. Springer. p175.

Ernstsen, V. (2006). Denitrification below the root zone. Plantekongres 92.3: 439-440.

Giller, P. S., Malmqvist, B. (2004). Biology of Habitats: The Biology of Streams and Rivers. Oxford University Press.

Goldsmith, R., and Ryder, G. (2013). Factors affecting contaminant loss in overland flow. Ryder Consulting Limited. Technical Review for Environment Southland. Dunedin, New Zealand.

Güler, C., and Thyne, G. D. (2004). Delineation of hydrochemical facies distribution in a regional groundwater system by means of fuzzy c-means clustering. Water Resources, v.40, p.1–11.

Güler, C., Thyne, G. D., McCray, J. E., and Turner, K. A. (2002). Evaluation of graphical and multivariate statistical methods for classification of water chemistry data. Hydrogeology Journal, 10(4), 455–474.

Guney, Y., Sarı, D., Cetin, M., Tuncan, M. (2007). Impact of cyclic wetting-drying on swelling behavior of lime-stabilized soil. Building and Environment, 42(2): 681-68.

Hale, S. S., Paul, J. F., and Heltshe, J. F. (2004). Watershed landscape indicators of estuarine benthic condition. Estuaries, 27(2): 283-295.

Horton, R. E. (1941). An approach toward a physical interpretation of infiltration-capacity. Soil Science Society of America Journal, 5(C): 399-417.

Hughes, B., Wilson, K., Rissmann, C., and Rodway, E. (2016). Physiographics of Southland: Development and application of a classification system for managing land use effects on water quality in Southland. Environment Southland Technical Report No. 2016/11. Invercargill, New Zealand.

Inamdar S. (2011). The use of geochemical mixing models to derive runoff sources and hydrologic flow paths. In: Levia D., Carlyle-Moses D., Tanaka T. (Eds). Forest Hydrology and Biogeochemistry. Ecological Studies (Analysis and Synthesis), v.216. Springer, Netherlands.

Isaac, M.J. (compiler) (1996). Geology of the Kaitaia area. Institute of Geological & Nuclear Sciences 1:250 000 geological map 1. 1 sheet + 43 p. Lower Hutt, New Zealand. GNS Science. QMAP Kaitaia.

Johnson, L., Richards, C., Host, G., and Arthur, J. (1997). Landscape influences on water chemistry in Midwestern stream ecosystems. Freshwater Biology 37(1): 193–208.

Jurgens, B. C., Mcmahon, P. B., Chapelle, F. H., and Eberts, S. M. (2009). An Excel ® Workbook for Identifying Redox Processes in Ground Water An Excel ® Workbook for Identifying Redox Processes in Ground Water.

Katsuyama, M., Ohte, N., and Kobashi, S. (2001). A three-component end-member analysis of streamwater hydrochemistry in a small Japanese forested headwater catchment. Hydrological Processes, 15(2), 249–260.

Katsuyama, M., and Ohte, N. (2002). Determining the sources of stormflow from the fluorescence properties of dissolved organic carbon in a forested headwater catchment. Journal of Hydrology, 268(1–4), 192–202.

Katsuyama, M., Kabeya, N., and Ohte, N. (2009). Elucidation of the relationship between geographic and time sources of stream water using a tracer approach in a headwater catchment. Water Resources Research, 45(6).

Kendall C., and McDonnell, J. J. (2008). Isotope Tracers in Catchment Hydrology. Elsevier Science B.V., Amsterdam. p.41-86.

Killick, M., Stenger, R., and Rissmann, C. (2015). Estimating soil zone denitrification for Southland. Technical Report. Environment Southland, Invercargill, New Zealand

King RS, Baker ME, Whigham DF, Weller DE, Jordan TE, Kazyak PF, Hurd MK. (2005). Spatial considerations for linking watershed land cover to ecological indicators in streams. Ecology Applications, 15: 137–53.

Krantz, D. E., and Powars, D. S. (2002). Hydrogeologic setting and potential for denitrification in groundwater, Coastal Plain of Southern Maryland: U.S. Geological Survey Water-Resources Investigations Report 00-4051.

Langmuir, D. (1997). Aqueous environmental geochemistry. Prentice Hall.

Lydersen, E., Larssen, T., Fjeld, E. (2004). The influence of total organic carbon (TOC) on the relationship between acid neutralizing capacity (ANC) and fish status in Norwegian lakes. The Science of the total environment, v.326(1-3), p.63-9.

Lynn, I. H., Manderson, A. K., Page, M. J., Harmsworth, G. R., Eyles, G. O., Douglas, G. B., Mackay, A. D., Newsome, P. J. F. (2009). Land Use Capability Survey Handbook – a New Zealand handbook for the classification of land 3rd edition. Hamilton, AgResearch; Lincoln, Landcare Research; Lower Hutt, GNS Science. 163p.

McDowell, R. W., Monaghan, R.M., Morton, J., 2003. Soil phosphorus concentrations to minimise potential P loss to surface waters in Southland. New Zealand Journal of Agricultural Research, 46:3.

McDowell, R. W., Monaghan, R. M., and Wheeler, D. (2005). Modelling phosphorus losses from pastoral farming systems in New Zealand. New Zealand Journal of Agricultural Research, 48(1): 131-141.

McDowell, R. W. (2006). Contaminant losses in surficial runoff from cattle, deer and sheep dung. Water, Air, and Soil Pollution 174(1-4): 211-222.

McKergow, L. A., Tanner, C. C., Monaghan, R. M., and Anderson, G. (2007). Stocktake of diffuse pollution attenuation tools for New Zealand pastoral farming systems. NIWA Client Report Report HAM2007–161, Prepared for Pastoral, 21. Hamilton, New Zealand.

McLaren, R.G., and Cameron, K.C. (1996). Soil Science: Sustainable production and environmental protection. 2nd Edition. Oxford University Press, New York.

McMahon, P., and Chapelle, F. (2008). Redox processes and water quality of selected principal aquifer systems. Groundwater 46(2): 259-271.

Milne, J.D.G., Clayden, B., Singleton, P.L. and Wilson, A.D. (1995). Soil Description Handbook. Manaaki Whenua Press. Lincoln, Canterbury, New Zealand

Ministry for the Environment. (2014). National Policy Statement for Freshwater Management. ME Report 1155.

Moldan, B., and Černý, J. (Eds.) (1994). Biogeochemistry of Small Catchments: A tool for Environmental Research. Published on behalf of the Scientific Committee on Problems of the Environment (SCOPE) of the International Council of Scientific Unions (ICSU) and of the United Nations Environment Programme (UNEP). Wiley and Sons, England.

Molenat, J., Gascuel-Odoux, C., Ruiz, L., Gruau, G. (2008). Role of water table dynamics on stream nitrate export and concentration in agricultural headwater catchment (France). Journal of Hydrology, v.348(3-4), p.363-378.

Monaghan, R.M., Smith, L.C., and Muirhead, R.W. (2016) Pathways of contaminant transfers to water from an artificially-drained soil under intensive grazing by dairy cows. Agriculture, Ecosystems and Environment, 220: 76-88.

Needelman, B.A., Gburek, W.J., Petersen, G.W., Sharpley, A.N., and Kleinman, P.J.A. (2003. Surface runoff anlong two agricultural hillslopes with contrasting soils. Soil Science Society of America, 68(3):914-923

Nichol, S., Harvey, M., and Boyd, I. (1997). Ten years of rainfall chemistry in New Zealand. Clean Air: Journal of the Clean Air Society of Australia and New Zealand, 31(1), 30.

Northland Regional Council, 2011. Northland River Water Quality Monitoring Network Report - 2008-2009.

Orchiston, T. S., Monaghan, R., and Laurenson, S. (2013). Reducing overland flow and sediment losses from winter forage crop paddocks grazed by dairy cows. In: Accurate and efficient use of nutrients on farms. (Eds. L.D. Currie and C L. Christensen). http://flrc.massey.ac.nz/publications.html. Occasional Report No. 26. Fertilizer and Lime Research Centre, Massey University, Palmerston North, New Zealand. 7 pages.

Panno, S. V., Kelly, W. R., Martinsek, A. T., and Hackley, K. C. (2006). Estimating background and threshold nitrate concentrations using probability graphs. Ground Water, 44(5), 697–709. https://doi.org/10.1111/j.1745-6584.2006.00240.x

Paul, E. A. (2013). Soil Microbiology, Ecology and Chemistry. Journal of Chemical Information and Modeling (Vol. 53). https://doi.org/10.1017/CBO9781107415324.004

Pearson, L. (2015a). Overland flow risk in Southland. Environment Southland. Technical Report No. 2015-06. Invercargill, New Zealand.

Pearson, L. (2015b). Artificial subsurface drainage in Southland. Environment Southland. Technical Report No. 2015-07. Invercargill, New Zealand.

Pearson, L., Couldrey, M., and Rodway, E. (2016). Spatial analysis of winter forage cropping in Southland and the implications for water quality management. Environment Southland. Technical Report No. 2016-13. Invercargill, New Zealand.

Ponnamperuma, F. (1972). The Chemistry of Submerged Soils. Advances in Agromomy 24(C): 29-96.

Reimann, C., and Garrett, R. G. (2005). Geochemical background-concept and reality. The Science of the Total Environment. https://doi.org/10.1016/j.scitotenv.2005.01.047

Rissmann, C. (2011a). Regional mapping of groundwater denitrification potential and aquifer sensitivity. Environment Southland Technical Report No. 2011-12. Invercargill, New Zealand.

Rissmann, C., Nicol, A., Cole, J., Kennedy, B., Fairley, J., Christenson, B., … Gravley, D. (2011). Fluid flow associated with silicic lava domes and faults, Ohaaki hydrothermal field, New Zealand. Journal of Volcanology and Geothermal Research, 204(1–4).

Rissmann, C. (2012). The extent of nitrate in Southland Groundwaters: Regional 5 year median (2007-2012 (June)). Environment Southland, Technical Report No. 2012-09. Invercargill New Zealand

Rissmann, C., Wilson, K., and Hughes, B. (2012). Waituna Catchment Groundwater Resources. Environment Southland, Technical Report No. 2012-04. Invercargill, New Zealand.

Rissmann, C. and Hodson, R. (2013). Role of baseflow and catchment geology over the surface water biogeochemistry of the Waituna Catchment - Redox gradients and nutrient speciation. Presentation to Hydrological Society, Palmerston North, November 19-22

Rissmann, C., and Lovett, A., 2016. Hydrochemical analysis for the Otane waste water treatment plant, GNS science consultancy report 2016/83:32p.

Rissmann, C., Rodway, E., Beyer, M., Hodgetts, J., Pearson, L., Killick, M., Marapara, T.R., Akbaripasand, A., Hodson, R., Dare, J., Millar, R., Ellis, T., Lawton, M., Ward, N., Hughes, B., Wilson, K., McMecking, J., Horton, T., May, D., and Kees, L. (2016a). Physiographics of Southland Part 1: Delineation of key drivers of regional hydrochemistry and water quality. Environment Southland Technical Report No. 2016/3. Invercargill, New Zealand.

Rissmann, C., Beyer, M., Rodway, E., Hodson, R., Ward, N., Ellis, T., Hodgetts, J., Pearson, L., Killick, M., Marapara, T., Akbaripasand, A., Dare, J., Kees, L, Snelder, T., Moriarty, E., Almond, P., and Webster-Brown, J. (2016b). Shrink-swell (cracking) soils as important conduits of ground and surface water microbial contamination? NZ Freshwater conference, Invercargill, New Zealand.

Rissmann, C., Marapara, T., Bloomberg, S., Lindsay, J., and Pearson, L. (2017). Evaluation of geospatial datasets and recognition of landscape gradients specific to water quality. e3Scientific Report no. 17035, prepared for Northland Regional Council. Invercargill, New Zealand

Rissmann, C. and Beyer, M. (2018). Waituna Catchment: Temporal Variation. Land and Water Science Report 2018/09. Prepared for Living Water. 11p.

Rissmann, C. and Pearson, L. (2018). Identifying Pollutant Sources within the Waimea Catchment: Applying hydrochemical tracers to surface water time series data. Land and Water Science Report 2018/15. p54.

Rissmann, C., Pearson, L., Lindsay, J., Beyer, M., Marapara, T., Badenhop, A., and Martin, A. (2018a). Integrated landscape mapping of water quality controls for farm planning – applying a high resolution physiographic approach to the Waituna Catchment, Southland. In: Farm environmental planning – Science, policy and practice. (Eds. L. D. Currie and C.L. Christensen). http:flrc.massey.ac.nz/publications.html. Occasional Report No. 31. Fertilizer and Lime Research Centre, Massey University, Palmerston North, New Zealand. 19 pages.

Rissmann, C., Pearson, L., Lindsay, J. Marapara, M., and Badenhop, A. (2018b). Waituna Catchment: Technical Information and Physiographic Application. Land and Water Science Report 2018/01. Prepared for Living Water, 133p.

Rodway, E., Rissmann, C., Beyer, M., Marapara, T. R., Hodgetts, J. (2016). Technical Chapter 1: Precipitation. Technical Report. No: 2016/3. Invercargill, New Zealand.

Rogers, K. M., Turnbull, R. E., Martin, A. P., Baisden, W. T., and Rattenbury, M. S. (2017). Stable isotopes reveal human influences on southern New Zealand soils. Applied Geochemistry, 82: 15-24.

Schoonover, J. E., and Crim, J. F. (2015). An Introduction to Soil Concepts and the Role of Soils in Watershed Management. Journal of Contemporary Water Research and Education, 154(1): 21-47.

Seitzinger, S., Harrison, J. A., Böhlke, J. K., Bouwman, A. F., Lowrance, R., Peterson, B., Tobias, C., and Van Drecht, G. (2006). Denitrification across landscapes and waterscapes: A synthesis. Ecological Applications. 16(6): 2064-2090.

Shiels, D. R. (2010). Implementing landscape indices to predict stream water quality in an agricultural setting: An assessment of the Lake and River Enhancement (LARE) protocol in the Mississinewa River watershed, East-Central Indiana. Ecological Indicators, 10(6): 1102–1110.

Smith, L. C., and Monaghan, R. M. (2003). Nitrogen and phosphorus losses in overland flow from a cattle-grazed pasture in Southland. New Zealand Journal of Agricultural Research, 46(3): 225-237.

Snelder, T. (2016). Performance testing of the Physiographics of Southland using random forest (RF) models. Water Land People report prepared for Environment Southland.

Snelder, T, Hughes, B, Wilson K, and Day, K. (2016). Physiographic Zones for the Southland Region: Classification system validation and testing report. Prepared for Environment Southland by LWP Ltd, Christchurch. 73p.

Srinivasan, M. S., Gburek, W. J., and Hamlett, J. M. (2002). Dynamics of stormflow generation—A hillslope-scale field study in east-central Pennsylvania, USA. Hydrological Processes, 16(3):649-665.

Strong, D. T., Turnbull, R. E., Haubrock, S., Mortimer, N. (2016). Petlab: New Zealand's national rock catalogue and geoanalytical database. New Zealand Journal of Geology and Geophysics, v.59(3), p.475–481

Tschritter, C., Westerhoff, R., Rawlinson, Z., and White, P. (2017). Aquifer classification and mapping at the national scale – Phase 1: Identification of hydrogeological units, GNS Science Report 2016/51. 52 p.

Tratnyek, P. G., Grundl, T. J., Haderlein, S.B. (Eds) (2012). Aquatic Redox Chemistry. American Chemical Society symposium series 1071; Oxford University Press, 20

Turnbull, I.M. and Allibone, A.H. (compilers) (2003). Geology of the Murihiku area. Institute of Geological and Nuclear Sciences Limited. 1:250 000 geological map 20. 1 sheet and 74 p. Lower Hutt, New Zealand.

Webb, T., Hewitt, A., Lilburne, L., McLeod, M., and Close, M. (2010). Mapping of vulnerability of nitrate and phosphorus leaching, microbial bypass flow, and soil runoff potential for two areas of Canterbury. Environment Canterbury Report no. 10. Canterbury, New Zealand.

Wieder, R.K., Novak, M., and Vile, A. (Eds.). (2004). Biogeochemical Investigations of Terrestrial, Freshwater, and Wetland Ecosystems across the Globe. Kluwer Academic Publishers, New York. p.748.

Wilson, S., Chanut, P., Rissmann, C., and Ledgard, G. (2014). Estimating time lags for nitrate response in shallow Southland groundwater. Lincoln Agritech Ltd: Environment Southland Publication no. 2014-03.

Wilson, S. R., Close, M. E., and Abraham, P. (2018). Applying linear discriminant analysis to predict groundwater redox conditions conducive to denitrification. Christchurch, New Zealand. Journal of Hydrology, 556: 611-624.

Wright, R. F. (1988). Influence of Acid Rain on Weathering Rates. In A. Lerman, and M. Meybeck, Physical and Chemical Weathering in Geochemical Cycles p.181-196. Oslo, Norway: Kluwer Academic Publishers.

Zomlot, Z., Verbeiren, B., Hysman, M., and Batelaan, O. (2015). Spatial distribution of groundwater recharge and base flow: assessment of controlling factors. Journal of Hydrology, Regional Studies, 4, 349–368.

Appendix 1. Correlation Matrix

	Easting			**Northing**			**Mean Altitude RSL**			**Median Altitude RSL**			**Cl**			**Conductivity**			**Mg**			**Na**			**SO_4**		
	Corr	No	2-Tail P	Corr	No	2-Tail P	Corr	No	2-Tail P	Corr	No	2-Tail P	Corr	No	2-Tail P	Corr	No	2-Tail P	Corr	No	2-Tail P	Corr	No	2-Tail P	Corr	No	2-Tail P
Easting																											
Prsn				-0.77	64.00	0.00	-0.21	64.00	0.10	-0.16	64.00	0.22	0.44	34.00	0.01	0.06	64.00	0.66	-0.30	34.00	0.08	0.39	34.00	0.02	0.32	34.00	0.06
Spmn				-0.74	64.00	0.00	-0.17	64.00	0.18	-0.12	64.00	0.33	0.46	34.00	0.01	0.08	64.00	0.54	-0.33	34.00	0.06	0.43	34.00	0.01	0.29	34.00	0.10
Kndl				-0.53	64.00	0.00	-0.14	64.00	0.10	-0.10	64.00	0.23	0.32	34.00	0.01	0.05	64.00	0.59	-0.21	34.00	0.08	0.27	34.00	0.03	0.18	34.00	0.13
Northing																											
Prsn	-0.77	64.00	0.00				-0.04	64.00	0.75	-0.05	64.00	0.69	-0.63	34.00	0.00	-0.14	64.00	0.28	0.05	34.00	0.78	-0.52	34.00	0.00	-0.36	34.00	0.03
Spmn	-0.74	64.00	0.00				-0.01	64.00	0.94	-0.04	64.00	0.78	-0.66	34.00	0.00	-0.22	64.00	0.08	-0.04	34.00	0.84	-0.58	34.00	0.00	-0.33	34.00	0.05
Kndl	-0.53	64.00	0.00				0.00	64.00	0.95	-0.02	64.00	0.84	-0.51	34.00	0.00	-0.14	64.00	0.10	-0.06	34.00	0.61	-0.43	34.00	0.00	-0.21	34.00	0.09
meanRSL																											
Prsn	-0.21	64.00	0.10	-0.04	64.00	0.75				0.98	64.00	0.00	-0.48	34.00	0.00	-0.56	64.00	0.00	-0.09	34.00	0.59	-0.46	34.00	0.01	-0.63	34.00	0.00
Spmn	-0.17	64.00	0.18	-0.01	64.00	0.94				0.97	64.00	0.00	-0.42	34.00	0.01	-0.55	64.00	0.00	-0.09	34.00	0.63	-0.46	34.00	0.01	-0.56	34.00	0.00
Kndl	-0.14	64.00	0.10	0.00	64.00	0.95				0.88	64.00	0.00	-0.32	34.00	0.01	-0.40	64.00	0.00	-0.06	34.00	0.63	-0.36	34.00	0.00	-0.41	34.00	0.00
medianRS																											
L Prsn	-0.16	64.00	0.22	-0.05	64.00	0.69	0.98	64.00	0.00				-0.47	34.00	0.00	-0.57	64.00	0.00	-0.17	34.00	0.33	-0.48	34.00	0.00	-0.58	34.00	0.00
Spmn	-0.12	64.00	0.33	-0.04	64.00	0.78	0.97	64.00	0.00				-0.41	34.00	0.02	-0.56	64.00	0.00	-0.14	34.00	0.42	-0.49	34.00	0.00	-0.56	34.00	0.00
Kndl	-0.10	64.00	0.23	-0.02	64.00	0.84	0.88	64.00	0.00				-0.31	34.00	0.01	-0.40	64.00	0.00	-0.10	34.00	0.42	-0.37	34.00	0.00	-0.39	34.00	0.00
Cl																											
Prsn	0.44	34.00	0.01	-0.63	34.00	0.00	-0.48	34.00	0.00	-0.47	34.00	0.00				0.63	34.00	0.00	0.27	34.00	0.12	0.89	34.00	0.00	0.46	34.00	0.01
Spmn	0.46	34.00	0.01	-0.66	34.00	0.00	-0.42	34.00	0.01	-0.41	34.00	0.02				0.58	34.00	0.00	0.21	34.00	0.23	0.85	34.00	0.00	0.34	34.00	0.05
Kndl	0.32	34.00	0.01	-0.51	34.00	0.00	-0.32	34.00	0.01	-0.31	34.00	0.01				0.44	34.00	0.00	0.16	34.00	0.20	0.71	34.00	0.00	0.26	34.00	0.04
Condy																											
Prsn	0.06	64.00	0.66	-0.14	64.00	0.28	-0.56	64.00	0.00	-0.57	64.00	0.00	0.63	34.00	0.00				0.79	34.00	0.00	0.79	34.00	0.00	0.52	34.00	0.00
Spmn	0.08	64.00	0.54	-0.22	64.00	0.08	-0.55	64.00	0.00	-0.56	64.00	0.00	0.58	34.00	0.00				0.78	34.00	0.00	0.78	34.00	0.00	0.53	34.00	0.00
Kndl	0.05	64.00	0.59	-0.14	64.00	0.10	-0.40	64.00	0.00	-0.40	64.00	0.00	0.44	34.00	0.00				0.58	34.00	0.00	0.62	34.00	0.00	0.40	34.00	0.00
Mg																											
Prsn	-0.30	34.00	0.08	0.05	34.00	0.78	-0.09	34.00	0.59	-0.17	34.00	0.33	0.27	34.00	0.12	0.79	34.00	0.00				0.52	34.00	0.00	0.10	34.00	0.56
Spmn	-0.33	34.00	0.06	-0.04	34.00	0.84	-0.09	34.00	0.63	-0.14	34.00	0.42	0.21	34.00	0.23	0.78	34.00	0.00				0.50	34.00	0.00	0.13	34.00	0.48
Kndl	-0.21	34.00	0.08	-0.06	34.00	0.61	-0.06	34.00	0.63	-0.10	34.00	0.42	0.16	34.00	0.20	0.58	34.00	0.00				0.36	34.00	0.00	0.07	34.00	0.54
Na																											
Prsn	0.39	34.00	0.02	-0.52	34.00	0.00	-0.46	34.00	0.01	-0.48	34.00	0.00	0.89	34.00	0.00	0.79	34.00	0.00	0.52	34.00	0.00				0.41	34.00	0.02
Spmn	0.43	34.00	0.01	-0.58	34.00	0.00	-0.46	34.00	0.01	-0.49	34.00	0.00	0.85	34.00	0.00	0.78	34.00	0.00	0.50	34.00	0.00				0.38	34.00	0.03
Kndl	0.27	34.00	0.03	-0.43	34.00	0.00	-0.36	34.00	0.00	-0.37	34.00	0.00	0.71	34.00	0.00	0.62	34.00	0.00	0.36	34.00	0.00				0.30	34.00	0.01
SO_4																											
Prsn	0.32	34.00	0.06	-0.36	34.00	0.03	-0.63	34.00	0.00	-0.58	34.00	0.00	0.46	34.00	0.01	0.52	34.00	0.00	0.10	34.00	0.56	0.41	34.00	0.02			
Spmn	0.29	34.00	0.10	-0.33	34.00	0.05	-0.56	34.00	0.00	-0.56	34.00	0.00	0.34	34.00	0.05	0.53	34.00	0.00	0.13	34.00	0.48	0.38	34.00	0.03			
Kndl	0.18	34.00	0.13	-0.21	34.00	0.09	-0.41	34.00	0.00	-0.39	34.00	0.00	0.26	34.00	0.04	0.40	34.00	0.00	0.07	34.00	0.54	0.30	34.00	0.01			